FEDERAL UNIVERSITY OF CEARÁ
SCIENCE CENTER
GEOLOGY DEPARTMENT
GEOLOGY GRADUATE PROGRAM

KAREN MARIA LEOPOLDINO OLIVEIRA

CHARACTERIZATION OF DEEPWATER RESERVOIRS IN A FRONTIER BASIN IN THE BRAZILIAN EQUATORIAL MARGIN: FROM SEISMIC PROCESSING TO MACHINE LEARNING APPROACH

FORTALEZA
2020

KAREN MARIA LEOPOLDINO OLIVEIRA

CHARACTERIZATION OF DEEPWATER RESERVOIRS IN A FRONTIER BASIN IN THE BRAZILIAN EQUATORIAL MARGIN: FROM SEISMIC PROCESSING TO MACHINE LEARNING APPROACH

Doctorate thesis submitted to Geology Graduate Program at Federal University of Ceará for the obtainment of the title of PhD in Geology. Study Area: Geodynamics and Mineral Resources.

Advisor: Prof. Dr. Raimundo Mariano Gomes Castelo Branco
Co-advisor: Prof. Dr. Francisco Nepomuceno Filho

US Advisor: Dr. Heather Bedle – University of Oklahoma

FORTALEZA

2020

Dados Internacionais de Catalogação na Publicação
Universidade Federal do Ceará
Biblioteca Universitária
Gerada automaticamente pelo módulo Catalog, mediante os dados fornecidos pelo(a) autor(a)

O47c Oliveira, Karen Maria Leopoldino.
Characterization of deepwater reservoirs in a frontier basin in the Brazilian Equatorial Margin: from seismic processing to machine learning approach / Karen Maria Leopoldino Oliveira. – 2020.
136 f. : il. color.

Tese (doutorado) – Universidade Federal do Ceará, Centro de Ciências, Programa de Pós-Graduação em Geologia, Fortaleza, 2020.
Orientação: Prof. Dr. Raimundo Mariano Gomes Castelo Branco.
Coorientação: Prof. Dr. Francisco Nepomuceno Filho.

1. Bacia do Ceará. 2. Exploração de petróleo. 3. Atributos sísmicos. 4. Machine Learning. I. Título.
CDD 551

KAREN MARIA LEOPOLDINO OLIVEIRA

CHARACTERIZATION OF DEEPWATER RESERVOIRS IN A FRONTIER BASIN IN THE BRAZILIAN EQUATORIAL MARGIN: FROM SEISMIC PROCESSING TO MACHINE LEARNING APPROACH

Doctorate thesis submitted to Geology Graduate Program at Federal University of Ceará for the obtainment of the title of PhD in Geology. Study Area: Geodynamics and Mineral Resources.

Approval Date: 11/08/2020.

COMITTE MEMBERS

To Marta, Felipe, and Levi.

ACKNOWLEDGEMENTS

It was four years of research lived intensely. I started, at the same time, two long rewarding journeys, the PhD degree and motherhood. Many people contributed directly or indirectly to my professional and personal growth, obviously such an outstanding achievement is not only because my own merits. There is a large list of people that have helped me achieve this goal. First, I would like to thank almighty God for giving me wisdom whenever I asked him and for all his gifts.

Second, I want to thank my mom Marta Leopoldino for the love, care, and compassion. Without my mom's love I would not be where I am today. To my husband Felipe and my son Levi for the great support during these four years, I would like to thank them for all love, patience, and strength this last few years, for being there unconditionally every time I needed them. To my brother Diego Leopoldino for caring so much about me (and for the help with computer things!!)

I am very thankful for my advisor Dr. Mariano Castelo Branco, who gave me the opportunity to learn more about geophysics during almost 11 years. I am grateful for his support and guidance. Also, my co-advisor Francisco Nepomuceno Filho who trusted me and showed me the "seismic data world". Thank you for sharing your knowledge, always motivating me to go beyond. I was so lucky to have had both of you as my advisors.

I am infinitely grateful to my US advisor Dr. Heather Bedle because she trusted me as her student when I sent an email asking for guidance without any recommendation letter (she is so brave!). Even before we met, she was so professional and available for me. I cannot thank her enough for everything she has done for me. Also, I thank her for showing me that you can be intelligent, wise, positive (always), a great mother, and still be humble and kind to others. To Dr. Kurt Marfurt for all constructive criticisms and to share the AASPI software for this research.

To Laboratório de Geofísica de Prospecção e Sensoriamento Remoto (LGPSR) and its great team. Thank you so much for all the memories we shared at field trips, at the University, and other social gatherings. It has been almost eleven unforgettable years that I will never forget.

To all my fellow graduate students at the Universidade Federal do Ceará and the Laboratório de Interpretação Sísmica, thank you so much for all the constructive discussions, excellent company, and support. Ana Clara, Márcio, Narelle, and Thiago.

This study was financed in part by the Coordenação de Aperfeiçoamento de Pessoal de Nível Superior - Brasil (CAPES) - Finance Code. Also, I acknowledge FUNCAP.

Additional support for this research was provided by the Fulbright Brazil. Special thanks to the main office ladies of Fulbright Brazil: Carolina Martins, Taynara Ramos, and Bibiana Silva. Thank you for your continuous support throughout the Fulbright grant (2019-2020).

I would also like to thank the various companies for their support and technologies; to Petrobras for the workstations and infrastructure; to Schlumberger for Petrel, to Brazilian National Oil and Gas Agency (ANP) for the geophysical dataset, To Laboratório de Sistemas e Banco de Dados (LSBD) for all the resources during my first years of PhD; to CimaGeo for the support in processing seismic data, and to the sponsors AASPI research consortium.

I would like to thank to all the staff in the geology and geophysics department and professors and friends at the University of Oklahoma who were kind and helped me during my nine months as a Fulbright Visiting Research. Dr. Heather Bedle, Dr. Kurt Marfurt, Karelia, Jose, Edimar, Javier, Rafael, Chris, Roberto, Julian, Laura, Carl, Peter, Clayton, David, Marta, Hannah, Hope, Caf, Francis, Swetal, Rebecca Fay, Leah Moser, and Ashley Tullius.

To my Brazilian family in Norman (OK) who made my exchange time more comfortable besides the distance from my family. Cláudia, Juliana, Alice, Letícia, Paulo, Olívia, Samuel, Edimar, Cláudia Boza, Aglaia, Lara, Michele, Fabio, Pedro, Eduardo (Panamanian, also).

To all Geology Department of at the Universidade Federal do Ceará. I began my journey as geologist there, as undergraduate student and I am “finishing” my academic career as a PhD geoscientist there. I have so much to thank to all my UFC professors. Some are still there, some of them are in other Universities, and other dear ones are in a better place (heaven). Thank you so much!

I would like to thank my friends and colleagues of the Municipality of Aquiraz for their important support during a brief period for the development of this thesis.

Lastly, but not less important, I would like to thank to my whole family and friends for all the love, compassion, help, and adventures during my endeavor. I do not feel comfortable to write a list of names. I am certain my family and friends know this acknowledgement is for them.

I would like to express my sincere gratitude to my committee members: Dr. Mariano Castelo Branco, Dr. Wander Amorim, Dr. Paulo Johann, Dr. Mateus Meira, Dr. Sérgio Lima Filho for their kind words and encouragement.

RESUMO

Nos últimos anos, a Margem Equatorial Brasileira chamou atenção para as novas descobertas de hidrocarbonetos, tanto na margem conjugada africana quanto na margem brasileira e na Guiana Francesa. Entretanto, estudos sobre o regime tectônico associados às margens transformantes, sua evolução, estruturas e potencial petrolífero ainda são escassos devido à grande complexidade geológica dessa região. Para suprir essa lacuna de conhecimento, foram realizadas pesquisas para melhor compreender as estruturas geológicas, assim como identificar possíveis locais para acúmulo de hidrocarbonetos em águas profundas da Bacia do Ceará. Foi realizada interpretação integrada de um grande volume de dados sísmicos 2D, um cubo sísmico, novos dados exploratórios de poço, bem como dados antigos de poços. Essa análise de dados refina a arquitetura da bacia e a evolução tectônica do Cretáceo ao Paleógeno, incluindo implicações para a prospecção de hidrocarbonetos em águas profundas da bacia. A análise também identifica possíveis acumulações de hidrocarbonetos em reservatórios turbidíticos e apresenta informações sobre as dimensões do rifte situado no talude. Os resultados revelam um alto potencial para as sequências drifte em águas profundas, onde a espessura dos sedimentos do intervalo Albiano-Cenomaniano-Turoniano atingem aproximadamente 3048 a 4894 m. Além disso, esta pesquisa mostra evidências de magmatismo do Cretáceo ao Paleógeno, indicadas pelos vulcões bem imageados e soleiras associadas nos dados sísmicos. A variedade de padrões estratigráficos e estruturais desenvolvidas ao longo do Cretáceo na bacia oferece potenciais de trapas para plays petrolíferos tanto no rifte quanto nas sequencias drifte da Bacia do Ceará. Além disso, análise de atributos sísmicos e uma abordagem não supervisionada de *machine learning* foram capazes de produzir imagens de alta resolução e mapear a geometria 3D da geomorfologia sísmica em diferentes níveis estratigráficos, do intervalo Albiano ao Turoniano. Uma melhor compreensão da geomorfologia sísmica e das análises de fácies sísmicas forneceram informações valiosas sobre uma bacia pouco explorada, oferecendo o melhor potencial para armadilhas estratigráficas em águas profundas. Essa abordagem pode ser usada em bacias de nova fronteira exploratória ou emergentes para ajudar a diminuir o risco de exploração.

Palavras-chave: Margem Equatorial Brasileira. Bacia do Ceará. Exploração de petróleo. Ambientes em águas profundas. Atributos sísmicos. *Machine learning*.

ABSTRACT

In recent years, the Brazilian Equatorial Margin has drawn attention due to its similarity to areas with new hydrocarbon discoveries in the African conjugated margin, and in French Guiana. However, studies on the tectonic regimes associated with transform margins and their evolution, structures, and petroleum potential are still lacking due to the geological complexity of this region. To address this knowledge gap, research has been done to better understand the geological structures, as well as to identify potential hydrocarbon accumulations in the deepwater Ceará Basin. To achieve this, we performed an integrated interpretation of a large 3D and 2D seismic data, new exploratory borehole data, as well as older well data with revised biostratigraphy. This data analysis refines the basin architecture and the Cretaceous-Paleogene tectonic evolution, including implications for hydrocarbon prospectivity in the Ceará Basin deepwater. The analysis also identifies potential hydrocarbon accumulations in turbiditic reservoirs and presents new insights about the dimensions of the underlying rift features situated in the continental slope. The results reveal a high potential for drift sequences in deepwater where the Late Albian-Early Cenomanian-Turonian sediments reach thicknesses of approximately 3048 to 4894 m. Moreover, this research shows evidence of Cretaceous to Paleogene magmatism, indicated by the well-imaged volcanoes and associated sills in the seismic data. The variety of stratigraphic and structural features developed through the Cretaceous history of the Mundaú sub-basin offers a variety of potential hydrocarbon traps and plays in a number of rift and post-rift sequences. In addition, a seismic attributes analysis and unsupervised machine learning approach were able to produce relatively high-resolution images and map the 3D geometry of ancient geomorphology across different stratigraphic levels from Albian to Turonian interval. A better understanding of the seismic geomorphology and seismic facies analysis provided valuable insights into an underexplored basin and offer the best potential for deepwater stratigraphic traps. This approach may be used on similar frontier or emerging hydrocarbon basins to help de-risking the petroleum exploration.

Keywords: Brazilian Equatorial Margin. Ceará Basin. Petroleum Exploration. Deepwater Environments. Seismic Attributes. Machine Learning.

TABLE OF CONTENTS

1	**INTRODUCTION**	**11**
1.1	**Motivation**	**11**
1.2	**Main Goal**	**13**
1.3	**Study Area and database**	**14**
1.4	**Structure of this thesis**	**17**
2	**ARTICLE 1: THE IMPORTANCE OF RECOGNIZING MULTIPLES IN LEGACY DATA: A CASE STUDY FROM THE BRAZILIAN EQUATORIAL MARGIN**	**19**
3	**ARTICLE 2: SEISMIC STRATIGRAPHIC PATTERNS AND CHARACTERIZATION OF DEEPWATER RESERVOIRS OF THE MUNDAÚ SUB-BASIN, BRAZILIAN EQUATORIAL MARGIN**	**26**
4	**ARTICLE 3: SEISMIC ATTRIBUTES, MACHINE LEARNING, AND ROCK PHYSICS ANALYSES – A PROMISING AID FOR HYDROCARBON PREDICTION IN A DEEPWATER BASIN OF THE BRAZILIAN EQUATORIAL MARGIN**	**75**
5	**CONCLUSION**	**115**
	REFERÊNCIAS	**117**
	APPENDIX A – LIST OF PAPERS AND ABSTRACTS RELATED TO THIS THESIS	**119**
	APPENDIX B – LIST OF PAPERS AND ABSTRACTS OF THE BEM's RESEARCH GROUP	**123**
	APPENDIX C –LIST OF FIGURES	**132**

1. INTRODUCTION

This thesis compiles the work I developed during my years as a PhD student at the Universidade Federal do Ceará and also includes some results of the research I conducted as a Fulbright visiting research at the University of Oklahoma. It presents the results of an integrated interpretation of a large 2D and 3D seismic data, new exploratory borehole data, as well as older well data with revised biostratigraphy. This data analysis refined the basin architecture and the Cretaceous-Paleogene tectonic evolution, including implications for hydrocarbon prospectivity in the Ceará Basin deepwater, in the Brazilian Equatorial Margin.

Thus, this chapter is dedicated to valuing the understanding of this margin as a new exploratory frontier both for Brazil and international oil companies. In addition, it justifies the purpose of this thesis, list the main goal, present the study area and the dataset, and explain the structure of this thesis.

1.1 Motivation

The Brazilian Equatorial Margin (BEM) has approximately 1,000,000 km² of sedimentary area and comprises the Foz do Amazonas, Pará-Maranhão, Barreirinhas, Ceará, and potiguar basins (Fig. 1-1a). The geological evolution of this margin is similar to the West African margin, being characterized by transform tectonism. In recent years, the Brazilian Equatorial Margin has drawn attention due to its similarity to areas with new hydrocarbon discoveries in the African conjugated margin, and in French Guiana. However, studies on the tectonic regimes associated with transform margins and their evolution, structures, and petroleum potential are still lacking due to the geological complexity of this region. Such basins and their structures still require more in-depth research on their genesis and geological significance, especially for the oil industry.

It is important to restate that in the African counterpart, production is having success in Nigeria, in Ghana with the Jubilee discovery, offshore Ivory Coast, and in Equatorial Guinea. New discoveries in offshore Suriname and Guyana confirm the potential of the region. In the last years, the Brazilian Equatorial Margin has been a subject of discussion in events as the Offshore Technology Conference (OTC) - where expert professionals from energy sector meet to exchange ideas and opinions to advance scientific and technical knowledge for offshore resources and environmental matters. At the 2016 OTC meeting, the highlight of the first day was a speech by the president of the Brazilian Institute of Oil, Gas and Biofuels (IBP) with the

theme “The perspective of investments by International Oil Companies (IOC) in the oil and gas sector in Brazil”, which had a convergence in the speeches made by the speakers of opportunities for the country. Among them are the revitalization of mature fields, a new frontier at BEM, and the development and production of the Pre-Salt. The OTC technical program in 2018, which celebrated 50 years, had a special discussion on “Investments in deepwaters in Brazil: an IOC perspective” (OTC, 2018). The geology of BEM is much less known than the geology of the South Atlantic basins, especially due to difficulties in interpretation caused by shear faults that resulted in a much more complex model for these sedimentary basins. The great challenge is to interpret the geology of the area in order to choose locations to drill with the probability of discovering oil and/or natural gas in commercial quantities that can be produced economically.

The 11th Round of Bids of the Brazilian National Agency of Oil, Natural Gas and Biofuels (ANP) in 2013 allowed dozens of blocks to be acquired by companies in all five basins of the BEM (Zalán, 2015). The ANP's most recent bidding round, the 15th in 2018, had 12 blocks offered in deep and ultra-deepwater in the Ceará Basin, totaling an area of approximately 8,500 km². The increase in bidding in the last several years reveals the escalating interest in the hydrocarbon potential of the BEM. According to ANP, BEM has potential for oil discovery in turbidite reservoirs from the late Cretaceous to the Paleogene, similar to the discoveries of the West African Margin.

Most oil and gas discoveries on Equatorial margins are associated with the presence of stratigraphic traps in turbidites. In addition to this, according to studies, 90 percent of the hydrocarbon discoveries in deepwater basins come from from turbiditic deposits, and their exploration becomes a relevant and active field in the international oil industry (Pang et al., 2005; Peng et al., 2005; Shanmugam, 2000; Stowa and Mayall, 2000; Pettingill and Paul, 2002). There exist many hot spots of deepwater exploration in the world, including West Africa, Brazil, and the Gulf of Mexico (Liu et al., 2016).

The deepwater of the BEM is underexplored, only three wells have been drilled, however available public domain data from ongoing seismic evaluation suggests that there is high potential for light oil discoveries in Upper Cretaceous turbidite sandstone reservoirs in stratigraphic traps. Previous works as Maia de Almeida et al. (2020) proved that reservoirs in a deepwater well comprise Cretaceous sandstones in a combined trap related to both an unconformity and a normal fault. However, they did not discuss the potential reservoirs in the

syn-rift and drift sequences. In this study, we improve the current geologic understanding of the basin, mapping the main geologic features using a large 2D seismic dataset, as well as identify regions of potential hydrocarbon accumulations in the deepwater Cretaceous-Paleogene sequences of Mundaú sub-basin. This analysis results in a new understanding of the basin that can be used to identify possible plays and to refine the basin architecture and its tectonic evolution, including implications for hydrocarbon prospectivity in the Ceará Basin deepwater.

Proceeding to the research, three deepwater wells, and three-dimensional (3D) seismic reflection data have been examined in the light of three main objectives: (i) identify deepwater architectural elements; (ii) using multiattribute to analysis major types of seismic facies which could be well related to sedimentary facies; (iii) identify key targets for future exploration. Besides the multiattribute seismic analysis, unsupervised machine-learning techniques as self-organizing map (SOM) and independent component analysis (ICA) were applied focusing on this same interval. These techniques provided additional insight to hydrocarbon potential in this area, and aided in understanding the distribution and classification of the deepwater geological elements. This research presents the first occurrence of subsurface large turbidite complex system based on the integration of the seismic attributes and machine learning techniques in the Ceará Basin. This, to our knowledge, is the most broad-brush overview of the seismic geomorphology of deepwater Ceará Basin within the public domain. These approaches may be used on similar frontier or emerging hydrocarbon basins to help de-risking the petroleum exploration.

1.2 Main Goal

The goal I aim to reach is provide significant advances in the knowledge of the Cretaceous-Paleogene tectonic evolution, including implications for hydrocarbon prospectivity in the Ceará Basin deepwater, using geophysical approaches. Seismic data processing, conventional seismic interpretation, seismic attributes and machine learning techniques were applied to improve the understanding of the seismic geomorphology and seismic facies, and thus reveal future opportunities. A comparison with successful Equatorial margin basins was made to increase the possibility of future discoveries in this area.

1.3 Study Area and database

The Ceará Basin is a frontier hydrocarbon producing basin with four fields in the shallow water domains of the Mundaú sub-basin (Xaréu, Atum, Espada and Curimã) (Figs. 1-1c and 1-2). In 2012, Petrobras drilled the 1 BRSA 1080 CES well, the first deepwater oil discovery in Ceará Basin, then two additional exploratory wells were drilled with more complete chronostratigraphic data collection. Two wells had previously been drilled in the deepwater in the 1990s, but data from these have not been publicly released, and thus are not correlated with the new wells.

This study is based on a large seismic reflection dataset and well data (Fig. 1-1c and 1-2), all of which were acquired by Petrobras and supplied by the Brazilian National Agency of Oil, Gas and Biofuels (ANP). We interpreted more than 1,589 km of post-stack time-migrated multichannel 2D seismic reflection profiles located between the slope and the abyssal plain of the Mundaú sub-basin (Fig. 1-2). Additionally, two prestack seismic lines were processed to assist in the interpretation and for depth information. A 3D seismic cube (Fig. 1-1c) was used for conventional seismic interpretation techniques, seismic attributes and machine learning techniques to investigate the seismic geomorphology and depositional environments from Albian to Turonian age interval.

The 2D seismic data set covers an area of approximately 7,125 km², on a seismic grid of ~4 km spacing, which was sufficient enough to confidently tie the different seismic units mapped in this study. The seismic sequence stratigraphic units were identified based on the newly available exploratory wells data 1 BRSA 1114 CES (2012), 1 BRSA 1150 CES (2013), 1 BRSA 1080 CES (2012), and older wells, including 1 CES 112 CE (1993), 1 CES 111 CE (1996), 1 CES 43 CE (1981) and 1 CES 81 CE (1983). These last two wells are located in shallow water. Well data includes standard log suites (i.e. gamma ray, density, resistivity, sonic, Vp, and Vs), checkshots, lithologic and geochemical data, formation tops, and biostratigraphic ages.

The 3D seismic survey was acquired in 2003 by CGG and covered ~1,107 km² of the deepwater Ceará Basin (Figure 1-1c). For the proposal of this research the seismic cube was cropped and covers an area of 765 km² with vertical geometry between -2772 and -5000 ms. It covers part of Premier Oil, Cepsa, Chevron, and Ecopetrol exploration blocks, as well as ANP's blocks of permanent offer (Fig. 1-1c).

Figure 1-1: (a) Regional topographic and bathymetric map of the Equatorial Atlantic showing conjugate margins in Brazil and Africa as well as the larger oceanic fractures zones in the area;

(b) The Ceará basin is divided in four sub-basins: Piauí-Camocim, Acaraú, Icaraí and Mundaú; (c) Relative location of the four producer fields (Xaréu, Atum, Curimã and Espada) of the Mundaú sub-basin. The location of the wells and 3D seismic data are shown. The topographic model is from the National Oceanic and Atmospheric Administration (NOAA). The structural data was compiled from Zalán & Warme (1985), Silva et al., (1999), and Morais Neto et al., (2003). The basin boundaries are from ANP and the sub-basins boundaries were adapted from Morais Neto et al., (2003).

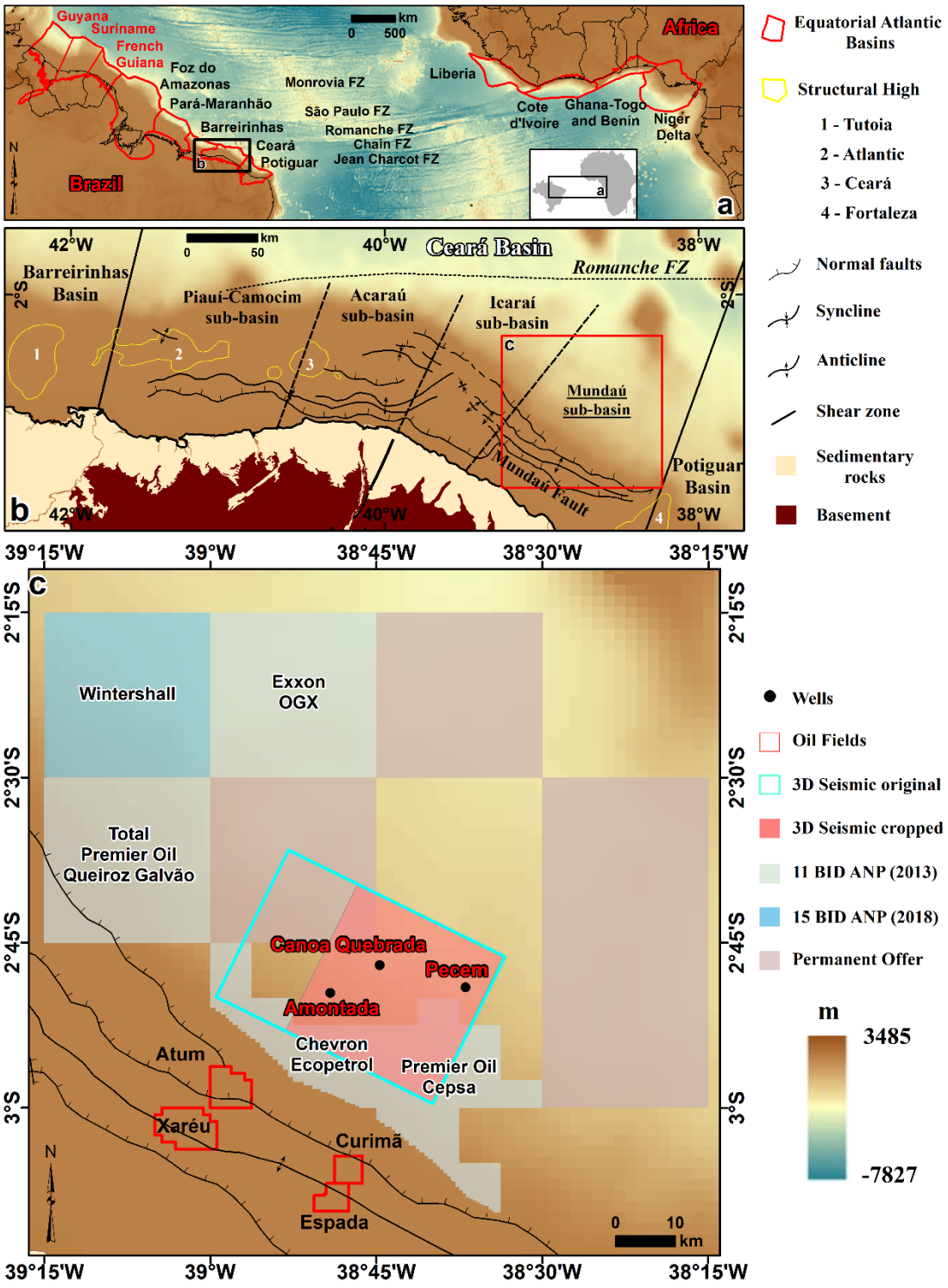

Figure 1-2: The location of the wells, seismic data (2D), and the blocks of ANP Bidding Rounds are displayed. Also, four producer fields (Xaréu, Atum, Curimã, and Espada) in the Mundaú sub-basin are outlined.

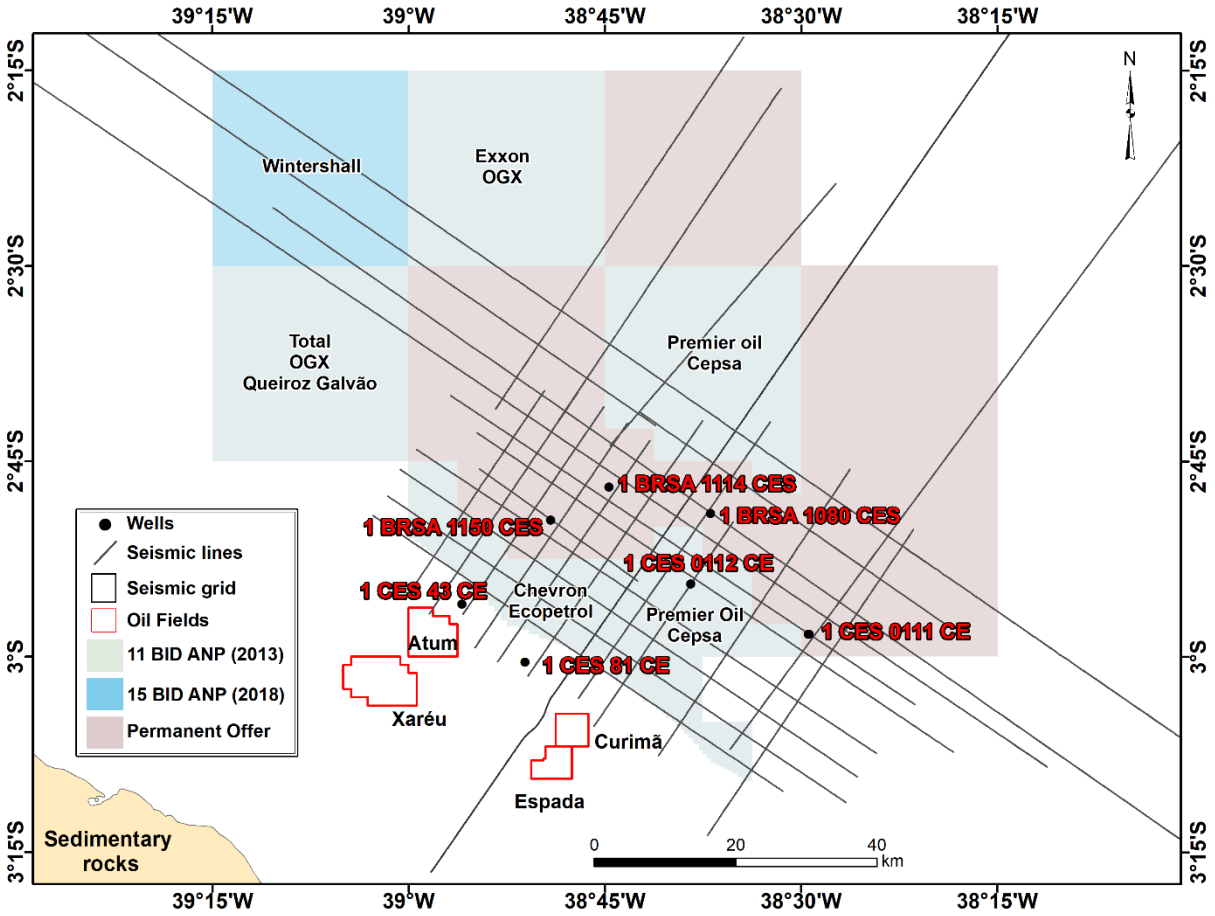

1.4 Structure of this thesis

This thesis contains three articles appended on each chapter. Two fully published articles and one unsubmitted first draft manuscript are presented. In Chapter 2, I analyzed a series of 2D seismic datasets, and I observed some migration artifacts (i.e. multiples) that were characterized by strong seismic horizons mimicking geological layering. So, a marine conventional processing was made in two regional 2D seismic lines in order to remove multiples and noise. Since the Equatorial Margins are marked by complex geological structures a velocity analysis was carefully performed. The reprocessing allowed a more accurate interpretation of subsurface geology in the area, which can increase chances in finding geological structures favorable to hydrocarbon accumulation.

In chapter 3, I improved the current geologic understanding of the basin, mapping the main geologic features using a large 2D seismic dataset, as well as identify regions of

potential hydrocarbon accumulations in the deepwater Cretaceous-Paleogene sequences of Mundaú sub-basin.

Chapter 4 uses a 3D seismic survey to present a broad-brush overview of the seismic geomorphology of the study area aiming at delineating the turbidite channels, as the sands are deposit in the channels and can accumulate the hydrocarbons, which can be exploited for the benefits of the petroleum industry. I used conventional seismic data interpretation techniques, 3D seismic attributes and unsupervised machine learning techniques to investigate the seismic geomorphology and depositional environments from Albian to Turonian age interval.

Chapter 5 presents a summary with the key findings and perspectives. The Appendix 1 contains the first page of each published article, and the conference abstracts related to this thesis. The Appendix 2 contains the first page of each published article of the BEM's research group that I have co-authored, as well as the abstracts presented on conferences. Lastly, the Appendix 3 contains the list of figures related to this thesis.

2. ARTICLE 1: THE IMPORTANCE OF RECOGNIZING MULTIPLES IN LEGACY DATA: A CASE STUDY FROM THE BRAZILIAN EQUATORIAL MARGIN

Authors: Karen M. Leopoldino Oliveira, Heather Bedle, Gabriel de A. Araujo, and Mariano Castelo Branco.

Published on **Interpretation**, 30 de junho de 2020.

Special Issue Interesting features seen on seismic data.

Reference:

Karen M. Leopoldino Oliveira, Heather Bedle, Gabriel de A. Araujo, and Mariano Castelo Branco, (2020), "The importance of recognizing multiples in legacy data: A case study from the Brazilian equatorial margin," *Interpretation* 8: SR17-SR21. https://doi.org/10.1190/INT-2019-0214.1

THE IMPORTANCE OF RECOGNIZING MULTIPLES IN LEGACY DATA: A CASE STUDY FROM THE BRAZILIAN EQUATORIAL MARGIN

Geological Feature: Stratigraphy of the Ceará Basin, offshore Brazil

Seismic Appearance: Strong seismic horizons mimicking geological layering

Alternative Interpretations: Multiples arising from poor seismic migration processing

Features with similar appearance: Strong seismic horizons reflecting basement and carbonates.

Formation: Rift sequence of the Ceará Basin

Age: Cretaceous

Location: Ceará Basin, offshore Brazil

Seismic data: Obtained by Brazilian National Petroleum Agency and reprocessed by the authors

Analysis tool: Reprocessing

Contributors: Karen M. Leopoldino Oliveira[1, 2], Heather Bedle[2], Gabriel de A. Araujo[3], and Mariano Castelo Branco[1].

[1] Programa de Pós-Graduação em Geologia, Universidade Federal do Ceará (UFC), Campus do Pici, Bloco 912, Fortaleza, Ceará, CEP 60440-554, Brazil. Email: karenleopoldino@gmail.com, mariano@ufc.br

[2] School of Geosciences, University of Oklahoma, 100 East Boyd St. Suite 710 Norman, OK 73019. Email: karenleopoldino@ou.edu, hbedle@ou.edu

[3] Departamento de Informática e Matemática Aplicada, Universidade Federal do Rio Grande do Norte, Natal, Brasil. Email: g.almeidaaraujo@gmail.com

2.1. Summary

The Ceará Basin is a deepwater exploration frontier basin that comprises part of the Brazilian Equatorial Margin. This basin has been receiving renewed attention from the petroleum industry since the discovery of important deepwater oil fields in its African counterpart. However, detailed seismic stratigraphic, depositional, and structural frameworks for the Ceará Basin are still lacking in literature. We analyzed a series of 2D seismic datasets and stumbled into the pitfalls of migration artifacts (i.e. multiples) ultimately realizing that

reprocessing was the best option to avoid the mistake of interpreting these artifacts as geologic features. Multiples can be difficult to identify in seismic data where they mimic the true geology of the region, and often present a pitfall for less experienced interpreters. Indeed, the identification and removal of multiples is crucial as they do not reflect the true geology in the subsurface and may otherwise lead to wrongful business decisions.

2.2. Miscorrelating

An example of a seismic profile processed without a careful analysis of the velocity model is shown in Fig. 2-1a and 2-2a and shows the occurrence of several multiples and noise (red arrows) that mimic geological events. These events are further exacerbated using seismic attributes such as amplitude volume technique (AVT) (e. g. Bulhões and Amorim, 2005) (Fig. 2-2a). Seismic interpreters can correlate and interpret these multiples as false horizons as they are well-marked and change their shape as it increases the order multiple (see blue lines in Fig. 2-1b).

2.3. Processing Data

A conventional processing sequence was applied to marine seismic data. The main steps of the processing flow applied was: 1) geometry definition; 2) deghosting; 3) deconvolution; 4) SRME multiple prediction; 5) spectral balance; 6) velocity analysis and NMO correction; 7) Kirchoff time migration; 8) AVT Attribute. In order to improve recognition and removal of multiples, we calculated their depth location by modeling and subsequently extracted them (Fig. 2-1a (red arrows) and b (blue and green lines)).

We used the Surface-Related Multiple Elimination (SRME) (Verschuur et al. 1992) that consists in attenuating multiples generated by the free surface. This method uses only the recorded data to predict all orders of free surface multiples. Due to timing and amplitude errors that arise in practice, the predicted multiples are typically subtracted from the data using adaptive filtering.

Figure 2-1: a) Seismic reflection section with the presence of the first multiple of the seabed and red layer multiple (red arrows) mixing with the signal and noise – a location map view is shown with the seismic profile, the Pecém well and the exploration blocks in Ceará Basin, Brazilian Equatorial Margin; (b) two multiples related to the seabed and another derived from

a slightly deeper horizon. Blue lines refer to seabed reflector and the green line refers to the red line layer.

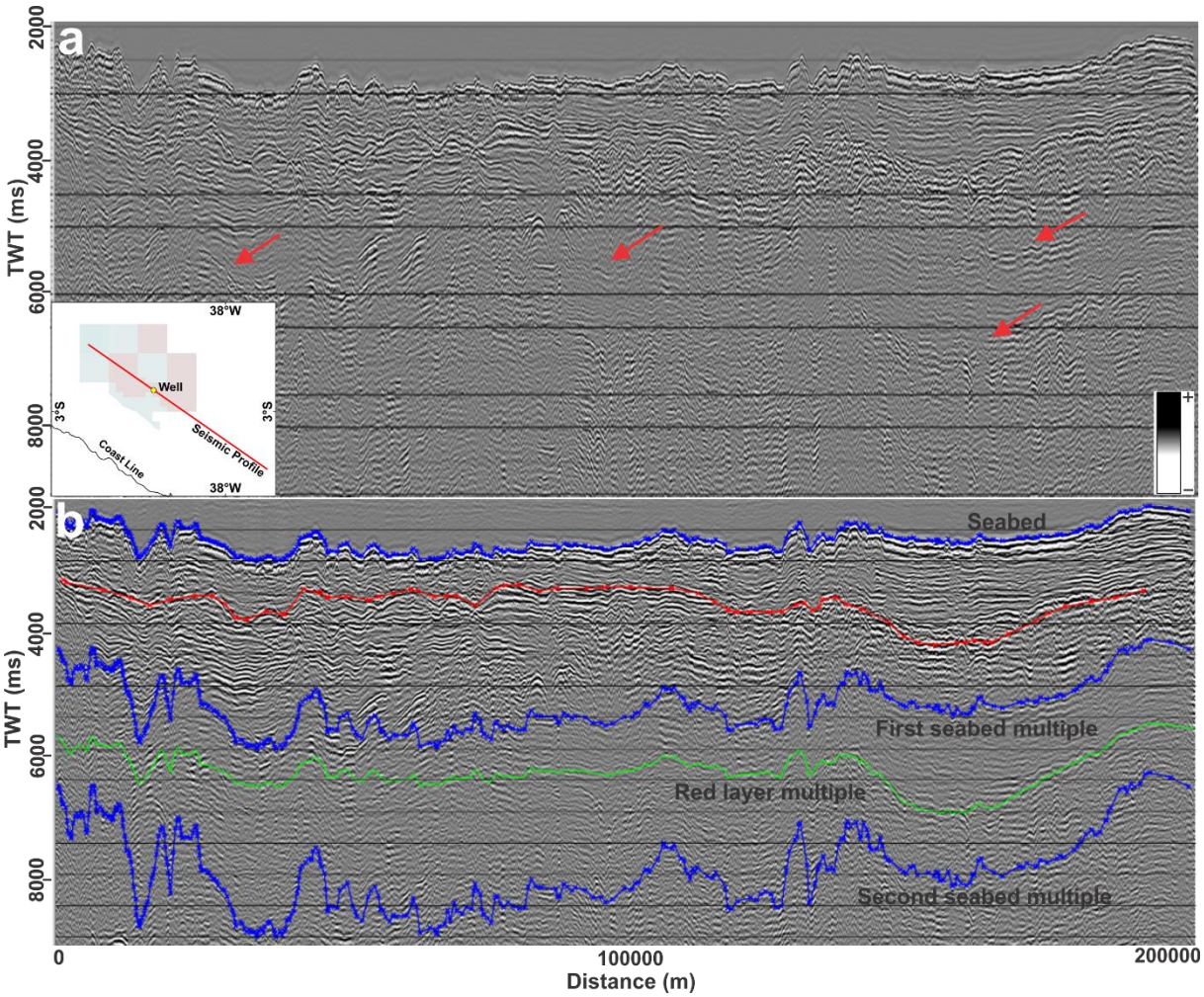

The velocity model was improved using commercial seismic processing software that uses constant velocity stack (CVS) theory. In this method, the complete seismic section is stacked several times, each with constant velocity, with a defined velocity increment. Using multiple panels, velocity analysis can be performed at any point of the seismic section with the aid of supergathers (gathers generated by collecting traces from adjacent CMPs) and the semblance function (Fig. 2-3). In this way, the analysis is completed anywhere in the seismic section and more sampling in the regions where the geology is more complex.

A frequency enhancing algorithm was employed to aid interpretation at both low and high frequencies, the AVT attribute introduced by Bulhões & Amorim (2005) (Fig. 2-2a and b).

Figure 2-2: (a) Seismic line obtained by Brazilian National Petroleum Agency (ANP) with the presence of multiples (red arrows); (b) reprocessed seismic line and true horizons can be mapped without bias. Note that multiples and noise were extracted, and the seismic signal is much better defined. Both lines are displayed with the amplitude volume technique (AVT) attribute as described by Bulhões and Amorim, (2005).

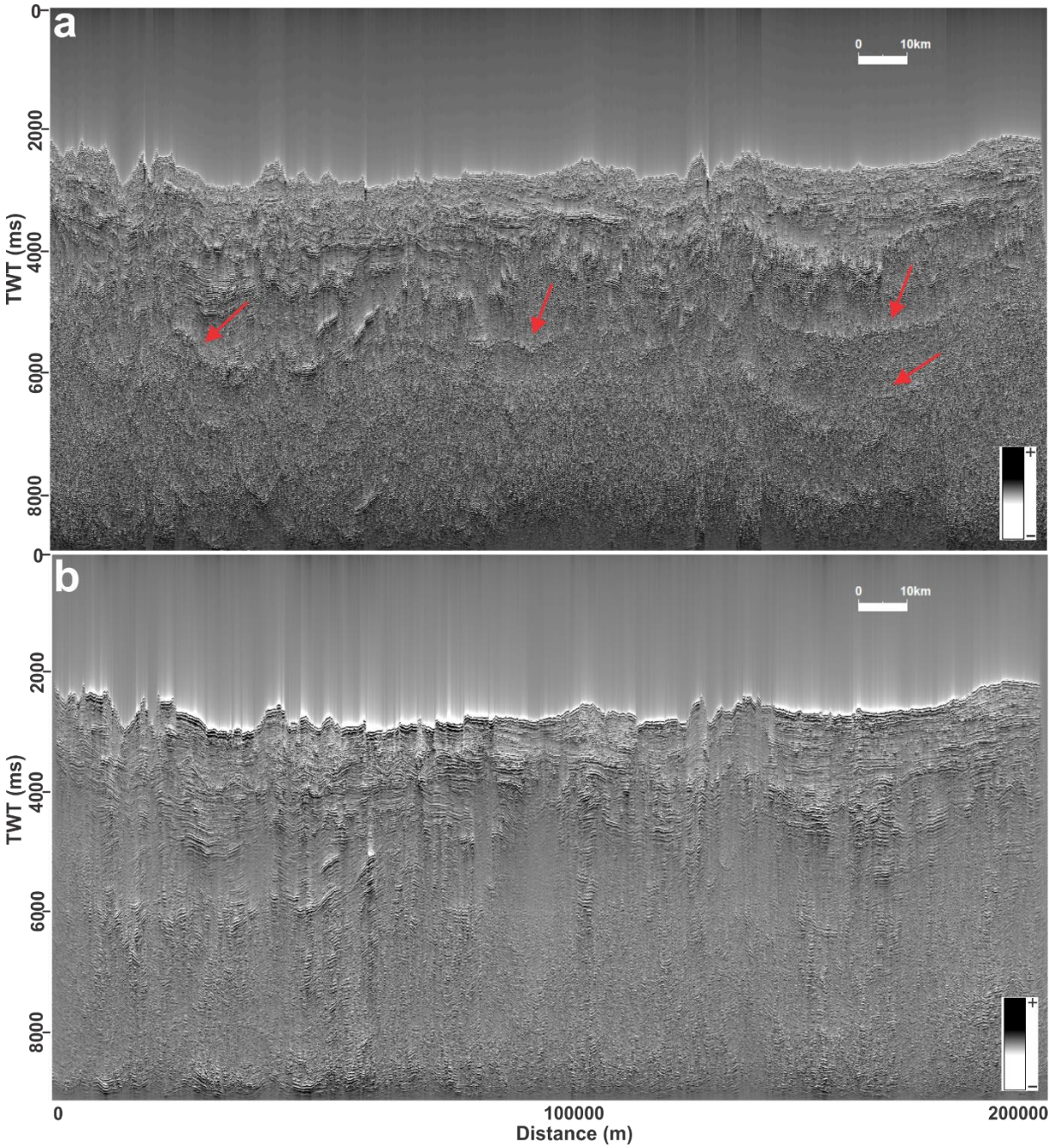

Figure 2-3: The three panels of velocity analysis of this seismic line. (a) the supergather panel is shown on the left as a function of time and offset; (b) the semblance panel; (c) the stacked section with each vertical red line representing a location where the velocity analysis was performed and green line the current location in analysis; (d) the result of this process is shown in a 2D velocity model.

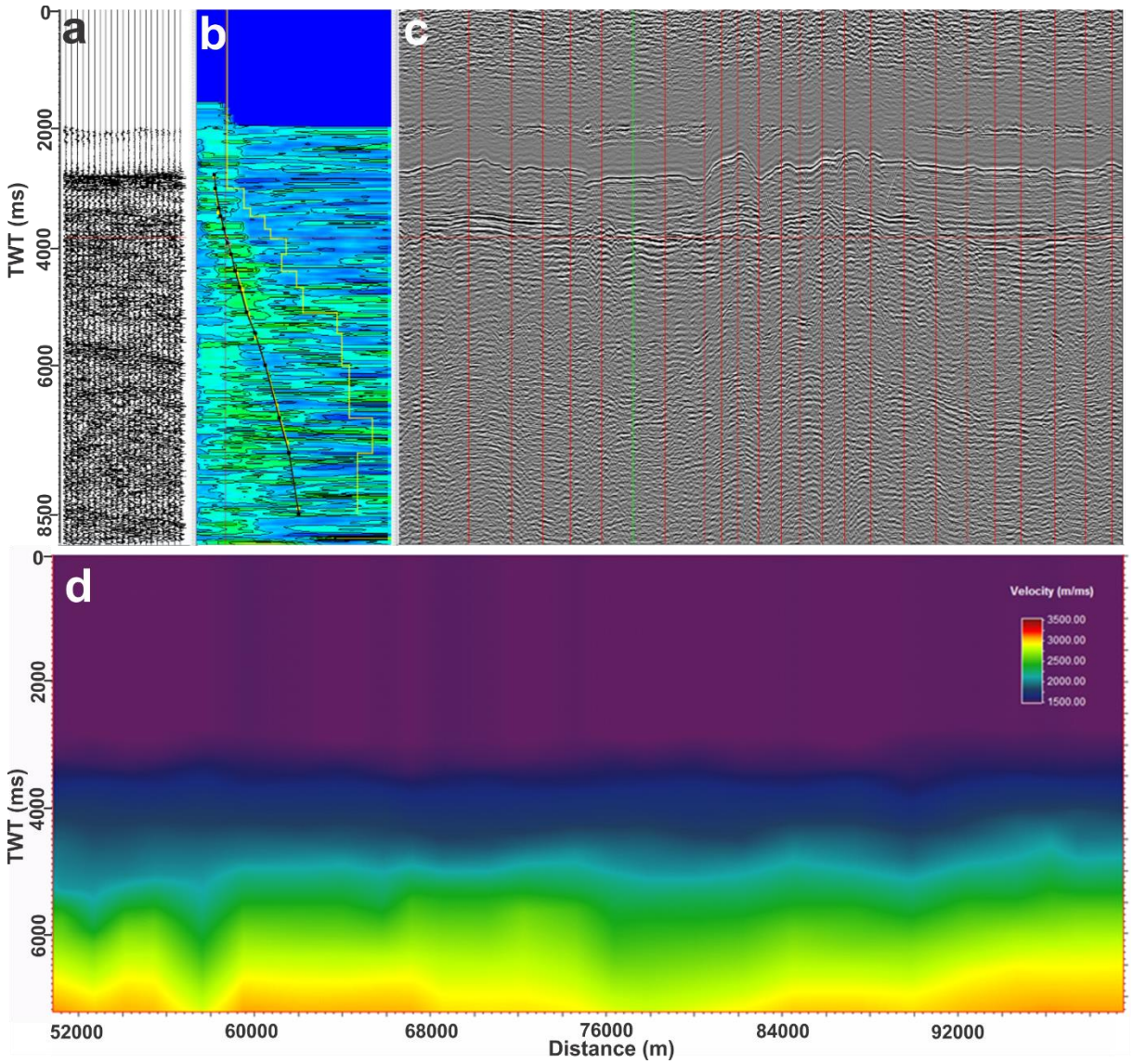

2.4 Remarks

The seismic section in Figure 2-2a does not have clarity and definition in several parts of the seismic line. The combined presence of noise and multiples combined usually confuses the interpreter with false horizons or mask true horizons, also high-frequency noise causes reflector discontinuity that makes it difficult to evaluate the lateral continuity. The multiples cause uncertainty in the seismic interpretation of the basal portions of the basin and the presence or absence of basement. Figure 2-2b shows that the reprocessing allows a more accurate interpretation of subsurface geology in the area, which can increase chances in finding

geological structures favorable to hydrocarbon accumulation. Noteworthy, the Pecém well was drilled on this line and was the first deepwater oil discovery in the Ceará Basin, and thus improved images may reveal other opportunities.

Acknowledgments

The authors are grateful to the Brazilian National Petroleum Agency (ANP) for the provision of seismic and well data. CImaGeo is also acknowledged for their support in seismic processing. The first author is grateful to the Fulbright Commission Brazil for a grant to support in her research in the United States. KMLO thanks the School of Geosciences, the University of Oklahoma, for providing facilities during her split PhD in the United States. This study was financed in part by the Coordenação de Aperfeiçoamento de Pessoal de Nível Superior - Brasil (CAPES) - Finance Code 001. We are also grateful to Florian Smith and two anonymous reviewers that greatly improved the quality of the paper, and the Associate Editor Sumit Verma for his constructive feedback.

References

Bulhões, E. M. & Amorim, W. N., 2005. Princípio da sismocamada elementar e sua aplicação à técnica de volume de amplitudes (TecVa): Ninth International Congress of the Brazilian Geophysical Society, Salvador, Brasil. https://doi.org/10.1190/sbgf2005-275

Verschuur, D. J., Berkhout, A. J., Wapenaar, C. P. A., 1992. Adaptive surface-related multiple elimination. GEOPHYSICS 57: 1166-1177.

3. ARTICLE 2: SEISMIC STRATIGRAPHIC PATTERNS AND CHARACTERIZATION OF DEEPWATER RESERVOIRS OF THE MUNDAÚ SUB-BASIN, BRAZILIAN EQUATORIAL MARGIN

Authors: Karen M. Leopoldino Oliveira, Heather Bedle; R. Mariano G. Castelo Branco, Ana Clara B. de Souza, Francisco Nepomuceno Filho, Márcio N. Normando, Narelle M. de Almeida, Thiago H. da Silva Barbosa

Published on **Marine and Petroleum Geology**, June 2020.

Special Issue Continental margins unleashed: From early inception to continental breakup

https://doi.org/10.1016/j.marpetgeo.2020.104310

Reference:

Leopoldino Oliveira, K.M., Bedle, H., Branco, R.M.G.C., de Souza, A.C.B., Nepomuceno Filho, F., Nomando, M.N., Maia de de Almeida, N., da Silva Barbosa, T.H., 2020. Seismic stratigraphic patterns and characterization of deepwater reservoirs of the Mundaú sub-basin, Brazilian Equatorial Margin. Mar. Pet. Geol. https://doi.org/10.1016/j.marpetgeo.2020.104310.

SEISMIC STRATIGRAPHIC PATTERNS AND CHARACTERIZATION OF DEEPWATER RESERVOIRS OF THE MUNDAÚ SUB-BASIN, BRAZILIAN EQUATORIAL MARGIN

Karen M. Leopoldino Oliveira[1,2,3], Heather Bedle [3]; R. Mariano G. Castelo Branco[1,2], Ana Clara B. de Souza[1], Francisco Nepomuceno Filho[4], Márcio N. Nomando[1], Narelle M. de Almeida[5], Thiago H. da Silva Barbosa[6]

[1] Programa de Pós-Graduação em Geologia, Universidade Federal do Ceará (UFC), Campus do Pici, Bloco 912, Fortaleza, Ceará, CEP 60440-554, Brazil. Email: karenleopoldino@gmail.com, mariano@ufc.br, anaclarageologia@alu.ufc.br, mnormando@gmail.com

[2] Laboratório de Geofísica de Prospecção e Sensoriamento Remoto (LGPSR). Universidade Federal do Ceará (UFC), Campus do Pici, Bloco 1011, Fortaleza, Ceará, CEP 60440-760, Brazil.

[3] School of Geosciences, University of Oklahoma, 100 East Boyd St. Suite 710 Norman, OK 73019. Email: karenleopoldino@ou.edu, hbedle@ou.edu

[4] Departamento de Física, Universidade Federal do Ceará (UFC), Campus do Pici, Bloco 922, Fortaleza, Ceará, CEP 60440-554, Brasil. Email: nepomuceno@fisica.ufc.br

[5] Departamento de Geologia, Universidade Federal do Ceará (UFC), Campus do Pici, Bloco 912, Fortaleza, Ceará, CEP 60440-554, Brasil. Email: narelle@ufc.br

[6] Departamento de Engenharia do Petróleo, Universidade Federal do Ceará (UFC), Campus do Pici, Bloco 709, Fortaleza, Ceará, CEP 60440-554, Brasil. Email: thiagohenrique@alu.ufc.br

ABSTRACT

In recent years, the Brazilian Equatorial Margin has drawn attention due to its similarity to areas with new hydrocarbon discoveries in the African conjugated margin, and in French Guiana. However, studies on the tectonic regimes associated with transform margins and their evolution, structures, and petroleum potential are still lacking due to the geological complexity of this region. To address this knowledge gap, research has been done to better understand the geological structures, as well as to identify potential hydrocarbon accumulations in the

deepwater Ceará Basin. To achieve this, we performed an integrated interpretation of a large 2D seismic data, new exploratory borehole data, as well as older well data with revised biostratigraphy. This data analysis refines the basin architecture and the Cretaceous-Paleogene tectonic evolution, including implications for hydrocarbon prospectivity in the Ceará Basin deepwater. 2D seismic interpretation was performed using modern concepts of continental break-up. To accomplish this, the transition of continental-oceanic crust was taken into account for restoration of the sediments of the rift stage in the basin. The analysis also identifies potential hydrocarbon accumulations in turbiditic reservoirs and presents new insights about the dimensions of the underlying rift features situated in the continental slope. The results reveal a high potential for drift sequences in deepwater where the Late Albian-Early Cenomanian-Turonian sediments reach thicknesses of approximately 3048 to 4894 m. Moreover, this research shows evidence of Cretaceous to Paleogene magmatism, indicated by the well-imaged volcanoes and associated sills in the seismic data. This analysis indicates that the Mundaú sub-basin can be classified as a volcanic passive margin that was developed during the oblique dextral separation between South America and Africa. The variety of stratigraphic and structural features developed through the Cretaceous history of the Mundaú sub-basin offers a variety of potential hydrocarbon traps and plays in a number of rift and post-rift sequences.
Keywords: Brazilian Equatorial Margin, Ceará Basin, Petroleum Exploration, Deepwater Environments, Turbidites.

3.1. INTRODUCTION

The Brazilian Equatorial Margin (BEM) in northeastern South America and the eastern part of the Equatorial South Atlantic Ocean is composed by five sedimentary basins along the coast. There are, from west to east, the Foz do Amazonas, Pará-Maranhão, Barreirinhas, Ceará, and Potiguar basins (Fig. 3-1a). These basins began their development during the Early Cretaceous, as a series of several continental rift basins through a complex evolution with tectonic regime varying from predominantly normal (distension) to predominantly strike-slip (transtension and transpression) regime. The geological evolution of this margin is similar to the West African margin as Ghana, Ivory Coast and Liberia (Fig. 3-1a), being characterized a transform margin (Françolin & Szatmari, 1987; Matos, 1999, 2000; Milani & Thomaz Filho, 2000; Maia de Almeida et al., 2019).

In recent years, new hydrocarbon discoveries in the African conjugated margin, Brazilian margin and in French Guiana have drawn attention to the BEM. However, studies on

the tectonic regimes associated with transform margins and their evolution, structures, and petroleum potential are scarce, partially due to the geological complexity (Zalán et al., 1985; Zalán & Warme, 1985; Soares et al., 2012; Nemčok et al., 2012; Krueger, 2012; Krueger et al., 2014; Davison et al., 2016; Maia de Almeida et al., 2019). Such basins and their structures require an in-depth research on their genesis and geological significance, especially for oil industry applications.

The exploration potential of Equatorial margins is exemplified by the Jubilee field in Ghana, which produced approximately 10,000 bopd only five years after the discovery and currently are producing more than 100,000 bopd (Karagiannopoulos, [updated 2018]). Other fields, also in Ghana's deepwater, such as Tweneboa-Enyenra-Ntomme (TEN) are also already producing oil. On the other hand, a much-publicized discovery in French Guiana was also announced in 2012 (Zaeydius field), however, six evaluation wells have since been classified as dry or with uneconomic (Zalán, 2015). Nevertheless, these analogue discoveries suggest potential for another world-class Jubilee-like oil system in deep and ultra-deepwaters of the BEM.

Figure 3-1: (a) Regional topographic and bathymetric map of the Equatorial Atlantic showing conjugate margins in Brazil and Africa as well as the larger oceanic fractures zones in the area; (b) The Ceará basin is divided in four sub-basins: Piauí-Camocim, Acaraú, Icaraí and Mundaú. The Romanche Fracture Zone and positive gravity anomalies were mapped using data from the World Gravity Map (WGM2012). The topographic model is from the National Oceanic and Atmospheric Administration (NOAA). The structural data was compiled from Zalán & Warme (1985), Silva et al., (1999), and Morais Neto et al., (2003). The basin boundaries are from ANP and the sub-basins boundaries were adapted from Morais Neto et al., (2003).

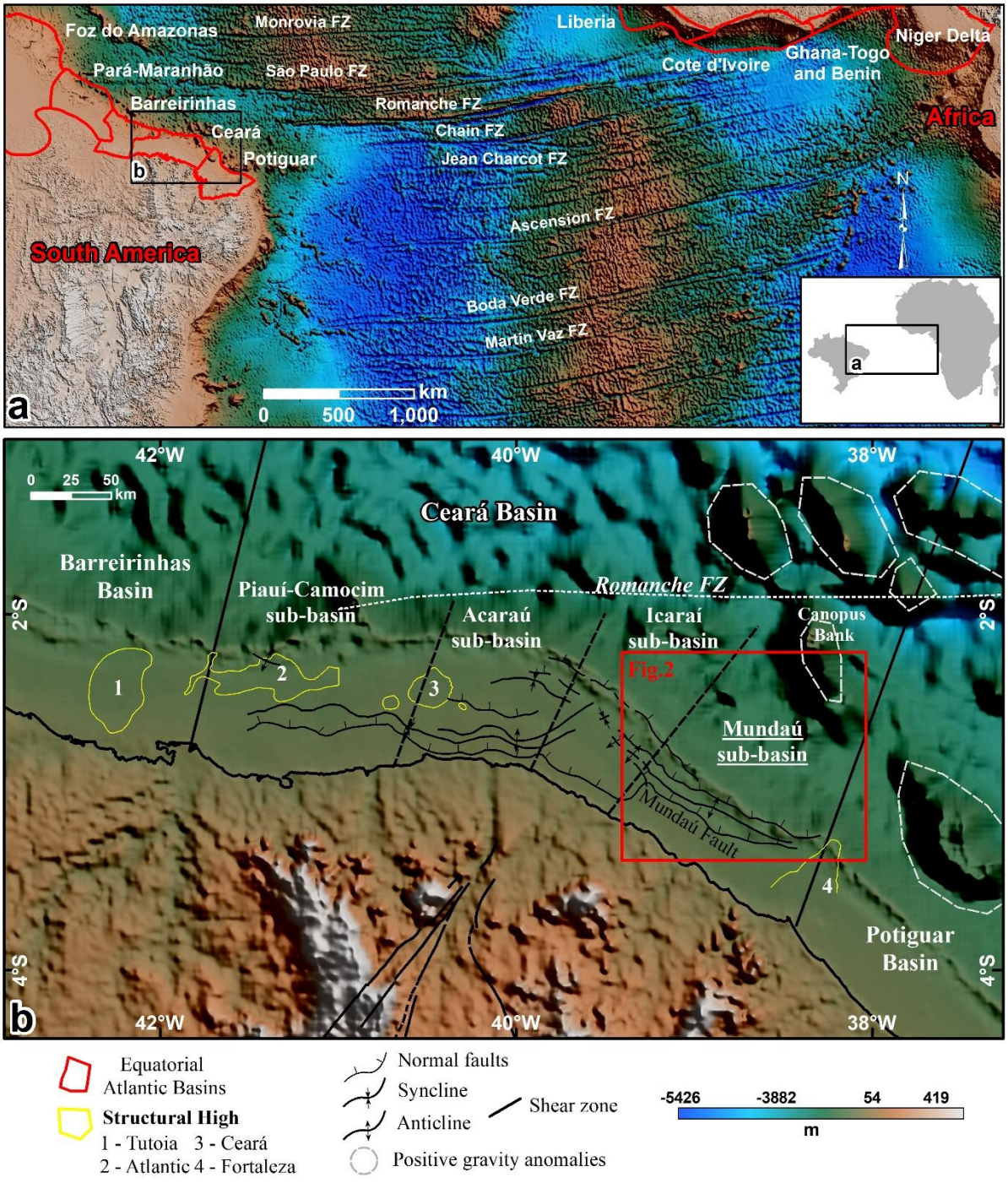

The 11th Round of Bids of the Brazilian National Agency of Oil, Natural Gas and Biofuels (ANP) in 2013 allowed dozens of blocks to be acquired by companies in all five basins of the BEM (Zalán, 2015). The ANP's most recent bidding round, the 15th in 2018, had 12 blocks offered in deep and ultra-deepwater in the Ceará Basin, totaling an area of approximately 8,500 km². According to ANP, BEM has potential for oil discovery in turbidite reservoirs from the late Cretaceous to the Paleogene, similar to the discoveries of the West African Margin. The increase in bidding in the last several years reveals the escalating interest in the hydrocarbon

potential of the BEM.

The Ceará Basin is a frontier hydrocarbon producing basin with four fields in the shallow water domains of the Mundaú sub-basin (Xaréu, Atum, Espada and Curimã) (Figs. 3-1b and 3-2). In 2012, Petrobras drilled the 1 BRSA 1080 CES well, the first deepwater oil discovery in Ceará Basin, then two additional exploratory wells were drilled with more complete chronostratigraphic data collection. Two wells had previously been drilled in the deepwater in the 1990s, but data from these have not been publically released, and thus are not correlated with the new wells.

Maia de Almeida et al., (2019) presented the petroleum system of the Mundaú sub-basin deepwater transitional sequence using the 1 BRSA 1080 CES well and seismic data. However, they did not discuss the potential reservoirs in the syn-rift and drift sequence. In this study, we improve the current geologic understanding of the basin, mapping the main geologic features using a large 2D seismic dataset, as well as identify regions of potential hydrocarbon accumulations in the deepwater Cretaceous-Paleogene sequences of Mundaú sub-basin. In addition, the seismic-stratigraphic interpretations are combined with new borehole data that includes detailed biostratigraphy data. This analysis results in a new understanding of the basin that can be used to identify possible plays and to refine the basin architecture and its tectonic evolution, including implications for hydrocarbon prospectivity in the Ceará Basin deepwater.

Figure 3-2: The location of the wells, seismic data (2D), and the blocks of ANP Bidding Rounds are displayed. Also, four producer fields (Xaréu, Atum, Curimã, and Espada) in the Mundaú sub-basin are outlined. The black polygon frame indicates the area presented in Figures 8, 9, 10 and 11.

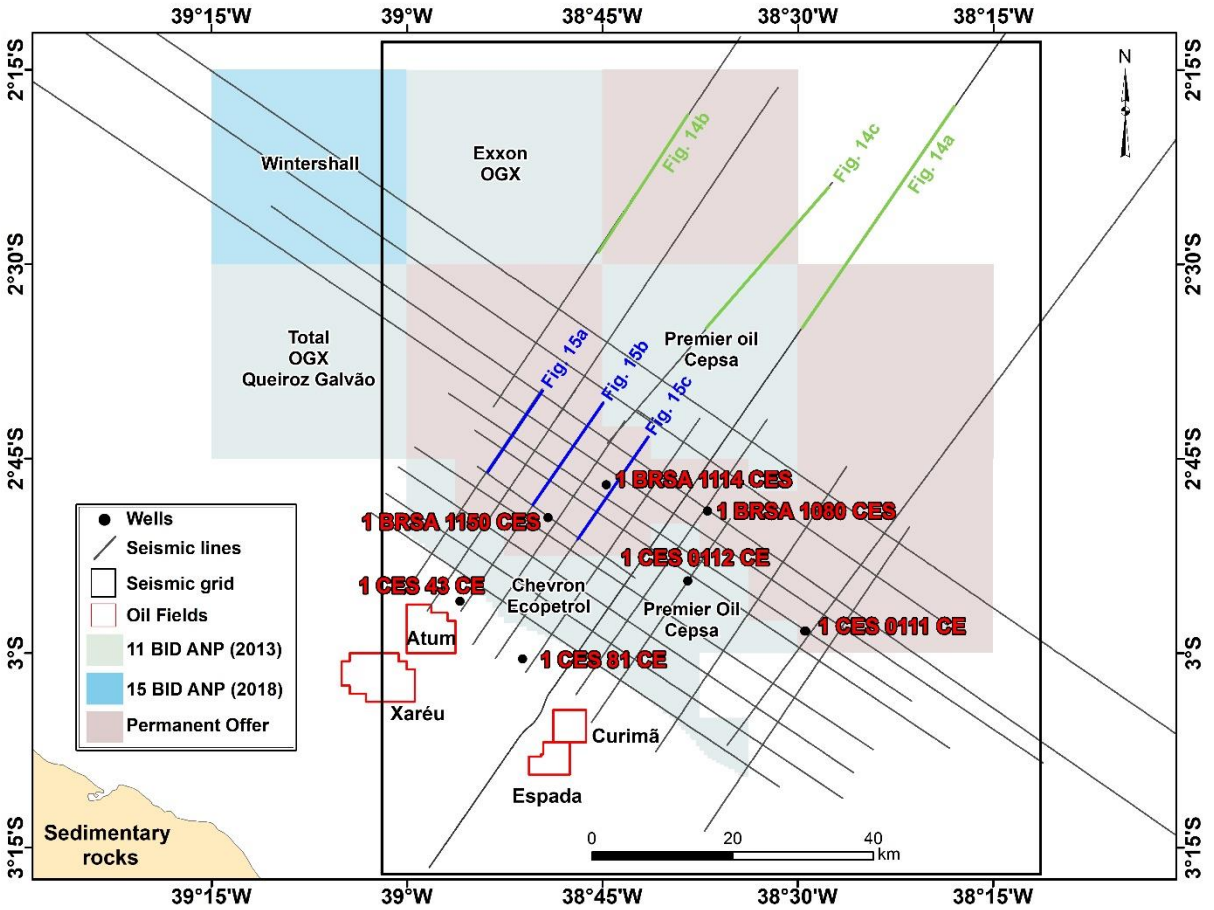

3.2 GEOLOGICAL SETTING

3.2.1. Ceará Basin

The Ceará Basin origin is related to the process of the Gondwana breakup during the Lower Cretaceous resulting in the Equatorial Atlantic opening. This basin is bounded to the east by the Fortaleza High, to the west by the Tutóia High, to the south by the Precambrian basement, and to the north by the Romanche Fracture Zone (RFZ) (Fig. 3-1b) (Costa et al., 1990). Due to the distinct tectono-stratigraphic character along and across the Margin, the Ceará Basin is divided into four sub-basins, from west to east: Piauí-Camocim, Acaraú, Icaraí and Mundaú (Morais Neto et al., 2003). The Piauí-Camocim is separated from the Acaraú sub-basin by the Ceará High. The Acaraú and Icaraí sub-basins have as common limit the Sobral-Pedro II lineament extension. In addition, the Icaraí is separated from Mundaú sub-basin by an important fault inflexion (Morais Neto et al., 2003).

Another defining characteristic of the basin are the intrusions and magmatic

extrusions, which sometimes generate guyots and bathymetric highs. Only a few volcanic rocks are dated from the shallow water (continental crust) offshore the Ceará and Potiguar basins, and they reveal ages spanning from 83 to 28 Ma (Santonian to Lower Oligocene; Mizusaki et al., 2002; McHone, 2006). However, there is no direct sampling and dating of any offshore seamount from the BEM, except for the Fernando de Noronha Archipelago (Jovane et al., 2016). Therefore, there is no clear assessment of the relationship between sedimentation and volcanic rocks in the seamounts, and the current age estimate for the latest volcanic emplacement ranges between the Coniacian and the Eocene, and thus has an uncertainty of more than 40 My (Jovane et al., 2016).

3.2.2. Mundaú sub-basin

The Mundaú sub-basin is regionally structured by a major fault, the Mundaú Fault, which has normal offset in the NW-SE direction and is NE-dipping (Antunes et al., 2008) (Fig. 2-1b). The tectono-sedimentary evolution of the Mundaú sub-basin consists of three major megasequences (Beltrami et al., 1994): syn-rift, transitional, and drift. The syn-rift phase is characterized by the development of NW-SE normal faults forming asymmetric half-grabens, and continental sedimentation marked by fluvial-deltaic sandstones and shales of the Mundaú Formation (Beltrami et al., 1994). The top of this unit is a regional stratigraphic reflector, called the “Electric Mark 100” (Costa et al., 1990) or “1000” (Beltrami et al., 1994; Condé et al., 2007) and is interpreted to be the result of a period of regional flooding that affected the basin during the lower Aptian (Pessoa Neto, 2004).

The transitional sequence, the Paracuru Formation (Fig. 2-3), is marked by the first marine incursions recorded in the sub-basin, within the fluvial, deltaic, and lacustrine sandstones. Limestones and subordinate evaporites (Trairi Member) were also deposited at this stage (~115 My) (Costa et al., 1990; Beltrami et al., 1994; Condé et al., 2007).

Figure 3-3: Ceará Basin litho-, chrono-, and tectonostratigraphic columns with the representation of the units recognized in the study area (modified from Conde et al., 2007). BS: Breakup sequence; UBA: Ubarana Fm.; GUA: Guamaré Fm.; TIB: Tibau Fm.

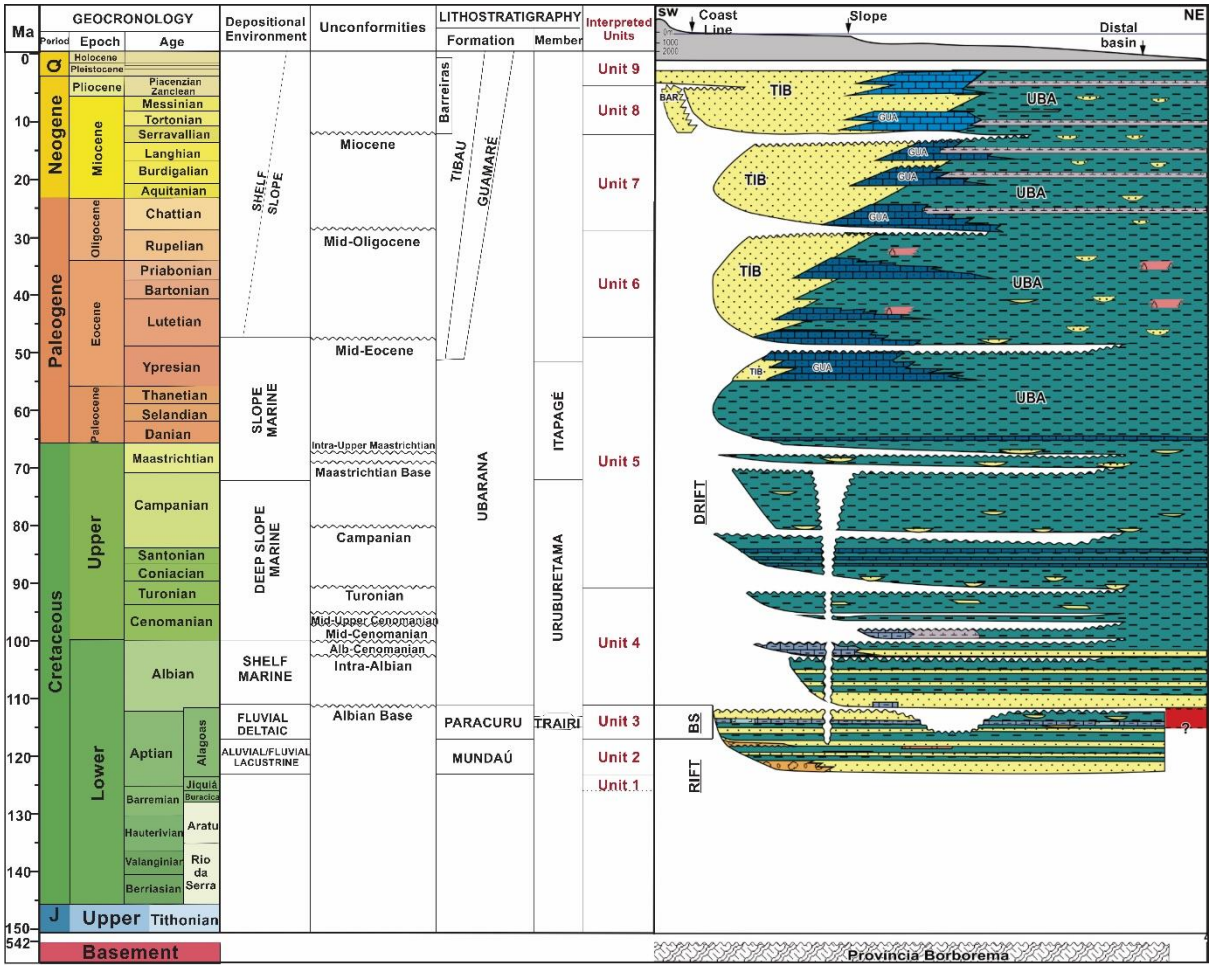

The drift or marine megasequence developed as a result of continental drift and a marked phase of thermal subsidence. The Ubarana Formation (from ~110 My to 65 My) comprises two members (Fig. 2-3) (Costa et al., 1990; Beltrami et al., 1994; Condé et al., 2007). The first one, the Uruburetama Member (~110 My to 75 My), corresponds to a marine transgression and consists of predominantly shales. The second member, Itapagé Member (from ~ 75 My to 65 My), corresponds to a regressive marine phase and consists of turbiditic shales and sandstones (Costa et al., 1990; Beltrami et al., 1994; Condé et al., 2007). The Guamaré Formation (from ~65 My to recent) consists of shelf carbonates, while the Tibau Formation (from ~65 My to recent) comprises proximal sandstones (Fig. 2-3). The clastic continental sediments of the Barreiras Formation comprise the youngest unit of the basin (Condé et al., 2007).

Magmatism in this basin occurred between the Mid-Eocene and Lower Oligocene. It was associated with a mafic event resulting in intrusive bodies of basalt and diabase, some of which were sampled in exploratory wells (Condé et al., 2007). Data from K-Ar and Rb-Sr dating (Mizusaki et al., 2002) indicate that the volcanic rocks vary in age from the Eocene (44 Ma, in the Ceará High area) to the Oligocene (32 Ma, in the Fortaleza High area). At north of Mundaú

sub-basin there is a seamount named the Canopus Bank, which is a north-northwest–trending intrusion, 80-km long, 40-km wide, covering an area approximately 2500 km². Its top reaches a depth of 150 m below sea level and is approximately 120 km² in area. Although seismic interpretation estimates the volcanic emplacement between 23 and 65 Ma, the hypothesis of seamount building because of multiple magmatic events is not disregarded (Maia de Almeida et al., 2019). Locally, near the Xaréu field (Fig. 3-2), a diabase sample provided a K-Ar age around 83 Ma, which may be related to the Cuó Magmatism - recorded in the Potiguar Basin and active in the Santonian-Turonian (Condé et al., 2007). Indeed, the geographical location and genetic determination of these rocks is essential for the geological study of the Ceará Basin, especially when it considers the influence of volcanic events in the generation, migration, and accumulation of hydrocarbons.

3.3. DATA

This study is based on a large seismic reflection dataset and well data (Fig. 3-4), all of which were acquired by Petrobras and supplied by the Brazilian National Agency of Oil, Gas and Biofuels (ANP). We interpreted more than 1,589 km of post-stack time-migrated multichannel 2D seismic reflection profiles located between the slope and the abyssal plain of the Mundaú sub-basin (Fig. 3-2). Additionally, two pre-stack seismic lines were processed to assist in the interpretation and for depth information. Seismic penetration to more than 9s TWT permitted the analysis of the entire seismic stratigraphic record of the abyssal plain down to the oceanic crust (Fig. 3-5). This data set covers an area of approximately 7,125 km², on a seismic grid of ~ 4 km spacing, which is sufficient enough to confidently tie the different seismic units mapped in this study.

The seismic sequence stratigraphic units were identified based on the newly available exploratory wells data 1 BRSA 1114 CES (2012), 1 BRSA 1150 CES (2013), 1 BRSA 1080 CES (2012), and older wells, including 1 CES 112 CE (1993), 1 CES 111 CE (1996), 1 CES 43 CE (1981) and 1 CES 81 CE (1983) which had revised biostratigraphy. These last two wells are located in shallow water. Well data includes standard log suites (i.e. gamma ray, density, resistivity, sonic, Vp, and Vs), checkshots, lithologic and geochemical data, formation tops, and biostratigraphic ages. Only three wells in deepwater have chronostratigraphic ages: 1 BRSA 1114 CES (2012), 1 CES 112 CE (1993), and 1 CES 111 CE (1996). This is the first deepwater study of the Ceará Basin where chronostratigraphic markers were used to refine the stratigraphic framework.

3.4. METHODS

Seismic interpretations of horizons and faults were carried out in the time domain (TWT). These horizons correspond to boundaries of sedimentary formations recognized in the wells and to major lithologic discontinuities. These seismic profiles were analyzed following a conventional 2D interpretation methodology by mapping key high-amplitude reflectors, and then the generation of surface-time, surface-depth, and isopach maps. Geological interpretation of the seismic units was based upon the interpretation of seismic parameters, such as amplitude, frequency, continuity, and external and internal geometries, as well as on the classical concepts of sequence stratigraphy (Vail et al., 1977). Initially, chronostratigraphic information from 1 BRSA 1114 CES, 1 CES 112 CE, and 1 CES 111 CE was plotted on the seismic lines. The well correlation used primarily the gamma ray and the sonic logs data (Segesman, 1980) (Fig. 3-4). Then, the most significant reflectors were mapped, in terms of continuity, amplitude, and tied to the well data, which provided chronological meaning, and aided in defining the seismic sequences.

A frequency enhancing algorithm was employed to aid interpretation at both low and high frequencies. This algorithm is similar to Amplitude Volume Technique Attribute (AVT) introduced by Bulhões & Amorim (2005). By introducing frequencies that enrich the recorded reflections, an attribute is created that emphasizes seismic stratigraphic packages and assists their correlation throughout the seismic section. The packets, or sequences, thus defined, bring together sets of reflections that have similar acoustic impedance characteristics (Figs. 3-5 to 3-7).

We constructed a number of time-thickness (isochron) maps (Figs. 3-8 and 3-9) in order to highlight the regional configuration of the main depocenters, their spatial and temporal migration, and their relationship with the deep crustal architecture of the basin. The isopach map is a key resource in understanding the stratigraphic thickness of the sediments, and it also represents thickness variations within each depositional unit (Bishop, 1960). Isopach maps are essential tools in the erosional and depositional sedimentary reconstruction as well as the recognition of turbiditic bodies.

Figure 3-4: (a) Correlation panel among the five deepwater wells showing interpreted seismic units, gamma ray, sonic logs, and calculated Vshale; (b) Four deepwater wells displaying the Paracuru Fm. interval of gamma ray and facies. The rocks of the Trairi Member are interbedded calcilutites and shales with high values of gamma ray. The 1 BRSA 1114 CES well data reveals that the Paracuru Formation in deepwater is composed of interbedded sandstones and shales in a subtle thickening pattern to the top; c) The five deepwater wells revealing the Unit 4 and 5 lithotypes. GR: Gamma Ray; Vsh: V shale; RS: Rift Sequence; BS: Breakup Sequence; DS:

Drift Sequences.

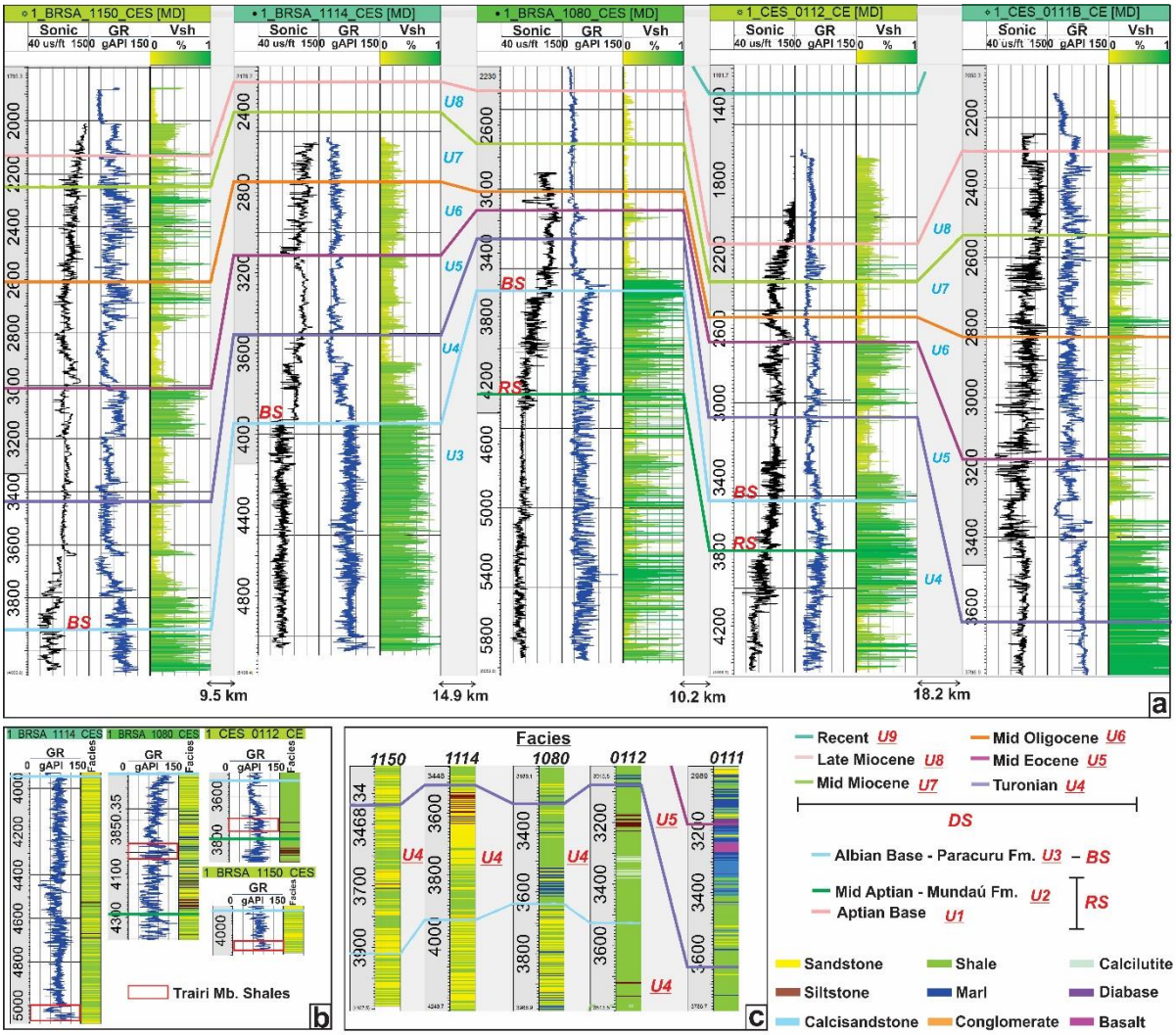

The major faults were picked and correlated from line to line. Next, the interval velocities of each seismic unit were obtained from check-shot data of the wells, so these interval velocities were finally corrected in order to fit the well tops. The defined velocity model was employed for a time to depth conversion. An average velocity obtained from the VSP of five deepwater wells was used. The average speed in the subsurface to the sedimentary package from this age was 2,668 m/s, while the average speed for water was 1,500 m/s. According to this data, it is inferred that the Late Albian-Early Cenomanian-Turonian depth is approximately 3048 to 4894m in the deepwater and ultra-deepwater. Geochemical data from five deepwater wells were obtained from lateral rock samples, and 399 samples were analyzed for Total Organic Carbon (TOC) and Rock-Eval pyrolysis analyses. In all, this corresponds to 200 samples in the Late Albian to Turonian interval. These measurements were conducted in shales, sandstones, marls, and conglomerates belonging to Ubarana Formation.

3.5. RESULTS

3.5.1. Seismic and structural interpretation

We here infer the tectono-sedimentary framework of the basin and its evolution based on seismic interpretation, structural and isochrons maps. These maps were organized from oldest to youngest, focusing on the stratigraphic patterns and thickness trend. Nine major horizons were interpreted on the seismic lines (Figs. 3-5, 3-6, 3-7 and 3-8), which were chosen based on lithologic and chronologic data obtained from the composite well logs, and using the main unconformities present in this basin as first interpreted by Condé et al. (2007). From those horizons, nine isochrons maps were generated and named as units from one to nine. (Figs. 3-3 and 3-9). The tenth horizon, the seabed, was also mapped and is the top of the most recent sedimentary interval.

Basement

In the basement structural map (Fig. 3-8a), the transition from continental crust to oceanic crust corresponds to a change from basement depths of less than 4000 ms on the continental shelf to depths of more than 6000 ms on the toe of slope over more than 20 km. Differing from the Barreirinhas Basin, the transitional zone between oceanic and continental crust in this basin is wide (more than 20 km) (Figs. 3-5, 3-8a and 3-10), as a result of being located between oceanic fracture zones. The basement was better identified at deepwater basin region, as the seismic lines tend to lose resolution in deeper parts at continental shelf. The basement is seismically characterized by chaotic internal reflectors at the continental shelf and contains seaward dipping reflector (SDR) in the continental slope and deepwater. This region is commonly cut by normal faults composed by horsts and grabens (Fig. 3-5a). On the continental shelf, the basement of the Ceará Basin is composed of Borborema Province rocks (Morais Neto et al., 2003). The basement of the ultra-deepwaters is composed of basaltic rocks of oceanic crust. Oceanic crust is characterized by transparent or chaotic seismic facies. In these facies, the presence of diffraction is noted in the upper part, and high-amplitude are observed in the lower portion near the Moho (Fig. 3-5c). Figure 3-8a displays a trend of the shallower basement to the southeast of the area, while the basement trends to the northwest at greater depths. The basement high in the south is related to the continental shelf. In the south, locally poor quality and less availability of seismic data increases uncertainty in the interpretation.

Figure 3-5: Seismic section showing the continental shelf, slope and deepwater segments in the study area. (a) On the continental shelf, the border fault controls the extensional faults, which form half-grabens and the basin depocenter; (b) The slope segment is characterized by SDRs and the four major landward-dipping faults mapped in this basin. A thick rift depocenter as well as anticline structures are interpreted. Synthetic and antithetic faults are interpreted in drift

sequence; (c) The deepwater segment is characterized by a thick drift sedimentary package, several high-amplitude reflectors, and high-angle and Cenomanian faults. The 1BRSA 1080 CES is shown in the up left. The Moho is interpreted on slope segment as a high-reflectivity zone around 9000 ms twt. Profile location (green line) is displayed on the right. Vertical scale in two-way traveltime (ms twt). The units mapped in this study are presented in yellow text.

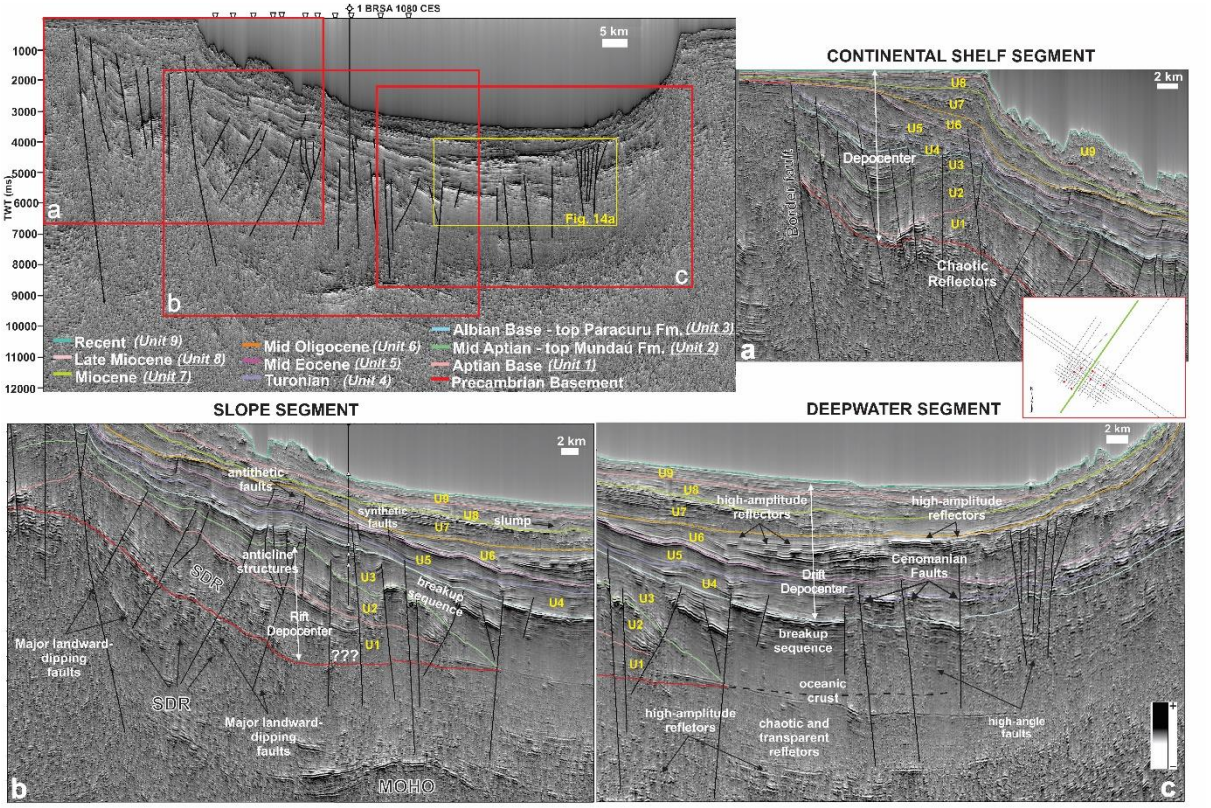

Unit 1 (Aptian base)

The Aptian base sequence U1 defined in this study underlays the basement and is below the Mid Aptian sequence that corresponds to top of Mundaú Formation (Figs. 3-5, 3-6, 3-7 and 3-8b). In shallow waters, beneath the top of Mundaú Formation, there are well-marked discontinuities in electric profiles, informally denoted as the 700 and 800 marks, which are consecrated by use for by over 30 years of exploration in the basin (Condé et al. 2007). Analyzing the seismic lines in deepwater (Figs. 3-5, 3-6, and 3-7), along with well data, there are some well-marked reflectors which allow a subdivision of the Mundaú Formation based on seismic facies. The top of this unit was defined as the Aptian base, based on previous research where the rocks have a high source rock potential (Brazilian Equatorial Margin Project Part 1 and 2 – Petrobras internal report). There is no information about rocks older than Aptian, however, Condé et al. (2007) suggested that there may be older deposits in the deepest portions of the basin, and they could be correlated to the Pendência Formation (Barremian age) of Potiguar Basin. The thicker package of this unit in seismic images (Fig. 3-5, 3-6 and 3-7)

corroborate that older rocks could be present.

This interval has seaward dipping reflectors in the slope with high-amplitude and continuous to sub-continuous, locally chaotic reflections with divergent patterns near faults (Fig. 3-6a), which are indicative of syn-tectonic deposition. In the deepwater, this formation has high-amplitude, concave downward reflectors, parallel, and continuous reflections (Figs. 3-5 and 3-6). It pinches-out approximately 40 km off of the continental shelf where the continental crust ends (Fig. 3-5), and its deposition had a thicker distribution to the east of the slope (Fig. 3-8b).

The faulted blocks often show parallel and high-amplitude reflectors to divergent and transparent reflector when approaching the faults indicating the presence of early syn-rift sediments infilling the grabens (Figs. 3-5 and 3-6). On the continental shelf, basinward-dipping faults form rotated blocks establishing a half-graben system. Convex, continuous to sub-continuous seismic reflections, sometimes presenting high-amplitudes, are observed inside the grabens. Normal faults affect the continental crust below the continental shelf. The continental slope displays this unit as filled horsts and grabens related to the complex evolution of this basin controlled by landward-dipping faults (Fig. 3-5, 3-6, 3-7, 3-8b and 3-9a). The greatest thickness (maximum of 1600 ms) of this sequence in relation to the basement is in the central region, following a trend NW-SE, while small values are on the continental shelf and in the north are due to contact with the continental crust boundary (Fig. 3-9a). The isochron map of this unit shows that most of the sedimentary package, up to 1300 ms (Fig. 3-9a), was accumulated on the continental slope, filled grabens.

Unit 2 (Mid Aptian)

The Mid-Aptian unit corresponds to the Mundaú Formation, which has another well log correlation and a strong reflection in seismic lines. The top of this unit is represented by the Mid-Aptian structural map (Fig. 3-8c). Two wells in deepwater reach the top of this unit. Similar to the previous unit described above, this interval also has seaward dipping reflectors. However, its seismic facies patterns are not homogeneous. Its upper part is predominantly marked by chaotic reflections, while strong and continuous reflections are marked in its lower part (Figs. 3-5, 3-6 and 3-7). The continental slope is composed of both highs and lows of this formation, having uniform sedimentary dispersion in the center and its greater depths lie at the north (Fig. 8c), where continental crust ends. This formation shows downlap over the early oceanic crust formed on the northern part of the basin (Fig. 5b). Figure 8k shows the extent of this surface in depth.

Figure 3-6:SW-NE dip seismic sections with stratigraphy uninterpreted and interpreted. The uninterpreted sections show the major antithetic faults and Mid-Eocene reflector. a) Interpreted section shows several anticline structures on the continental slope where it is related to the rift stage. Oligocene faults are shown in this section. Reflector SDRs were interpreted in the basement. The 1 BRSA 1080 well and its hydrocarbon evidence are labeled (black dots); b) Oligocene faults and SRD reflectors were also interpreted in this section; c) Interpreted section shows the interpreted horizons and Cenomanian reactivation faults. Note that seismic in C AVT attribute was not applied. The location is depicted in all the stratigraphic uninterpreted sections. Vertical scale in two-way traveltime (ms twt). The units mapped in this study are presented in yellow text.

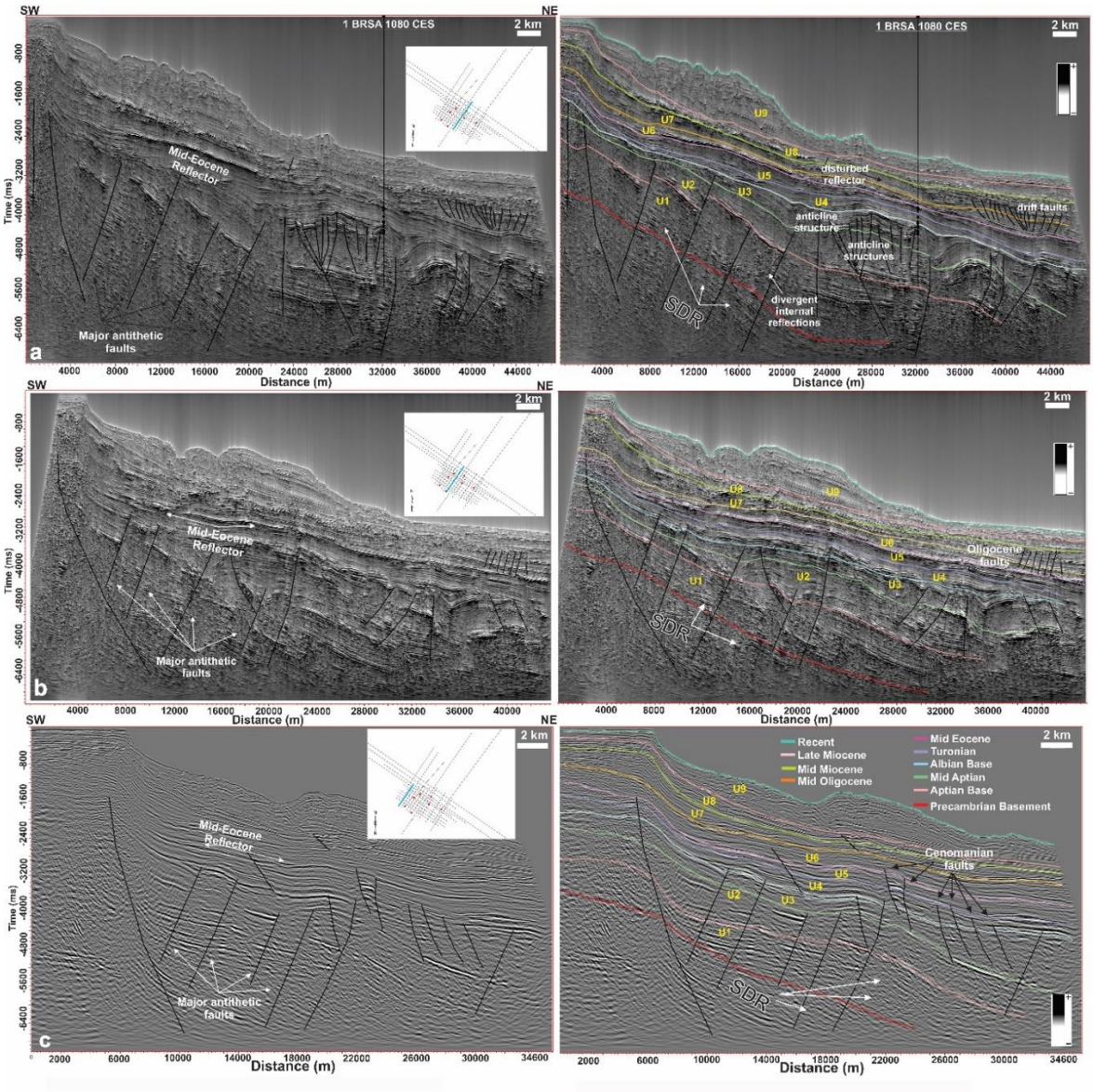

The top of the rift stage, on the continental shelf and in deepwater, is represented by this unit. Rift-related basement faults formed horsts and grabens within the area of the current continental shelf (Figs. 3-5a, and 3-9b). The syn-rift sequence (Unit 2) is very thick in the study area, with more than 1000 ms of sediments. The depocenter within the extent of the modern continental shelf reflects the adjustment between the border fault and the fault near the

slope (Fig. 3-5a). When compared with the previously described sequence, Unit 1, the syn-rift sequence has the greatest thickness (maximum of 1250 ms) in northeast of the area, while a slight thinning of this sequence is observed on the southeastern side of continental slope (Fig. 3-9b).

Unit 3 (Albian Base)

The base of this sequence is the Mid Aptian horizon (Fig. 3-8c) and the top of the sequence is the Albian Base horizon (Fig. 3-8d) that corresponds to the top of Paracuru Formation. This unit is considered a breakup sequence (Soares et al., 2012) as its deposition comprises an unconformity-bonded stratigraphic interval, which was controlled by the tectono-stratigraphic events triggered by the breakup. At this age, the oceanic crust began to form, and this sequence is overlying it, being the first sequence to be deposited on top of oceanic crust (Figs. 3-5 and 3-10). The breakup was finalized during the lower Albian in this segment of Equatorial Margin, where syn-wrench sedimentation took place (Brazilian Equatorial Margin Project Part 1 and 2 – Petrobras internal report). This unit has seismic facies that are parallel to sub-parallel, high amplitude and continuous reflectors. The sequence becomes thicker in the distal part of the basin, especially in the northwest. Unlike the previously described sequence that has a uniform sedimentation in the northeast of the area, this already has a more uniform distribution, even if subtle, to the northwest, making the area more regular in terms of deposition (Fig. 3-8d). The greatest thickness (maximum of 1600 ms) of this sequence in relation to Unit 2 is in the extreme north (Fig. 3-9c). The small values are on the continental slope mainly in southeast, highlighting one NW-SE trending, elongated feature in northeast (Fig. 3-9c). Figure 8l shows the coverage of the top horizon of this unit in depth. Some magmatic features interpreted as sills were imaged by high-amplitude reflections (Fig. 3-7a and 3-7b).

The entire Aptian-Albian interval, as well as underlying sequences, are cut by normal faults, suggesting active tectonic in these ages. The 1 BRSA 1080 CES well, where oil was discovered, was positioned where there is a high of Mundaú Formation formed by a fault and probably mobile shales (Fig. 3-6a). The isochron map between the top of Mundaú Formation and the top of Paracuru Formation (Unit 3) reveals that the sedimentary depositional preference to the northwest has greater thicknesses, while the continental slope has smaller thickness values, mainly in the east (Fig. 3-9c). Figure 3-9j displays the depth thickness of unit.

Unit 4 (Albian Base-Turonian)

This Unit marks the beginning of the drift sequence. Its base is composed of

conglomerates representing deposits of low sea system tract (Fig. 4c -1 BRSA 1150 CES and 1 BRSA 1114 CES wells), and seismically is composed of plane-parallel and high-amplitude seismic reflectors (Figs. 3-5 and 3-6). The top of this unit corresponds to a Turonian age horizon (~89 Ma) (Figs. 3-5 and 3-10) related to a maximum flooding surface and anoxic event that has a very characteristic high-amplitude seismic character and can be easily correlated throughout the Equatorial margin (Trodstorf et al. 2007). The 1 BRSA 1080 CES and 1 CES 0112 CE wells present a low sand supply during the deposition at the base of this sequence, while the shale input was high, representing predominantly shelf to deepwater environments (Fig. 3-4c). However, the 1 BRSA 1114 CES and 1 BRSA 1150 CES reveals a high sand supply in the whole sequence (Fig. 3-4c). The structural map presents increased depths in the northwest of study area, with regular sediment distribution on the continental slope (Fig. 3-8e).

Figure 3-7: NW-SE strike seismic sections with stratigraphy uninterpreted and interpreted and the location of the BRSA 1080 well is shown together with the location of hydrocarbon evidence (black dots); a) Interpreted section showing the presence of magmatic bodies as sills and vent. Mass transport and a paleocanyon is interpreted in the drift sequences. Red polygon indicates the area displayed in Figure 13a; b) Several sills and a magmatic body are shown in this section; c) Paleocanyons, canyons, and a basement high were interpreted in this section. The location is depicted in all the stratigraphic uninterpreted sections. Vertical scale in two-way traveltime (ms twt). The units mapped in this study are presented in yellow text.

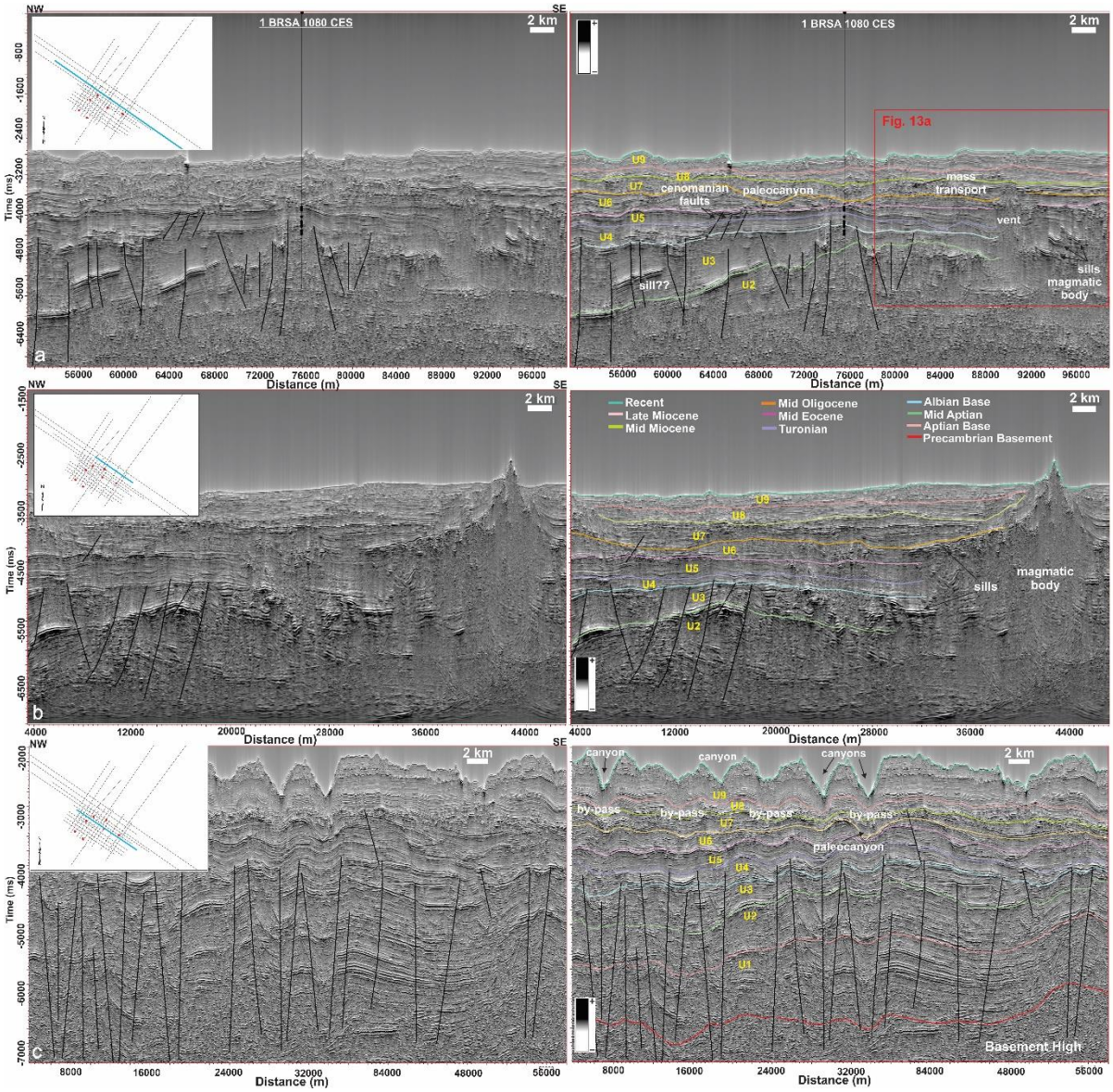

The Cenomanian faults have a similar orientation to the rift faults, which seem to be linked at depth (Figs. 3-5b and 3-5c). This suggests that the Cenomanian faults formed as a result of a phase of reactivation of the older and deeper rift structures. Given the evidence that rifting terminated in the late Aptian (Figs. 3-5 and 3-10), the extensional phase responsible for the formation of these late faults may have been triggered by processes of 'post-rift relaxation' (Morgan 1983; Burov & Cloetingh 1997; Burov & Poliakov 2003). The lack of known regional tectonic events in the margin during the Late Cretaceous makes it difficult to suggest alternative scenarios for the formation of the Cenomanian faults. The isopach map of this interval (Unit 4) shows smaller thickness when compared to the others due to the large number of erosive events that occurred in this period (four events in 10 Ma) (Condé et al., 2007) (Fig. 3-3). Beyond that, most of the sediments, up to 500 ms, were accumulated on the continental slope in a ponded depocenter (Figs. 3-9d and 3-11a). Thick sedimentary packages are observed in the deepwater

suggesting that the sediments also bypassed this area and continued further downslope (Fig. 3-11a). The thickness, when compared to the previous unit above described, is smaller. It reaches a greater depth to the northeast and northwest, with a thin feature among them following a trend NE-SW, probably associated with the Romanche Fracture Zone structures.

Figure 3-8: Structural maps from ten major horizons interpreted with seismic, and two structural maps migrated in time and depth. The location of five deepwater wells and the four major faults are shown. Parts (a) through (j) display time structure maps, parts (k) and (l) display depth structures. CS: continental shelf; OC: oceanic crust.

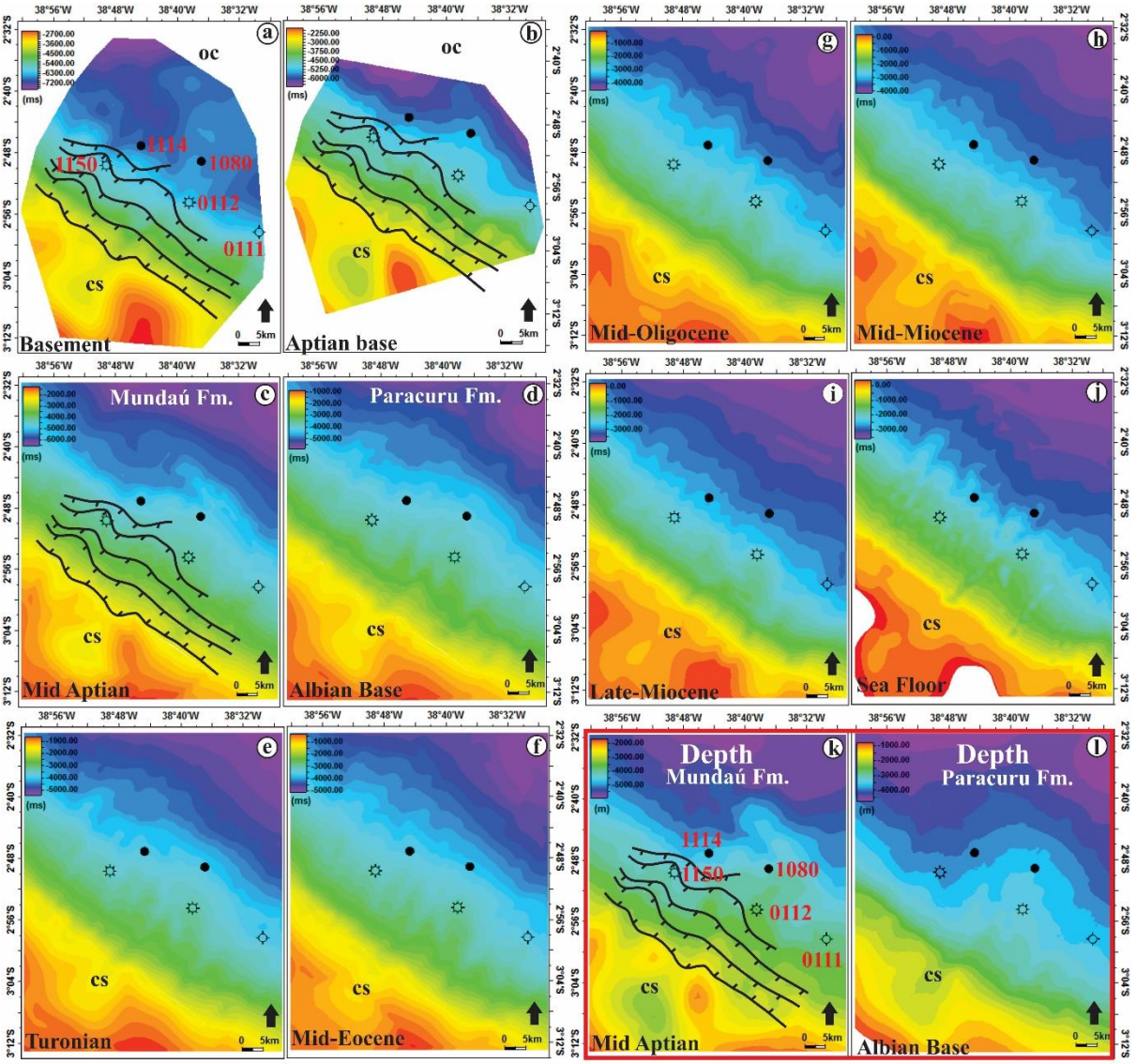

Unit 5 (Turonian-Mid Eocene)

The top of this is represented by Mid-Eocene unconformity horizon (Fig. 3-8f) that is very expressive in this basin, especially in distal areas. It is the seismic reflector most representative of drift phase, with a high acoustic impedance, in all of the deep and ultra-deepwater seismic lines (Fig. 3-6). In this sequence, during the Campanian (~78 Ma), the sea

level dropped, marking the change from mainly transgressive to regressive sequences (Trosdtorf et al., 2007). The Maastrichtian was a time of tectonic quiescence, and in this basin, sediments were deposited in a regressive sequence called the Itapagé member (Condé et al., 2007). This interval is composed of plane-parallel, sometimes continuous or chaotic seismic reflections (Figs. 3-5, 3-6 and 3-7). This interval has greater thicknesses on the continental shelf and to the northwest of the distal part of the sub-basin (Fig. 3-9e). It has a more uniform sedimentary distribution in the western portion of the study area. The 1 BRSA 1150 CES and the 1 CES 111 CE wells have greater thickness of this unit, while the 1 BRSA 1080 CES well has smaller thickness (170 ms) (Fig. 3-4a and 3-9e).

On the continental slope, this sequence is intersected by basinward-dipping faults (Fig. 3-6c). In the deepwater, this sequence is intersected by vertical faults related to the reactivation of the Romanche Fracture Zone and emplacement of magmatic bodies (Fig. 3-5c). The isochron map between the Turonian and Mid-Eocene (Unit 5) shows the depositional thickening infilling a Turonian ponded depocenters, which are wider (up to 10 km in the continental shelf) than the Late Albian mini-basins, represented on the Late-Albian to Turonian isochron (Fig. 3-9d). Comparing these isochron maps, some Late Albian mini-basins coalesced into larger basins during Turonian time, while others were buried. As previously described above, depositional thickening is observed in the northwest region, suggesting sediments also bypassed the area into the deepwater (Fig. 3-11b). The continental shelf has a better sedimentary distribution due to adjustment of the border fault and to the regressive event related to the Itapagé Member (Figs. 3-5 and 3-11b).

Figure 3-9: Isochron maps from eight units from the studied seismic lines, and one isochron map migrated in depth. These maps show sediment thickness distribution. The location of five deepwater wells and the four major faults are also shown in the figure for reference. Parts (a) through (i) display time structure maps, part (j) displays the depth structure. CS: continentalshelf; OC: oceanic crust.

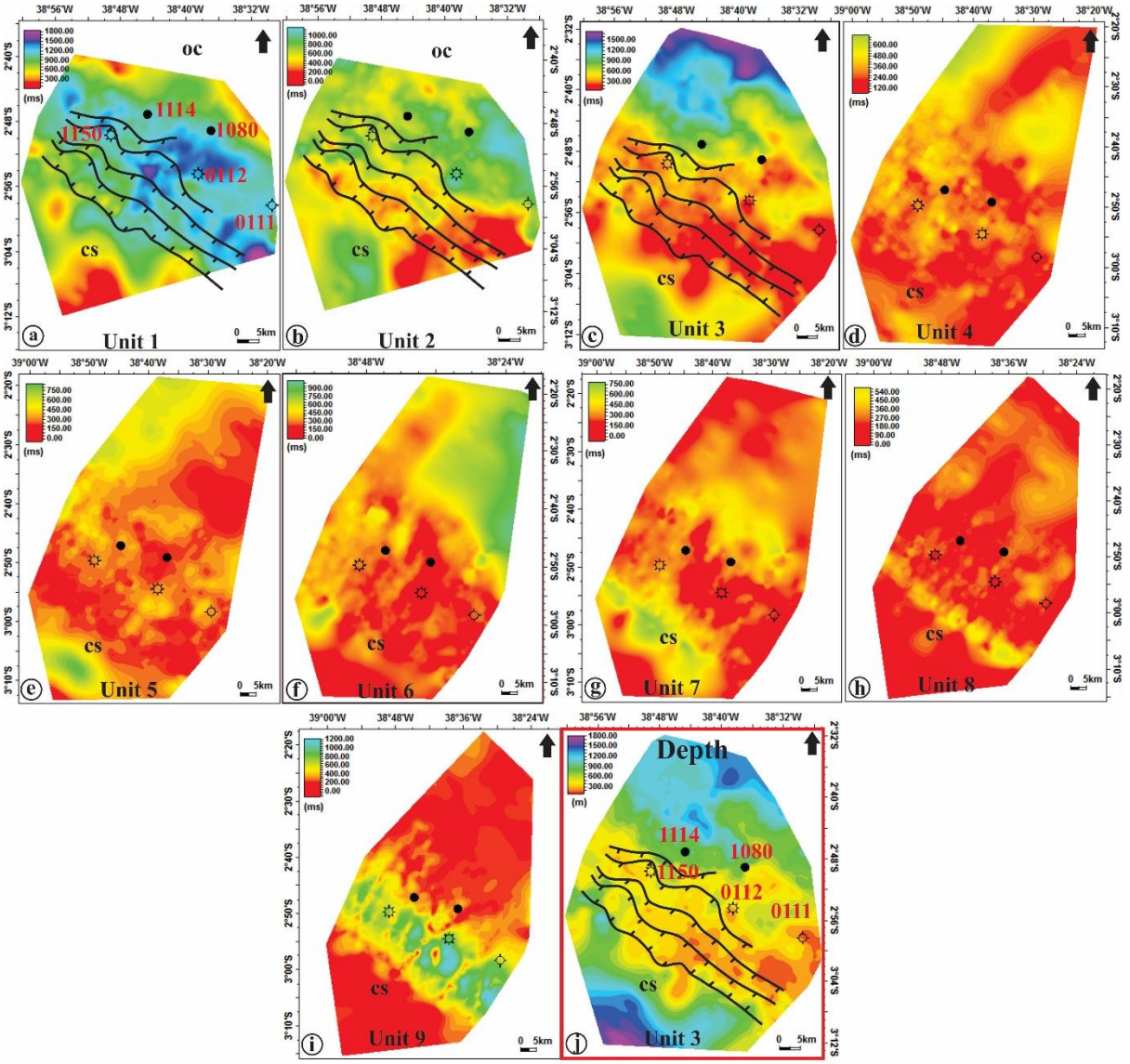

Unit 6 (Mid Eocene – Mid Oligocene)

The top of this unit is represented by a Mid Oligocene unconformity (Figs. 3-5, 3-6, 3-7 and 3-8g). The structural map reveals that this unit has greater depths in the north trending to NW-SE direction (Fig. 3-8g). Seismic facies are parallel to sub-parallel, often with a high-amplitude and continuous reflector. It has a strong seismic reflector and is well-marked on electrical profiles (Figs. 3-4 and 3-6). The top of this unit corresponds to the Rupelian-Chattian boundary unconformity (Trosdtorf et al., 2007). During the Oligocene, conditions changed from regressive in the Rupelian to transgressive in the Chattian, and formed the Oligocene unconformity (Haq et al., 1987). This interval is thicker on the northeast part of the distal sub-basin, and thinner in the continental shelf and the continental slope from the center to the east (Fig. 3-8g).

The isochron map (Fig. 3-9f) between the Mid-Eocene and the Mid Oligocene

unconformity (~27 Ma) horizons represent the thickness of Unit 6. On the continental shelf and on the continental slope most of sediments were eroded and deposited into deepwater environments, mainly in northeast of this basin (Fig. 3-11c). On the continental shelf there are three Mid-Eocene mini-basins and additional sedimentary deposition occurring to the west of the continental slope (Fig. 3-9f). At the toe of the continental slope, this sequence is intersected by oceanward-dipping faults that change their direction to landward-dipping faults (Fig. 3-6a).

Unit 7 (Mid Oligocene-Mid Miocene)

The top of this unit corresponds to a Mid-Miocene age horizon (Figs. 3-5, 3-6, 3-7, 3-8h, and 3-10) that is related to the top of a large transgressive event observed across the whole Brazilian Equatorial Margin, which gave origin to a large carbonate ramp (Trosdtorf et al., 2007). Seismic facies are uniform, parallel, and continuous reflectors. Common zones of internal disturbed reflections related to high sediments input have been recorded (Fig. 3-7a). In the continental slope there are transparent zones in seismic data associated with depositional changes and is characterized by the presence of disturbed discontinuous seismic reflection (Fig. 3-6a). The structural map presents a uniform sedimentary deposition in the study area, with depths ranging from 500 ms in the continental slope to 4300 ms in distal part (Fig. 3-8h). The greatest thickness (maximum of 700 ms) of this unit in relation to Unit 6 is in the upper and lower slope, which trends to the NW-EW, while the small values are on the middle slope and the northwestern distal region (Fig. 3-9g).

This was a time of erosion on the continental slope and deposition as its toe, as gullies and channels are observed on the slope (Fig. 3-11d). The isochron map for this sequence (Fig. 3-9g) shows that in the continental shelf three Mid-Eocene depocenters became wider, and the continental slope was partially eroded, and sediments were deposited in its toe (Fig. 3-11d).

Unit 8 (Mid Miocene to Late Miocene)

The structural map of Figure 3-8i presents the top of this unit, Late Miocene age, as an irregular relief in the continental slope. The relatively continuous reflectors with different impedance contrast indicate the existence of lithological intercalation between sands and clays (Fig. 3-4a – Vshale). The greater thickness of this unit is in the upper continental slope, while the slope was eroded at this time forming by-pass zones to sediments supplies in deepwater (Figs. 3-7c and 3-11e). Like Unit 7, the structural map presents a uniform sedimentary deposition with depths ranging from 400 ms in the continental shelf to 3500 in distal part (Fig.

3-8i).

The isochron map between these horizons (Unit 8) represents the sedimentary deposition during these ages (Fig. 3-9h). The top of the continental slope has the greatest thickness.

Figure 3-10: (A) SW-NE schematic geological section showing the architecture of the segments and stratigraphic interpretation. Note the thick package of rift sequences in the continental slope segment, and the thick package of drift in the deepwater segment. The projected location of the BRSA 1080 well, the oil discovery, is marked. (B) The isochron map of the syn-rift sequences. (C) The thickness map of the Transitional sequence (breakup sequence). (C) The thickness map of the drift sequences. COB: Continental-oceanic boundary; CS: continental shelf; OC: oceanic crust; TWT: two-way traveltime.

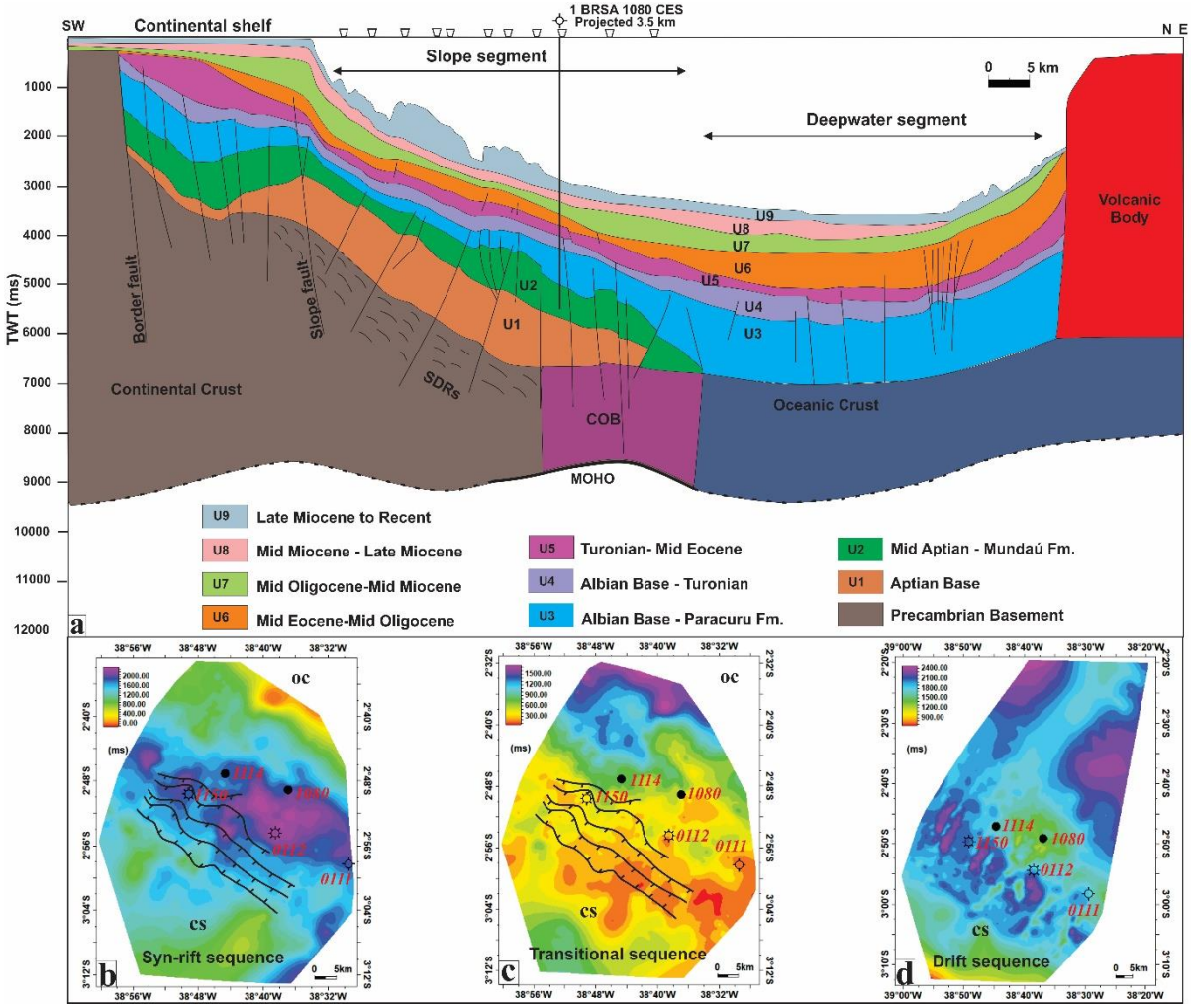

Unit 9 (Late Miocene to Recent)

Currently, the sea floor is a highly eroded surface cut by canyons (Fig. 3-7c) with unconsolidated sediments. The greater depths of this unit are in the northeast (Fig. 3-8j). The greatest thickness (maximum of 1200 ms) of this unit in relation to Unit 8 is in the continental slope (Fig. 3-9i) revealing an increase in the sediment supply in the Ceará Basin. This

deposition dynamic was also observed by Krueger (2012) in the Barreirinhas Basin, which had a deformation episode at this age that coincides to paleogeographic changes in the north of South America.

The Late Miocene to recent isochron map (Fig. 3-9i) represents the sedimentary accumulation in Unit 9. Sediments are thicker in the eastern region of the continental slope (Fig. 3-11f). The Late Miocene progradation that took place on the Brazilian Equatorial margin is not only related with the global cooling, but also to the adjustment of the drainage system due to due to an Andean tectonic event (Altamira-Areyan, 2009).

The toe of the continental slope has been eroded in the Upper Miocene age and continues to be eroded allowing sediments to be deposited in the abyssal plain, mainly in the NW and NE domains of this basin (Fig. 3-11f).

3.5.2. Well Data

The sedimentary package of the rift stage reveals a significant thickness, sampled in the 1 BRSA 1080 CES well, of approximately 1600 m, which reached the greatest depth of the Mid Aptian Mundaú Formation (Fig. 3-4a). The base of the rift stage has not yet been reached by any of the deepwater wells in this basin to date.

Analyzing the data from the five wells drilled in the deepwater of the Ceará Basin, four of these reached the Late Aptian Paracuru Formation; however, only two sampled the entire depth of the interval: the 1 CES 112 CE and the 1 BRSA 1080 CES (Fig. 3-4a). In both, the total thickness was approximately 302 m and 647 m respectively, with the latter having 86 m more than the total thickness reported for this formation by Beltrami et al. (1994). Also, the 1 BRSA 1114 CES well crosses more than 1170 m of the Paracuru Formation without reaching its base (Fig. 3-4a). Out of these, more than 1000 m overlies the Trairi Member (81 m), which means that the upper interval of the Paracuru Formation in this well is thicker than 1000 m (Fig. 3-4b).

The stratigraphic chart of this basin shows 5 My as the duration of sedimentary deposition established for the Paracuru Formation (Condé et al., 2007) (Fig. 3-3). An estimation of sedimentation and depositional age can be made, as the entire formation has three different lithologic units which occurred in 5 My. This reveals that the 1000 m of the upper interval in the 1 BRSA 1114 CES well would have been deposited within approximately 1.7 My, with a sedimentation rate of 588 m/Myr. This value is high for the depositional patterns sag-like basins, as interpreted by the depositional environment of the Paracuru Formation (Beltami et al., 1994, Morais Neto et al., 2003). This analysis corroborates the Conde et al. (2007) assumption that

the sediments deposited in this formation were influenced by active tectonism. This also is shown in the seismic interpretation of this work, and in that of Maia de Almeida et al. (2019).

Well data reveals that the Paracuru Formation in deepwater is composed of interbedded sandstones and shales in a subtle thickening pattern to the top (Fig. 3-4b – 1 BRSA 1114 CES well). Also, the 1 BRSA 1114 CES well reveal that there was a progressive infill of the basin no matter what the depositional environment of that formation was. The rocks of the Trairi Member as sampled by four wells are interbedded calcilutites and shales, and these shales present high values of gamma ray (Fig. 3-4b). Condé et al. (2007) described this formation in shallow waters as a rich organic matter shales, proving this range has hydrocarbon potential. Maia de Almeida et al. (2019) used geochemical data from 1 BRSA 1080 CES and described the rocks of Paracuru Formation to have good generation potential based on the good to very good amount of organic matter present.

Siliciclastic reservoirs in the rift and transitional sequences, having similar shallow water fields as their analogue basins, were targeted in four wells. In one case (1 CES 0111 CE), the well did not reach the target section; in two cases (1 CES 0112 CE and 1 BRSA 1114 CES), the siliciclastic reservoirs of the Paracuru Formation were of low quality. In the most successful case (1 BRSA 1080 CES), oil was found in sandstones of this same formation, well test results were promising and reliable, but the quantity is not yet commercially viable (Maia de Almeida et al., 2019).

On the other hand, the oil found in Ubarana Formation is 40°API and gas oil ratio 136m³/m³ as sampled in the 1 BRSA 1114 CES well. In the only case of hydrocarbon presence, the 1 BRSA 1050 CES well, which targeted deepwater turbidites of the Ubarana Formation, no commercial reservoir was found. However, between 3.617 and 3.624 it had hydrocarbon evidence. These wells present a metric interbedded sandstones and shales (Fig. 3-4c).

The 1 CES 111 CE well was drilled in the eastern region of the area on a basement high (Fig. 3-7c) and volcanic bodies were reported in the cutting samples description. Hydrocarbons were not found, and this well was considered dry. The analysis of drill cuttings indicated that argillites were deposited in deepwater and that they do not characterize typical deposits generated by gravitational flows. They also do not present favorable characteristics for the formation of good reservoirs. However, it should be emphasized that the analysis of electric well data shows that this section is composed of interbedded sandstones and argillites. Apparently, only the argillite sections with more cohesive portions were sampled. Twelve samples were analyzed with the foraminifera method, in order to obtain paleoenvironmental indications. From 2361.60 and 2366.60 m the samples indicate a domination of planktonic

forms. These are sometimes well preserved or oxidized in the middle-lower batial environment. From 2485-2494m, the data suggests a dominance of oxidized planktonic forms, with the presence of agglutinating forms of Cyclammina sp. These, although scarce, are also indicative of sedimentation in deeper water environments in the Mid-Miocene age.

Figure 3-12a illustrates the values of TOC percentage of rocks from Aptian to Turonian age. Analyzing the last interval, from Early Cenomanian and Cenomanian-Turonian, twenty-six samples presented TOC between 1.0 and 1.5%, with fair potential as source rocks; fifty-seven presented TOC between 1.0 and 2.0%, with a good potential as source rock; eighteen samples presented TOC between 2.0 and 4.0% indicating a very good source rocks; seven samples presented TOC values from 4.0 to up 6% indicating excellent source rocks.

A total of 106 samples from four wells was used for Maximum Temperature (Tmax) analysis (Fig. 3-12b). Of these, eighty-five samples have Tmax between 400 and 430ºC and are considered immature according to Tissot & Welte (1984), while 21 samples have Tmax values between 430 and 445 ºC and are considered to be within the mature zone. Thus, according to well data, the depth of Early Cenomanian and Cenomanian-Turonian source rocks at deepwater of Mundaú-sub basin occurs approximately between 3,400 and 3,900 m below sea water bottom. At this depth and deeper, there is the additional possibility of oil and gas generation.

On a graph of Hydrogen Index (HI) versus Maximum Temperature (Tmax), seven samples plot within the oil window zone (Fig. 3-12c). Considering the Hydrogen Index (mgHC/gTOC) versus Oxygen Index (mgCO2/gTOC) of the samples from Albian to Turonian obtained from the recent three wells, it was verified that they have mainly Type II and some samples are Type III organic matter (Fig. 3-12d). According to Tissot & Welte (1984), Type II organic matter, which is derived from autochthonous marine organic matter deposited in a reducing environment, is favorable to oil and gas generation; while Type III organic matter, which is originated from terrestrial plants, is favorable to gas generation at great depths. Well data analyses support that the drift sequence, characterized by the Ubarana Formation, has a high potential to be a source rock (geochemical graphs) as well as a good reservoir (Fig. 3-4c-facies).

Figure 3-11: Interpreted depositional environments in the drift units and location of the five deepwater wells used in this study. The drift deposition in slope segment reveals an active dynamic of erosion with canyons and gullies developed during its evolution. CS: continental shelf.

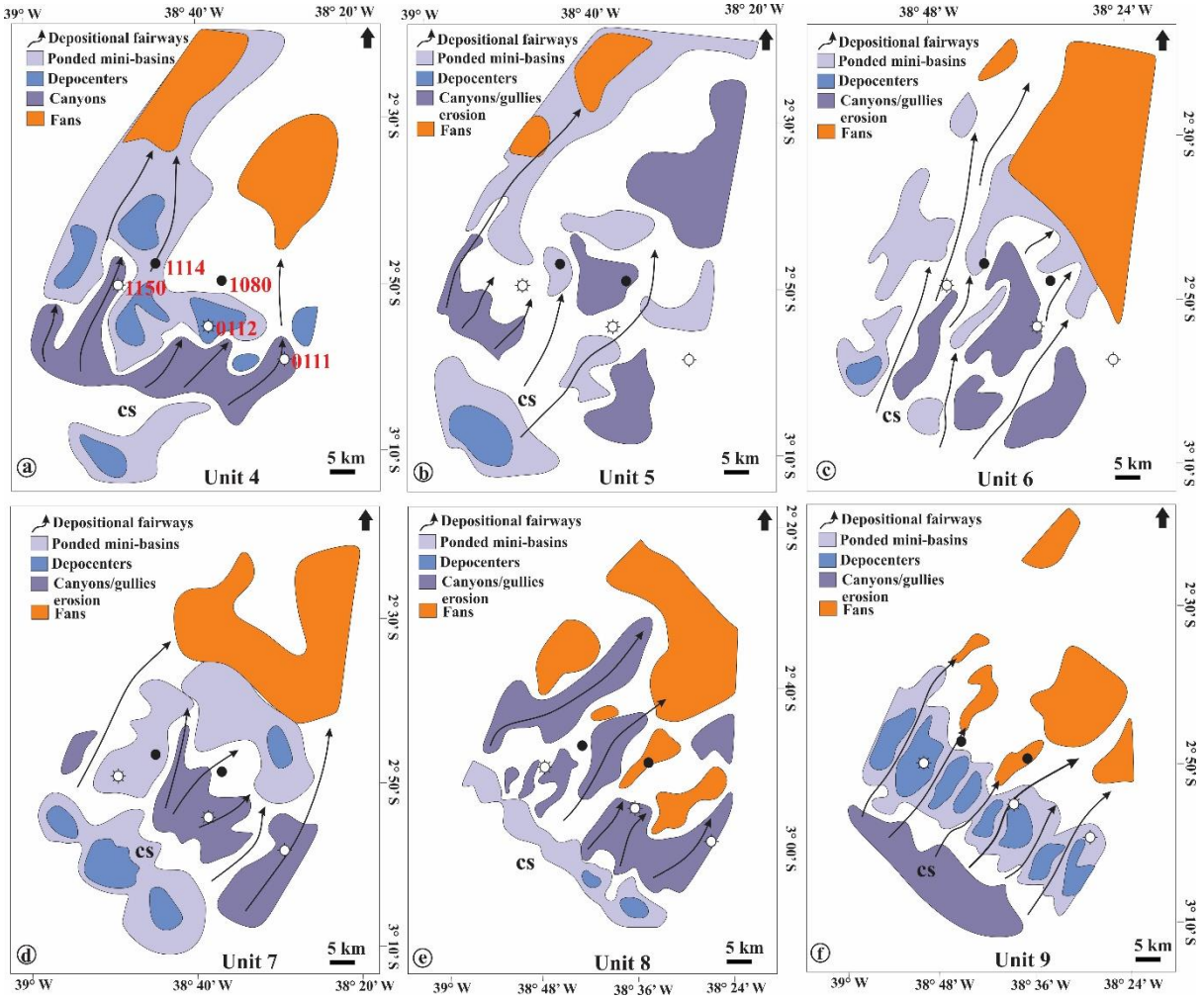

Magmatism

Sill complexes and hydrothermal vents are imaged by numerous high-amplitude reflections primarily within the Cretaceous successions (Figs. 3-7a, 3-13 and 3-14). Hydrothermal vents are characterized by diffuse and irregular seismic features that were identified below the top of the Oligocene unconformity (Fig. 3-7a). Sills were mapped inside the breakup sequence and in the Unit 6 (Figs. 3-13 and 3-14). In the ultra-deepwater, the Unit 6 is almost completely offset by vertical faults related to the reactivation of the Romanche Fracture Zone and emplacement of magmatic bodies (Figs. 3-5c and 3-14a). Most of the magma appears to be intrusive, with the exception of the magmatic body imaged in the Figure (3-7b) and the Canopus Bank (Figs. 3-2, 3-5 and 3-10).

3.6. DISCUSSION

3.6.1. Basin architecture

Continental shelf segment

The continental shelf segment forms a significant depocenter up to 22 km wide (Fig. 3-10). This segment is underlain by Precambrian basement, which was cut by NW–SE-trending, planar, high-angle extensional fault systems bounding a series of horst and graben structures infilled by wedge-shaped syn-rift sediments growth strata (units 1 and 2). The thickness reaches up 1200 ms in the central part of the graben (Figs. 3-5a, 3-10a and 3-10b), but accommodation space is related to the main phase of rifting in the Aptian age. Oceanward-dipping faults are predominant features and the deposition of syn-rift stage was controlled by the border fault that which appears in most of the equatorial margin basins and is well marked by potential field data (Silva Filho et al., 2007). Extensional reactivation of the major faults, and deposition of the breakup sequence (Figs. 3-5a and 3-10c), occurred during the earlier Albian and reaches up 800 ms into the central part of the depocenter. Following the end of the rift phase in the upper Aptian, the basin was infilled with a thick (~1700 ms) post-rift sediment sequence during Late Cretaceous–Late Miocene thermal subsidence. All the units described in this work are present in this shelf segment. In addition, the reservoir potential of the rift, breakup and drift sequences within the shelf segment is exemplified by the Curimã, Espada, Xaréu, and Atum fields that are producing in shallow waters.

The greatest thicknesses of drift sediment sequence correspond to Unit 5 on the mini-basin (~800 ms) (Figs. 3-9e and 3-11b) and Unit 7 age within three mini-basins (~700 ms) (Figs. 3-9g and 3-11d). The period between these two units correspond to Unit 6 (Mid-Eocene to Mid-Oligocene), whose top is related to a major regional unconformity, the “Oligocene unconformity”, identified in the Brazilian Equatorial Margin (Conde et al., 2007; Trosdtorf et al., 2007) throughout the west African margin (*e.g.* (Massala et al., 1992; Séranne et al., 1992; McGinnis et al., 1993; Meyers et al., 1996; Rasmussen, 1996; Mauduit et al., 1997; Nzé Abeigne, 1997; Karner & Driscoll, 1999; Mougamba, 1999; Séranne & Nzé Abeigne, 1999; Cramez & Jackson, 2000; Lavier et al., 2000), and Eastern Margins of Brazil (Rosseti et al., 2013).

Figure 3-12:(a) Plot of total organic carbon (TOC) versus depth showing the source rock generation potential; (b) Tmax versus Depth displaying the maturity of organic matters; (c) Hydrogen Index versus Tmax showing the maturity and the kerogen type; (d) Modified Van Krevelen diagram presenting the primary composition.

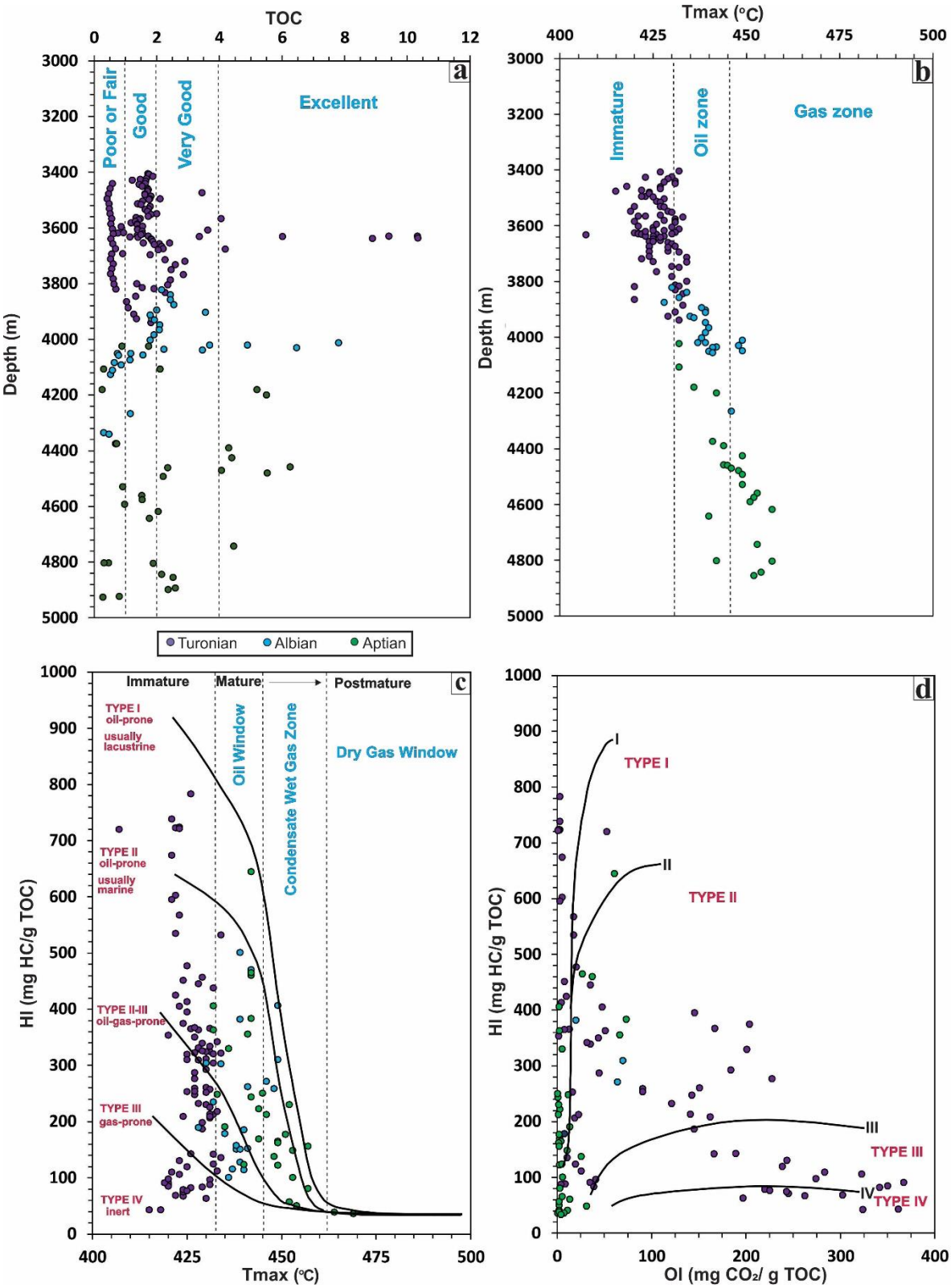

Slope segment

Landward-dipping faults are a predominant feature in this part of the basin and are in contrast to non-volcanic margins, in which the oceanward-dipping faults are a major tectonic feature (Abreu, 1998). These landward-dipping faults affected the outer edge of the continental

crust. The slope developed structures of horsts and grabens formed under the control of extensional landward-dipping faults, contrast with the orientation of the ones within the continental shelf. The structural maps of the Basement, Aptian base and Mid Aptian horizons document the presence of a well-developed, NW–SE-trending extensional fault system. Four majors NW-SE faults were mapped in the seismic data set (Figs. 3-5, 3-6, 3-7). This segment has well-developed rifted strata and depression strata with depocenter thickness over 2640 ms (Figs. 3-5b, 3-10a and 3-10b). Mello et al. (1994) presented that in the Equatorial Atlantic the most important deepwater petroleum source rocks are associated with deeply buried syn-rift sediments. Seismic facies of units 1 and 2 reveal wedge/lens strong reflection configurations indicating syn-rift deposition. The main depocenters of Unit 1 are up to 2000 ms thick, are located along the syn-rift hanging wall faults. The assumption of older rocks from Barremian or Jurassic ages is not disregarded due to the fact of the great thickness of these unit and the presence of the sedimentary column from these ages in the conjugated margin (Elvsborg and Dalode, 1985; Brownfield and Charpentier, 2006). The Mundaú Fm. presents anticline structures caused by high dip faults and flower structures (Fig. 3-5b). The deposition of syn-rift sequence ends in the toe of the slope segment when the proto-oceanic crust begins to form (Figs. 3-5b and 3-10a).

The breakup sequence (Unit 3) has a greater thickness in relation to the syn-rift sequences as the continental crust is transforming to oceanic crust (Fig. 3-10b) (Soares et al., 2012). In comparison with syn-rift deposition, the drift deposition (Units 4 to 9) has a less representative thickness demonstrating the basin dynamics of erosion and deposition during its development (Fig. 3-10d). Seismic data reveals a contrast of the structural styles of the intervals deposited above and below the Paracuru Formation (Figs. 3-5, 3-6 and 3-7). The structural framework of basement and syn-rift sequences is characterized by the presence of large antithetic normal faults, which were formed during the rift stage of the Brazilian equatorial margin and persisted until end of Albian (Pellegrini & Ribeiro, 2018). The structural framework of drift sequences is characterized by synthetic and antithetic small faults, from upper Cenomanian to later Eocene ages, which occur mainly in the slope (Fig. 3-5b). This same type of fault also occurs in the Barreirinhas Basin (Pellegrini & Ribeiro, 2018).

Figure 3-13:Figure 13: Seismic lines with stratigraphy uninterpreted and interpreted detailed section showing magmatic bodies. a) NW-SE strike section interpreted showing sills, vents and magmatic bodies; b) SW-NE dip section showing several high-amplitude reflectors associated with sills and a massive magmatic body. Red polygon indicates the area in Figure 14b; c) SW-NE dip section showing sills, vents, a mini-volcano, and a large magmatic body. Red polygon

indicates the area in Figure 14c. All the magmatic features with the exception of the vents are presented in this area until the late Eocene.

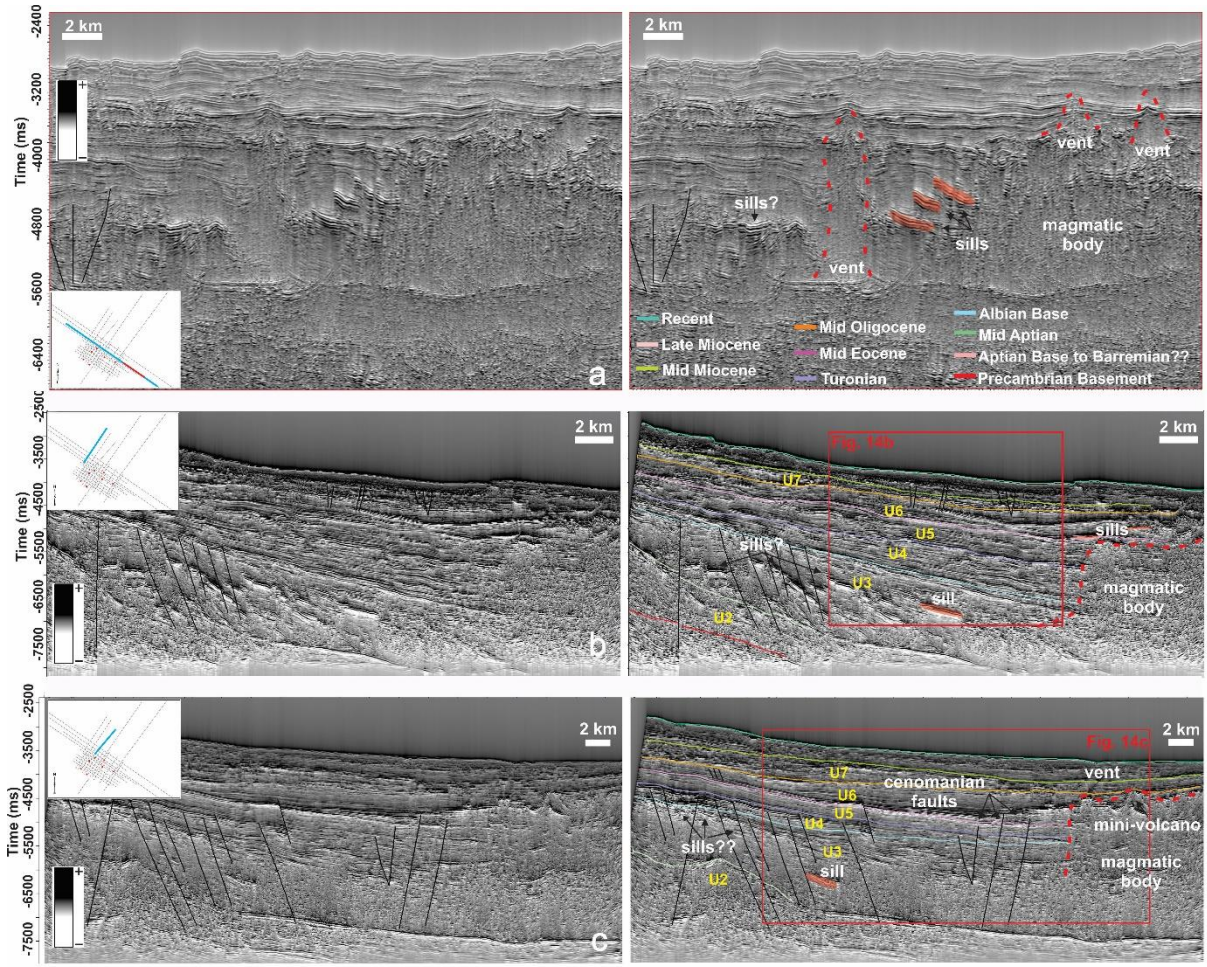

Deepwater segment and magmatism

High-angle faults and flower structures are a predominant feature in this part of the basin as well as bodies related to magmatism: sills and vents (Figs. 3-5c and 3-14a). These faults probably developed and deformed the sediments of the drift stage by reactivation of breakup faults, as its approaches the Romanche Fracture Zone (Fig. 3-1b). The transitional sequence has a thicker sedimentary distribution in this region and the drift sedimentary infilling has, in general, parallel to sub-parallel seismic reflection patterns. The detailed interpretation of the sedimentary fill reveals a considerable depocenter of drift sequences (2300 ms thick) (Figs. 3-5c, 3-10a, and 3-10d). A thicker sedimentary overburden is the ideal site for the maturation of the Late Albian to Turonian source rocks present at the base of the drift sequences. Inside this depocenter, a few bright spots associated to updip pinch-out are clearly visible (Fig. 3-14a). Such depositional geometries are typical of turbidite bodies saturated with hydrocarbons; some are trapped in mixed stratigraphic-structural traps by possible sills bodies.

These plays are very similar to the basin's African counterpart, with exception of the turbidites mixed by sills bodies that consists in an atypical play. All of them, point to hydrocarbon potential in the Mundaú sub-basin.

Sill complexes and hydrothermal vents imaged by seismic lines in the distal Mundau sub-basin are similar in style and position to the sills observed in the Cretaceous–Paleogene sediments of the others volcanic margins basins (e.g. Skogseid & Eldholm 1989; Skogseid et al. 1992, Larsen & Marcussen 1992). It is no possible to decipher the exact age of the magmatism in the deepwater because there are no geochronological data over these features. Only a few magmatic rocks were recovered in the 1 CES 111 CE well into Unit 5 (Fig. 3-4c), however, this well does not reached the breakup and rift sequences. Based on the seismic-stratigraphic interpretation, we suggest that this magmatism most probably related to a syn-rift phase (pre-break-up) event, and a reactivation event until Early Oligocene. In the eastern part of the BEM, within the Potiguar Basin, magmatic events are interpreted to have occurred during the syn-rift phase (Fonseca et al. 2019).

We propose that the architecture of this basin is best classified as a volcanic margin. Volcanic rifted margins and continental flood basalts are among the Largest Igneous Provinces (LIP) on Earth (Abreu, 1998). Examples of conjugate volcanic rifted margins in the South Atlantic Ocean are Pelotas (Brazil) and Walvis (Namibia) basins. Zálan (2015) classified the Mundaú sub-basin and Potiguar basin as transitional passive margins and the onshore rift of Potiguar Basin as volcanic passive margin. However, strong evidence points out that this margin can be considered volcanic: (1) the presence of basement and rifts filled by seaward dipping reflectors; (2) the COB is placed where the SDRs abut against the tabular body of oceanic crust, and (3) absence of exhumed mantle between the continental crust and oceanic crust. In addition, Hollanda et al. (2018) recognized a Cretaceous LIP in South America, known as the Equatorial Atlantic Magmatic Province (EQUAMP), owing to the fact that magmatic products of the Sardinha Formation and Rio Ceará-Mirim Group were found over an area of about 700,000 km² in the neighboring basins. In addition, Leopoldino Oliveira et al. (2018) show evidence of volcanic bodies (dykes) near coastlines in the Potiguar Basin imaged by potential field methods.

3.6.2. Implications for the petroleum potential

Magmatism

Senger et al. (2017) explained about the effects of igneous intrusions on the petroleum system. Magmatic activity has, mostly through improved source rock maturation and compartmentalization, performed a key role in the petroleum systems of many basins including

the onshore-offshore Taranaki Basin in New Zealand (Stagpoole & Funnell, 2001), the Faroe-Shetland and Rockall Trough Basins in the North Atlantic (Rohrman, 2007; Schofield et al., 2015), the Møre-Vøring basins offshore mid-Norway (Aarnes et al., 2015), the Sverdrup Basin of Arctic Canada (Jones et al., 2007), the Siberian Tunguska Basin (Svensen et al., 2009) and the Brazilian basins such as the Parnaiba basin (Miranda et al., 2016). The potential regional impact of igneous intrusions on hydrocarbon migration has been well documented in Western Australia (Holford et al., 2013) and the Brazilian basins (Thomaz Filho et al., 2008).In fact, igneous intrusions may both create new migration pathways if they are fractured and permeable, or they can act as fluid flow barriers if they are mineralized and impermeable. Also, igneous intrusions may form hydrocarbon traps directly and indirectly. Similarly, to sealing faults, impermeable intrusions such as dykes, sills, and vents cross-cutting stratigraphy, may generate numerous traps for migrating hydrocarbons (Senger et al., 2017). Besides, most igneous intrusions that are not fractured and altered are impermeable and hence may act as a good sealing rocks (e.g., Wu et al., 2006). In addition, non-altered intrusions may behave as a lateral and top seal for hydrocarbon accumulations (Thomaz Filho et al., 2008).

The deepwater of Mundau sub-basin presents igneous intrusions from Cretaceous to Paleogene strata. This differs from the shallow water region where magmatism occurred between the Mid-Eocene and Lower Oligocene, but with local samples of Santonian-Turonian age (Mizusaki et al., 2002; Conde et al., 2007). Maia de Almeida et al., (2019) also observed a magmatic intrusion inside the breakup sequence in the deepwater domain (Unit 3). Due to large presence of igneous features in the deepwater segment of the Mundaú sub-basin, an atypical petroleum system can exist there. For hydrocarbon generation, magma intrusions are responsible for the increase in temperature in the system and consequent maturation of the organic matter. As seen in Figure 3-12a the drift stage, Turonian age samples, has immature sequences with a good and excellent TOC potential. Regarding the oil migration, if those intrusions are fractured and have permeability, they will act as a migration route, if they are impermeable, they will form a structural trap preventing the passage of fluids. Figure 3-14a presents turbiditic bodies from Oligocene age with a clear proximity of sills that may act as seals. Furthermore, the mapping of this igneous activity is important also to E&P activities since they can represent drilling risks.

Rift-drift structural trap opportunity

The presence of a well-developed rift architecture in the deepwater Ceará Basin (Figs. 3-5, 3-6 and 3-7) provides further opportunities for structural trapping in the basin and

expectations of post-rift stratigraphic traps, as in the African counterpart (MacGregor et al. 2003; Dailly et al. 2013; Scarselli et al., 2018). In Ghana, the hydrocarbons would have accumulated mostly in structural traps afforded by the widespread rotated fault blocks associated with the rifted basins and half-graben (Antobreh et al., 2009). Maia de Almeida et al. (2019) compared the petroleum system in shallow water and deepwater of Mundau sub-basin and suggested that an importance source interval can exist in the initial syn-rift sequence. Thus, the numerous interconnecting Cenomanian faults would have the potential to allow charging of deepwater post-rift reservoirs from rift sources. (Fig. 3-5, 3-6 and 3-7). Early drift stage reservoirs have been found to be of good quality based on well data from the continental shelf of the Ceará Basin (Conde et al., 2007) and Côte d'Ivoire margin (MacGregor et al. 2003). Additional post-rift hydrocarbon charge may come from Cenomanian source rocks on the equatorial margin (Morrison et al. 2000; MacGregor et al. 2003; Dailly et al. 2013). Recent exploration efforts have documented the presence of high-quality Upper Cretaceous turbidite reservoirs in the inner slope offshore Ghana (Jubilee field) and Côte d'Ivoire (Paon discovery; Dailly et al. 2013; Coole et al. 2015; Martin et al. 2015). Detailed seismic analysis and drilling have indicated that these reservoirs extend into the deepwater of the Ivorian Tano Basin (Martin et al. 2015).

Turbidite Play

According to Maia de Almeida et al., (2019), based only in the 1 BRSA 1080 CES well, the source rocks of Ubarana Formation was considered immature, although its excellent TOC values. The authors also described that gas was found in this formation in reservoirs with hyaline sandstones intercalated to greenish dark to light shales, and it was migrated from transitional source rocks along faults. As described in the well data results, oil was found in Ubarana Formation in the 1 BRSA 1114 CES and 1 BRSA 1150 CES wells with 40 °API, however no commercial quantity. Also, the interval between Albian base to Turonian age has a good percentage of sandstones and shales as demonstrated by Vsh and facies log (Fig. 3-4a and 3-4c), and from rock samples in these wells.

According to Veeken (2007), the configuration and nature of basin infill are affected by factors such as tectonic subsidence, input of sediment supply, morphology of the substratum, eustatic sea level changes, base-level profile, and climatic conditions. In the deepwater of the Mundaú sub-basin, based on seismic interpretation, the drift deposits were mainly influenced by sediment input from the continental shelf and slope instabilities (e.g. canyons and slumps in Figs.3-7 and 3-11) and volcanic emplacement represented by sills, mini-volcano, and

hydrothermal vents (Figs. 3-7, 3-13, and 3-14). The deepwater Ubarana Formation from Albian to Turonian age consists primarily of turbidites and has potential as a hydrocarbon play (as shown in Figures 3-14 and 3-15). In this region, the main control on the distribution of turbiditic sands is the post-rift seabed geomorphology that were occasionally affected by sills intrusion (Figs 3-7, 3-11, 3-13, and 3-14). These features could develop highs that would form structures against which sands would onlap and pinch out, creating the potential for accumulation of reservoirs and opportunity for stratigraphic traps to develop (Fig. 3-14a). These turbidites are extensive and are commonly associated with mass transport deposits, which is also seen in the east Brazilian margin (e.g. Fiduck et al., 2004; Mohriak, 2005; Gamboa et al., 2010). The interpreted turbiditic sandstones have reflectors with high acoustic impedance contrasts, low frequency, lens external geometry, and variable lateral extension, ranging from 5 to 8 km (Figs. 3-14 and 3-15).

Figure 3-14:SW-NE dip seismic lines with stratigraphy uninterpreted and interpreted detailed section showing turbiditic bodies in deepwater. a) Interpreted section showing several bright spots and turbidites of the Late Albian to Turonian possibly saturated with hydrocarbons. These turbidites were interpreted with updip pinch-out and some of them are associated with magmatic bodies. Also, mass-transport are clearly associated with these turbidites. Turbidites from the Late Eocene were also interpreted with updip pinch-out and associated with magmatic bodies (red forms); b) Interpreted section showing several high-amplitude reflectors with patterns probably associated with turbidites of the Late Albian to Turonian; c) Interpreted section showing turbidites of the Late Albian to Turonian. Faults connecting rift, transitional, and drift sequences were interpreted near these turbiditic bodies. This indicates a possible play where the migration occurs directly from rift and transitional source rocks to drift turbiditic reservoir. The seismic section B and C are also shown in a larger view in Figure 13.

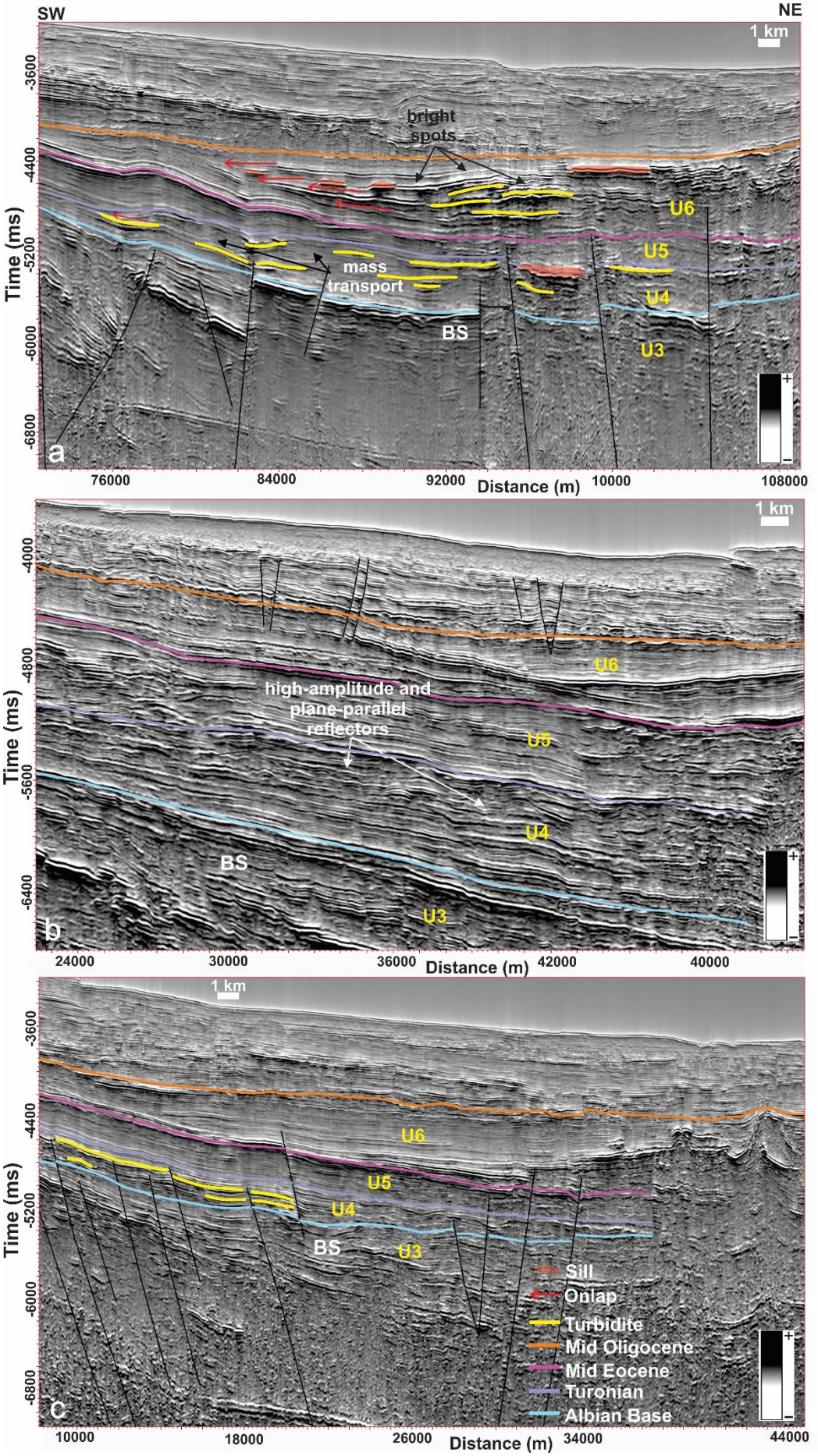
SW
NE
1 km
bright spots
mass transport
BS
U6
U5
U4
U3
Time (ms)
-3600
-4400
-5200
-6000
-6800
76000
84000
92000
10000
108000
Distance (m)
a
1 km
high-amplitude and plane-parallel reflectors
BS
U6
U5
U4
U3
Time (ms)
-4000
-4800
-5600
-6400
24000
30000
36000
42000
40000
Distance (m)
b
1 km
BS
U6
U5
U4
U3
Sill
Onlap
Turbidite
Mid Oligocene
Mid Eocene
Turonian
Albian Base
Time (ms)
-3600
-4400
-5200
-6000
-6800
10000
18000
26000
34000
44000
Distance (m)
c

There are two possible source rocks for this play: the marine shales of the Aptian Paracuru Formation, and the marine shales of the Late Albian-Early Cenomanian Ubarana Formation. In the first case, the hydrocarbons generated by shales of Paracuru Formation migrated through Cenomanian faults and unconformity traps. In the second case, the hydrocarbons generated by marine shales of the Ubarana Formation migrate directly from source rock to reservoir. The seal rocks are the shales of the Ubarana Formation itself, and stratigraphic traps were created by as depositional pinch-out and structure formed by volcanic bodies.

Figure 3-15: SW-NE oriented seismic lines with stratigraphy uninterpreted and interpreted detailed section showing turbiditic bodies in deepwater. a) Interpreted section showing turbidites of the Late Albian to Turonian age. Faults connecting rift, transitional, and drift sequences were interpreted near these turbiditic bodies. This indicates a possible play where the migration occurs directly from the rift and transitional source rocks to drift turbiditic reservoir; b) Interpreted section showing turbidites of the Late Albian to Turonian where updip pinch-out was interpreted. These reflector patterns show interbedding of turbidite and shales; c) Interpreted section displaying turbidites of the Late Albian to Turonian with updip pinch-out. Faults connecting rift, transitional, and drift sequences were interpreted near these turbiditic bodies. This indicating a possible play where the migration occurs directly from the rift and transitional source rocks to drift turbiditic reservoir. The 1 BRSA 1114 well and its hydrocarbon evidence are labeled (black dots).

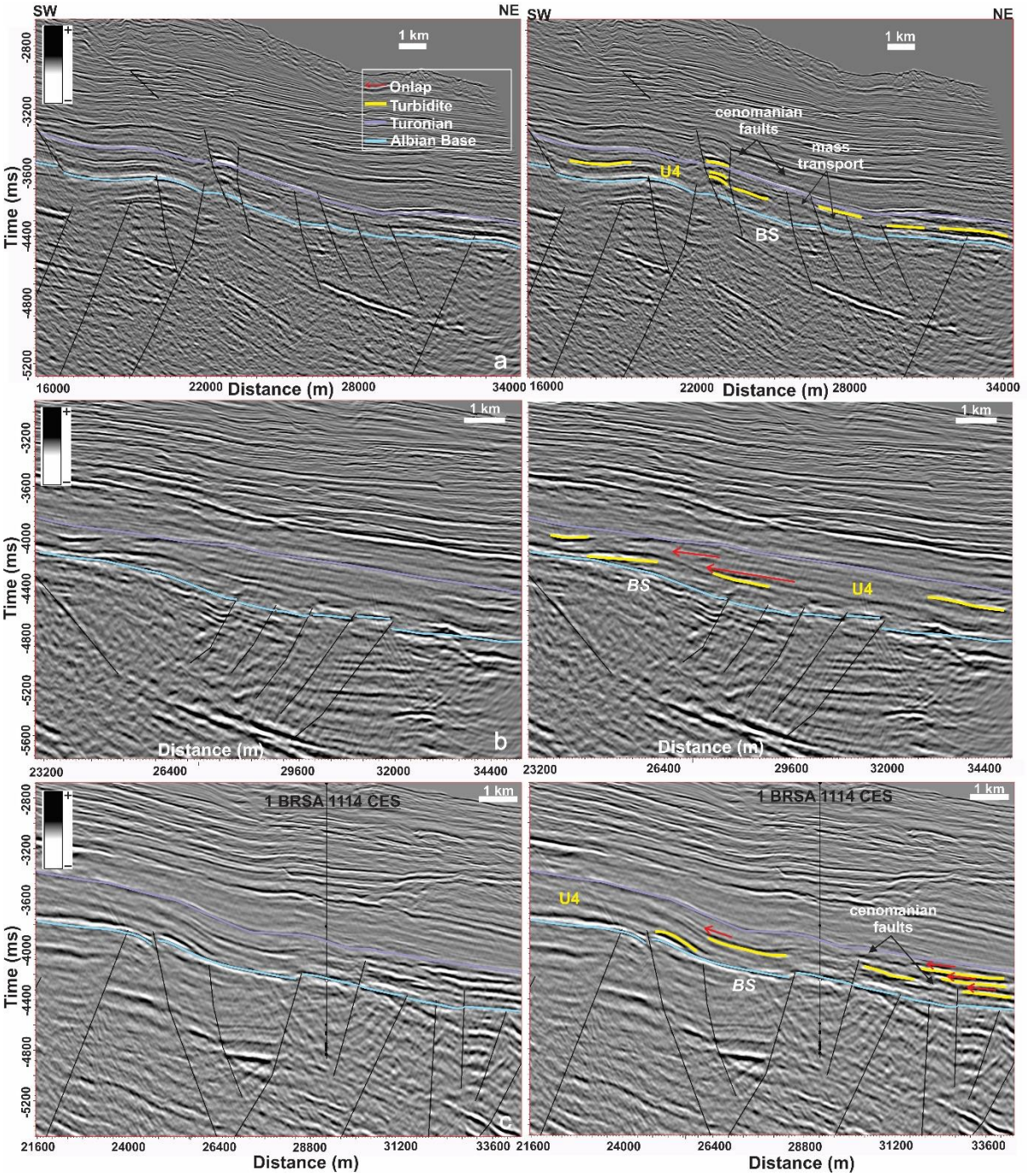

Based on the geochemical data, the depth of Early Cenomanian and Cenomanian-Turonian source rocks at deepwater of Mundaú sub-basin occurs approximately between 3,400 and 3,800 m below sea water bottom. Also, the depth of source rocks from Late Albian-Early Cenomanian and Cenomanian-Turonian is approximately from 3048 to 4894 m in the deepwater and ultra-deepwater based on the conversion of time to depth. Thus, it can be inferred that source rocks of the drift stage from deepwater's Mundaú sub-basin are at the oil window depth, since the source rocks reached the burial depth greater than 3,400 m below the sea floor. Unit 4 (Figs. 3-9d and 3-11a) reveals the most likely areas of deepwater turbiditic deposits in

the Mundaú sub-basin, which corresponds to Late Albian-Turonian ages, an analogue to the play found in the Jubilee field offshore Ghana.

3.7. CONCLUSIONS

New well data combined with 1,589 km of 2D seismic lines allowed for a new geological evaluation of the deepwater stratigraphy of Ceará Basin and its architectural framework. In this study, new insights were presented on the influence of structural features on the depositional elements and their distribution. The interplay between sedimentation and tectonics plays a key role in controlling sediment trapping and spatial distribution as well as the petroleum implications of this region. The following observations and interpretations have been made:

(1) The Aptian rift system in Mundaú sub-basin might supply further opportunities for structural trapping in the basin, and expectations of drift stratigraphic-structural traps through interconnecting faults. Four majors landward-dipping faults were mapped in all seismic data, which would have the potential to allow charging of deepwater drift reservoirs from rift source rocks.

(2) The seismic interpretation reveals evidence of Cretaceous to Paleogene magmatism in the region as indicated by the well imaged volcanoes and associated sills at depth. The proximity of deepwater turbidites plays with magmatic rocks could have established an atypical petroleum system.

(3) The variety of stratigraphic and structural features developed through the Cretaceous history of the basin offer high-trapping potential for a number of plays in the rift as well as in the drift sequences. The type of plays are: (1) the developed rift system with major faults which can act as long-distance migration pathways; (2) turbiditic bodies; (3) turbiditic bodies associated with magmatic intrusion. Identification of potential plays associated with turbiditic sandstones of the Ubarana Formation can be correlated to Jubilee play in Guinea Gulf and Zaedyus play in French Guiana.

(4) The sediments from Late Albian-Early Cenomanian-Turonian age are at depths ranging from 3048 to 4894 m in the deepwater and ultra-deepwater domains. Since the top depth of the oil window occurs from about 3,400 and 3,800 m in the deepwater Mundaú sub-basin, the analyses of geochemical data suggest that in this basin there must be a generation of oil and/or gas at deepwater plays.

(5) Our data strongly suggest that the architecture of this basin is a volcanic passive margin. Volcanic passive margins are associated with the extrusion and intrusion of large

volumes of magma, predominantly mafic, and represent distinctive features of Larges Igneous Provinces, in which regional fissural volcanism predates localized syn-magmatic break-up of the lithosphere. The criteria used to justify our assertion are: (1) the presence of basement and rifts filled by volcanics (seaward dipping reflectors); (2) the absence of exhumed mantle between the continental crust and oceanic crust; (3) the large presence of igneous intrusions; (4) and the presence of a LIP in the equatorial margin, based on igneous intrusions between two basins near the Ceará Basin.

Acknowledgements

The authors are grateful to the Brazilian National Petroleum Agency (ANP) for the provision of seismic and well data, and to Schlumberger for software licenses. The first author also thanks to Federal University of Ceará (LGPSR – Laboratório de Geofísica de Prospecção e Sensoriamento Remoto, and LSBD – Laboratório de Sistemas e Banco de Dados) for their support to this study. CImaGeo is also acknowledged for their support in seismic processing. The first author is grateful to the Fulbright Commission Brazil for a grant to support in her research in the United States. KMLO thanks the School of Geosciences, the University of Oklahoma, for providing facilities during her split PhD in the United States. This study was financed in part by the Coordenação de Aperfeiçoamento de Pessoal de Nível Superior - Brasil (CAPES) - Finance Code 001. We are also grateful to Davide Gamboa and to an anonymous reviewer for their constructive discussion and comments, and also the editor Tiago Alves for their help in improving the quality of the original manuscript.

References

Aarnes, I., Planke, S., Trulsvik, M. and Svensen, H. 2015. Contact metamorphism and thermogenic gas generation in the Vøring and Møre basins, offshore Norway, during the Paleogene-Eocene thermal maximum. Journal of the Geological Society, 172(5), 588-598. https://doi.org/10.1144/jgs2014-098

Abreu, V. S., 1998. "Geologic evolution of conjugate volcanic passive margins: Pelotas Basin (Brazil) and offshore Namibia (Africa). Implication for global sea level changes." Diss., Rice University. https://hdl.handle.net/1911/19338.

Altamira-Areyan, A., 2009, The ribbon continent of northwestern South America. Ph.D. Thesis. University of Houston. 215 p.Antobreh, A., Faleide, J., Tsikalas, F., & Planke, S. (2009). Rift–shear architecture and tectonic development of the Ghana margin deduced from multichannel seismic reflection and potential field data. Marine and Petroleum Geology, 26 (3),

345-368. https://doi.org/10.1016/j.marpetgeo.2008.04.005

Antunes, A.F., Jardim de Sá, E.F., Araújo, R.G.S., Lima Neto, F.F. 2008. Caracterização tectonoestrutural do Campo de Xaréu (Sub-Bacia de Mundaú, Bacia do Ceará – NE do Brasil): abordagem multiescala e pluriferramental. Revista Brasileira de Geociências. 38(1 - suplemento): 88-105.

Beltrami, C.V.; Alves, L.E.M.; Feijó, F.J. 1994. Bacia do Ceará. B. Geoci. Petrobras, v. 8, n. 1, p. 117-125.

Bishop, M. S. (1960). Surface mapping. John Willey New York p.198

Bulhões, E. M., Amorim, W. N., 2005. Princípio da sismocamada elementar e sua aplicação à técnica de volume de amplitudes (TecVa): Ninth International Congress of the Brazilian Geophysical Society, Salvador, Brasil. https://doi.org/10.1190/sbgf2005-275

Burov, E. & Cloetingh, S. 1997. Erosion and rift dynamics: new thermomechanical aspects of post-rift evolution of extensional basins. Earth and Planetary Science Letters, 150, 7–26. https://doi.org/10.1016/S0012-821X(97)00069-1

Burov, E. & Poliakov, A. 2003. Erosional forcing of basin dynamics: new aspects of syn-and post-rift evolution. In: NIEUWLAND, D.A. (ed.) New Insights into Structural Interpretation and Modelling. Geological Society, London, Special Publications, 212, 209–223, https://doi.org/10.1144/GSL.SP.2003.212.01.14.

Brownfield, M. E. & Charpentier R. R. 2006. Geology and total petroleum systems of the Gulf of Guinea Province of west Africa: U.S. Geological Survey Bulletin 2207-C, 32 p.

Condé, V.C.; Lana, C.C.; Pessoa Neto, O.C.; Roesner, E.H.; Morais Neto, J.M.; Dutra, D.C., 2007. Bacia do Ceará. B. Geoci. Petrobras, v. 15, n. 2, 347- 355 p.

Coole, P., Tyrrell, M. & Roche, C. 2015. Offshore Ivory Coast: reducing exploration risk. GeoExpro, 12, 80–84.

Costa, I.G.; Beltrami, C.V.; Alves, L.E.M.,1990. A Evolução tectono-sedimentar e o "habitat" do óleo na Bacia do Ceará. B. Geoci. Petrobras, v. 12, n. 1, 65-74 p.

Cramez, C. & Jackson, M.P.A., 2000. Superposed deformation straddling the continental oceanic transition in deepwater Angola. Marine and Petroleum Geology, 17: 1095-1109. https://doi.org/10.1016/S0264-8172(00)00053-2

Dailly, P., Henderson, T., Hudgens, E., Kanschat, K. & Lowry, P. 2013. Exploration for Cretaceous stratigraphic traps in the Gulf of Guinea, West Africa and the discovery of the Jubilee Field: a play opening discovery in the Tano Basin, Offshore Ghana. In: Mohriak, W.U., Danforth, A., Post, P.J., Brown, D.E., Tari, G.C., Nemčok, M. & Sinha, S.T. (eds) Conjugate Divergent Margins. Geological Society, London, Special Publications, 369, 235–248,

https://doi.org/10.1144/SP369.12

Davison, I., Faull, T., Greenhalgh, J., Beirne, E. O., Steel, I. 2016, Transpressional structures and hydrocarbon potential along the Romanche Fracture Zone: a review, in M. Nemčok, S. Rybár, S. T. Sinha, S. A. Hermeston and L. Ledvényiová (eds.), Transform Margins: Development, Controls and Petroleum Systems: London, Geological Society, Special Publications, v. 431, p. 235–248.

Elvsborg, A. & Dalode J. 1985. Benin hydrocarbon potential looks promising: Oil and Gas Journal, v. 82, p. 126–131.

Falkenhein, F., Martins Neto, M., Guerra, W.J. 2001. Brazilian Equatorial Margin Project Part. 1: Final Report. Brazilian National Agency of Petroleum, Natural Gas and Biofuels Internal Report.

Falkenhein, F., Martins Neto, M., Guerra, W.J. 2001. Brazilian Equatorial Margin Project Part. 2: Final Report. Brazilian National Agency of Petroleum, Natural Gas and Biofuels Internal Report

Fiduk, J.C., Brush, E.R., Anderson, L.E., Gibbs, P.B., Rowan, M.G., 2004. Salt defor- mation, magmatism, and hydrocarbon prospectivity in the Espírito Santo Basin, offshore Brazil. In: Post, P.J., Olson, D.L., Lyons, K.T., Palmes, S.L., Harison, P.F., Rosen, N.C. (Eds.), Salt-sediment Interactions and Hydrocarbon Prospectivity: Concepts, Applications, and Case Studies for the 21st Century. GCSSEPM 24th Annual Research Conference, pp. 370-392.

Fonseca, J.C.L.G., Vital, H., Perez, Y.A.R. et al. 2019. Seismic stratigraphy of a deep water basin in the Brazilian equatorial margin: the eastern portion of Potiguar Basin and Touros High. Geo-Mar Lett. https://doi.org/10.1007/s00367-019-00626-7

Françolin, J.B.L., Szatmari, P. 1987. Mecanismo de rifteamento da porção oriental da margem norte brasileira. Revista Brasileira de Geociências. 17(2):196-207.

Gamboa, D., Alves, T.M., Cartwright, J., & Terrinha, P. 2010. MTD distribution on a 'passive' continental margin: The Espírito Santo Basin (SE Brazil) during the Palaeogene. Marine and Petroleum Geology, v. 27, (7), 1311-1324. DOI:10.1016/j.marpetgeo.2010.05.008

Haq, B.U., Hardenbol, J., Vail, P.R., 1987. Chronology of fluctuating sea levels since the Triassic (250 million years ago to present): Science, v. 235, p. 1156–1167. https://doi.org/10.1126/science.235.4793.1156

Holford, S., Schofield, N., Jackson, C., Magee, C., Green, P. and Duddy, I. 2013. Impacts of igneous intrusions on source and reservoir potential in prospective sedimentary basins along the western Australian continental margin, West Australian Basins Symposium, Abstracts. http://hdl.handle.net/10044/1/32040

Hollanda, M. H. B. M., Archanjo, C. J., Macedo Filho, A. A., Fossen, H., Ernst, R. E, de Castro D. L., Melo, A. C., Oliveira, A. L. 2018. The Mesozoic Equatorial Atlantic Magmatic Province (EQUAMP) A New Large Igneous Province in South America. Springer Geology Book Series: Dyke Swarms of the World: A Modern Perspective 87-110 p. https://doi.org/10.1007/978-981-13-1666-1_3

Jones, S.F., Wielens, H., Williamson, M.C. and Zentilli, M. 2007. Impact of magmatism on petroleum systems in the Sverdrup basin, Canadian Arctic islands, Nunavut: a numerical modelling study. Journal of Petroleum Geology, 30(3), 237-256.

Jovane, L., Picanco Figueiredo, J., Pavani Alves, D., Iacopini, D., Giorgioni, M., Vannucchi, P., Silva de Moura, D., Hilario Bezerra, F., Vital, H.,Rios, I. & C. Molina, E. 2016. Seismostratigraphy of the Ceará Plateau: Clues to Decipher the Cenozoic Evolution of Brazilian Equatorial Margin. Frontiers in Earth Science, vol. 4, 90. https://doi.org/10.3389/feart.2016.00090

Karagiannopoulos L. 2018 Dec 24. Ghana's first oil exploration licensing round attracts global majors. Reuters; [accessed 2019 Apr 28]. https://www.reuters.com/article/us-ghana-oil-exploration/ghanas-first-oil-exploration-licensing-round-attracts-global-majors-idUSKCN1ON0XQ

Karner, G.D. & Driscoll, N.W., 1999. Tectonic and stratigraphic development of the West African and eastern Brazilian Margins: insights from quantitative basin modelling;. In: N.R. Cameron, R.H. Bate and V.S. Clure (Editors), The Oil and Gas Habitats of the South Atlantic. Geological Society, London, pp. 11-40. https://doi.org/10.1144/GSL.SP.1999.153.01.02

Krueger, A., 2012, The Brazilian Equatorial Margin from Rift to Drift: Faulting, Deposition, and Deformation in the Offshore Barreirinhas Basin. Ph.D. Thesis. University of Houston, 168p.

Krueger, A.,Murphy, M.,Burke, K., Gilbert, E. 2014. The Brazilian Equatorial Margin: A Snapshot in Time of an Oblique Rifted Margin: Adapted from extended abstract prepared in conjunction with oral presentation at AAPG 2014 Annual Convention and Exhibition, Houston, Texas, April 6-9. Search and Discovery Article #30325. http://www.searchanddiscovery

Larsen, H.C. & Marcussen, C. 1992. Sill-intrusion, flood basalt emplacement and deep crustal structure of the Scoresby Sund region, east Greenland. In: Storey, B.C., Alabaster, T. &Pankhurst, R.J. (eds) Magmatism and the Causes of Continental Break-up. Geological Society, London, Special Publications, 68, 365– 386, https://doi.org/10.1144/GSL.SP.1992.

068.01.23

Lavier, L., Steckler, M., Brigaud, F., 2000. An Improved Method for Reconstructing the Stratigraphy and Bathymetry of Continental Margins: application to the Cenozoic Tectonic and Sedimentary History of the Congo Margin. AAPG Bull., 84(7): 923-939. https://doi.org/10.1306/A9673B6C-1738-11D7-8645000102C1865D

Leopoldino Oliveira, K. M., De Castro, D. L., Castelo Branco, R. M. G., De Oliveira, D. C., Alvite, E.N.C., Jucá, C.C.A., Castelo Branco, J. L., 2018. Architectural framework of the NW border of the onshore Potiguar Basin (NE Brazil): An aeromagnetic and gravity based approach. Journal of South American Earth Sciences, v. 8, 700-714 p. https://doi.org/10.1016/j.jsames.2018.10.002

Macgregor, D.S., Robinson, J. & Spear, G. 2003. Play fairways of the Gulf of Guinea transform margin. In: Arthur, T.J., Macgregor, D.S. & Cameron, N.R. (eds) Petroleum Geology of Africa: New Themes and Developing Technologies. Geological Society, London, Special Publications, 207, 131–150. https://doi.org/10.1144/GSL.SP.2003.207.7

Maia de Almeida, N., T. M. Alves, F. Nepomuceno Filho, G. Satander Sá Freire, A. C. Braga de Souza, M. Nunes Normando, et al., Tectono-sedimentary evolution and petroleum systems of Mundaú Sub-Basin: A new deepwater exploration frontier in equatorial Brazil, (in press; preliminary version published online Ahead of Print 01 August 2019): AAPG Bulletin, doi: 10.1306/07151917381

Martin, J., Duval, G. & Lamourette, L. 2015. What lies beneath the deepwater tano basin. GeoExpro, 12, 28–30.

Massala, A., de Klasz, I., de Klasz, S., Laurin, B., 1992. translated: Benthic foraminifera of stratigraphic interest from the Congo Basin. In: R. Curnelle (Editor), African geology; First meeting on the Stratigraphy and paleogeography of West Africa sedimentary basins; Second African meeting on Micropaleontology. Elf-Aquitaine Research Centre, pp. 411.

Matos, R.M.D. 1999. Tectonic evolution of the equatorial South Atlantic. In: Mohriak, W.U., Talwani, M. (eds.). Atlantic rifts and continental margins, AGU Geophysical Monograph, 115:331-354. https://doi.org/10.1029/GM115p0331

Matos, R. M. D., 2000, Tectonic evolution of the Equatorial South Atlantic, in W. U. Mohriak and M. Talwani (eds.), Atlantic Rifts and Continental Margins: Geophysical Monograph, v. 115 (AGU), p. 331-354.

Mauduit, T., Guerin, G., Brun, J.P., Lecanu, H., 1997. Raft tectonics: effects of basal slope angle and sedimentation rate on progressive extension. J. Structural. Geol., 19(9): 1219-1230. https://doi.org/10.1016/S0191-8141(97)00037-0

McGinnis, J.P., Driscoll, N.W., Karner, G.D., Brumbaugh, W.D., Cameron, N., 1993. Flexural response of passive margins to deep-sea erosion and slope retreat: Implications for relative sea-level change. Geology, 21: 893-896. https://doi.org/10.1130/0091-7613(1993)021%3C0893:FROPMT%3E2.3.CO;2

McHone, J. G. 2006. Igneous Features and Geodynamic Models of Rifting and Magmatism Around the Central Atlantic Ocean. Available online at: http:// www.mantleplumes.org/CAMP.html

Mello, M.R., Mohriak, W.U., Koutsoukos, E.A.M., Bacoccoli, G., 1994. Selected petroleum systems in Brazil. AAPG Memoir 60, 499–512.

Meyers, J.B., Rosendahl, B.R., Austin, J.A.J., 1996. Deep-penetrating MCS images of the South Gabon Basin: implications for rift tectonics and post-breakup salt remobilization. Basin Research, 8: 65-84. https://doi.org/10.1111/j.1365-2117.1996.tb00115.x

Milani, E. J., & Thomaz Filho, A. 2000. “Sedimentary basins of South America,” in Tectonic Evolution of South America, Vol. 31, eds U. G. Cordani, E. J. Milani, A. Thomaz Filho, and D. A. Campos (Rio de Janeiro: International Geological Congress), 389–449.

Miranda, S.F., Cunha, P.R.C., Caldeira, J.L., Michelon, D., Aragao, F.B. 2016. The atypical igneous sedimentary petroleum systems of the Parnaiba basin: Seismic, well-logs and analogues. AAPG International Conference & Exhibition, Abstracts. https://doi.org/10.1190/ice2016-6471370.

Mizusaki, A. M. P., ThomaZ Filho, A., Milani, E. J., Césero, P. 2002. Mesozoic and cenozoic igneous activity and its tectonic control in the northeastern region of Brazil, South America. Journal of South America Earth Sciences, Oxford, v. 15, 183-198 p. https://doi.org/10.1016/S0895-9811(02)00014-7

Mohriak, W.U., 2005. Interpretação geológica e geofísica da Bacia do Espírito Santo e da região de Abrolhos: Petrografia, datação radiométrica e visualização sísmica das rochas vulcânicas. Boletim de Geociencias da Petrobras 14 (1), 133 - 142.

Morais Neto, J.M., Pessoa Neto, O.C., Lana, C.C., Zalán, P.V. 2003. Bacias Sedimentares Brasileiras: Bacia do Ceará. Fundação Paleontológica Phoenix, v. 57, 1-6 p.

Morgan, P. 1983. Constraints on rift thermal processes from heat flow and uplift. Tectonophysics, Processes of Continental Rifting, 94, 277–298, https://doi.org/ 10.1016/0040-1951(83)90021-5

Morrison, J., Burgess, C., Cornford, C. & N’zalasse, B. 2000. Hydrocarbon systems of the Abidjan margin, Côte d’Ivoire. Offshore West Africa. Fourth Annual Conference, 21–23 March 2000, Abidjan. Pennwell Publishing, Tulsa, OK.

Mougamba, R., 1999. Chronologie et architecture des systemes turbiditiques Cenozoique du prisme sédimentaire de l'Ogooué. (Marge Nord-Gabon). Ph.D. Thesis, Université des Sciences et Technologies de Lille, Lille, 219 pp.

Nemčok, M., Henk, A., Allen, R., Sikora, P.J., Stuart, C. 2012, Continental break-up along strike-slip fault zones: observations from the Equatorial Atlantic, in W. U. Mohriak, A. Danforth, P. J. Post, D. E. Brown, G. C. Tari, M. Nemčok and S. T. Sinha, S. T. (eds), Conjugate Divergent Margins: London, Geological Society, Special Publications, v. 369, p. 537-556. http://dx.doi.org/10.1144/SP369.8

Nzé Abeigne, C.R., 1997. Evolution post-rift de la marge continentale Sud-Gabon: contrôles tectonique et climatique sur la sédimentation. Ph.D. Thesis, Université Montpellier II, 2 vol. 195 pp.

Pellegrini, B. S., Ribeiro, H. J. P. R., 2018. Exploratory plays of Pará-Maranhão and Barreirinhas basins in deep and ultra-deep waters, Brazilian Equatorial Margin. Brazilian Journal of Geology v. 48, 3, 485-502. http://dx.doi.org/10.1590/2317-4889201820180146

Pessoa Neto, O.C. 2004. Blocos basculados truncados por discordância angular: lições aprendidas em trapeamento combinado de hidrocarbonetos, Bacia do Ceará, Nordeste do Brasil. Boletim de Geociências Petrobras, Rio de Janeiro, v. 12, n. 1, p. 59-71

Rasmussen, E.S., 1996. Structural evolution and sequence formation offshore South Gabon during the Tertiary. Tectonophysics(266): 509-523. https://doi.org/10.1016/S0040-1951(96)00236-3

Rohrman, M. 2007. Prospectivity of volcanic basins: Trap delineation and acreage de-risking. AAPG bulletin, 91(6), 915-939. https://doi.org/10.1306/12150606017

Rossetti, D.F., Bezerra, F.H.R. and Dominguez, J.M.L. (2013) Late Oligocene-Miocene Transgressions along Equatorial and Eastern Margins of Brazil. Earth-Science Reviews, 123, 87-112. http://dx.doi.org/10.1016/j.earscirev.2013.04.005

Scarselli, N., Duvel, G., Martin, J., Mc Clay, k., Toothill, S. 2018. Insights into the Early Evolution of the Côte d'Ivoire Margin (West Africa).Geological Society, London, Special Publications, 476, 16 March 2018, https://doi.org/10.1144/SP476.8

Schofield, N., Holford, S., Millett, J., Brown, D., Jolley, D., Passey, S., Muirhead, D., Grove, C., Magee, C., Murray, J., Hole, M., Jackson, C., Stevenson, C. 2015. Regional Magma Plumbing and emplacement mechanisms of the Faroe-Shetland Sill Complex: Implications for magma transport and petroleum systems within sedimentary basins. Basin Research, 29(1), 41-63. https://doi.org/10.1111/bre.12164

Segesman, F.F., 1980. Well-logging method. Geophysics 45 (11), 1667–1684.

Senger, K., Millett, J., Planke, S., Ogata, K., Eide, C. H., Festøy, M., Galland, O., Jerram, D. A. 2017. Effects of igneous intrusions on the petroleum system: a review. First Break: Technical Article, 35, 6, 47-56 p. https://doi.org/10.3997/1365-2397.2017011

Séranne, M. & Nzé Abeigne, C., 1999. Oligocene to Holocene sediment drifts and bottom currents on the slope of Gabon continental margin (west Africa). Consequences for sedimentation and southeast Atlantic upwelling. Sedimentary Geology, 128: 179-199. https://doi.org/10.1016/S0037-0738(99)00069-X

Séranne, M., Seguret, M., Fauchier, M., 1992. Seismic super-units and post-rift evolution of the continental passive margin of southern Gabon. Bull. Soc. Géol. France, 163(2): 135-146.

Silva Filho, W. F., De Castro, D. L., Corrêa, I. C. S., Freire, G. S. S. 2007. Estruturas rasas na margem equatorial ao largo do nordeste brasileiro (Estado do Ceará): análise de relevo e anomalias gravimétricas residuais. Revista Brasileira de Geofísica, 25 (1), 65-77. https://dx.doi.org/10.1590/S0102-261X2007000500007

Silva, S.R.P., Maciel, R.R., Severino, M.C.G. 1999. Cenozoic tectonics of Amazon Mouth Basin: Geo-Marine Letter, v. 18, p. 256-262.

Skogseid, J. & Eldholm, O. 1989 Voring plateau continental margin: seismic interpretation, stratigraphy, and vertical movements. In: Eldholm, O., Thiede, J., Taylor, E. et al. (eds) Proceedings of the Ocean Drilling Program, Scientific Results. Ocean Drilling Program, College Station, TX, 993–1029.

Skogseid, J., Pedersen, T., Larsen, V.B. 1992. Vøring Basin: subsidence and tectonic evolution. In: Larsen, R.M., Brekke, H., Larsen, B.T. & Talleras, E. (eds) Structural and Tectonic Modelling and its Application to Petroleum Geology. Norwegian Petroleum Society, Special Publications, 1, 55–82. https://doi.org/10.1016/B978-0-444-88607-1.50009-7

Soares, D. M., Alves, T. M., Terrinha, P. 2012, The breakup sequence and associated lithospheric breakup surface: Their significance in the context of rifted continental margins (West Iberia and Newfoundland margins, North Atlantic): Earth and Planetary Science Letters, v. 355–356, p. 311–326.

Stagpoole, V. & Funnell, R. 2001. Arc magmatism and hydrocarbon generation in the northern Taranaki Basin, New Zealand. Petroleum Geoscience, 7(3), 255-267. https://doi.org/10.1144/petgeo.7.3.255

Svensen, H., Planke, S., Polozov, A.G., Schmidbauer, N., Corfu, F., Podladchikov, Y.Y., Jamtveit, B. 2009. Siberian gas venting and the end-Permian environmental crisis. Earth and Planetary Science Letters, 277(3-4), 490-500. https://doi.org/10.1016/j.epsl.2008.11.015

Thomaz Filho, A., Mizusaki, A.M.P., Antonioli, L. 2008. Magmatism and petroleum exploration in the Brazilian Paleozoic basins. Marine and petroleum geology, 25(2), 143-151. https://doi.org/10.1016/j.marpetgeo.2007.07.006

Tissot, B.P., Welte, D.H. 1984. Petroleum Formation and Occurrence. Springer Verlag, Berlin. 1155 p.

Trosdtorf, I., Jr.; Zalán, P.V.; Figueiredo, J.J.P.; Soares, E.F. 2007. Bacia de Barreirinhas. B. Geoci. Petrobras, v. 15, n. 2, 331-339 p.

Vail, P. R., Mitchum, R. M. JR & Thompson, S. III. 1977. Seismic stratigraphy and global changes of sea level, part 3: relative changes of sea level from coastal onlap. In: Payton C. E. edition. Seismic stratigraphy applications to hydrocarbon exploration, AAPG. memoir 26 p. 63–97. https://doi.org/10.1306/M26490C5

Veeken PCH (2007) Seismic stratigraphy, basin analysis, and reservoir characterization. Elsevier Ltd, Oxford

Wu, C., Gu, L., Zhang, Z., Ren, Z., Chen, Z., Li, W. 2006. Formation mechanisms of hydrocarbon reservoirs associated with volcanic and subvolcanic intrusive rocks: Examples in Mesozoic-Cenozoic basins of eastern China. AAPG Bulletin, 90(1), 137-147. https://doi.org/10.1306/07130505004

Zálan P. V. and Warne, J. E. 1985. Tectonics and sedimentation of the Piauí-Camocim Sub-basins, Ceará Basin, Offshore Northeastern Brazil: Série Ciência-Técnica-Petróleo (17), PETROBRAS, Rio de Janeiro, 71 p.

Zalán, P.V. 2015. Similarities and Differences between Magma-Poor and Volcanic Passive Margins – Applications to the Brazilian Marginal Basins. Conference Paper - 14th International Congress of the Brazilian Geophysical Society held in Rio de Janeiro, Brazil, 37-42 p. https://doi.org/10.1190/sbgf2015-007

Zalán, P.V., Nelson, E. P., Warme, J., Davis, T. L. 1985, The Piaui Basin: rifting and wrenching in an equatorial Atlantic transform basin, in K. T. Biddle and N. Christie-Blick (eds.), Strike-Slip Deformation, Basin Formation, and Sedimentation, Society of Economic Paleontologists and Mineralogists, Tulsa, Special Publication, v. 37, p. 177-192. doi 10.2110/pec.85.37.0177

4. ARTICLE 3: SEISMIC ATTRIBUTES, MACHINE LEARNING, AND ROCK PHYSICS ANALYSES – A PROMISING AID FOR HYDROCARBON PREDICTION IN A DEEPWATER BASIN OF THE BRAZILIAN EQUATORIAL MARGIN

Manuscript invited by the **Geological Society Special Publications** to be submitted to a book entitled "Seismic geomorphology: subsurface analyses, data integration, and paleo-environment reconstruction".

A technical article from this chapter was invited for publication on the **AAPG Geophysical Corner website** with publication scheduled for January 2021.

ABSTRACT

We utilize 3D seismic reflection data and robust rock-physics models that are applied to a new well dataset to investigate the subsurface of the Mundaú sub-basin. A seismic attributes analysis and unsupervised machine learning approach were able to produce high-resolution images to allow the mapping of the 3D geometry of ancient geomorphologic features across stratigraphic levels, from the Albian to the Turonian interval. Meaningful deepwater elements were identified using seismic attributes and machine learning techniques (i.e. channel complex, point bars, feeder channels, faults, depocenters, dendritic lobes, smaller channels and distributaries). In addition, petrophysical analysis aided to train a deep convolutional network to allow S-wave modeling, and synthetic seismic generation to more fully understand and interpret the seismic data. The well validation helped to interpret sand-prone deposits; the rock-physics modeling allowed insight into the lithologies that were deposited. Machine learning techniques, including self-organizing maps (SOMs) and independent component analysis (ICA) revealed additional details regarding the seismic geomorphology which allowed a seismic facies classification. Moreover, a better understanding of the seismic amplitudes and geomorphology, tied with seismic facies analysis provided valuable insights into the geomorphology of this under-researched basin.

Keywords: Equatorial margin; Turbidites; Seismic geomorphology; Facies classification; Seismic attributes; Machine learning.

4.1. INTRODUCTION

The Brazilian Equatorial Margin (BEM), in the Equatorial South Atlantic Ocean, is composed of five sedimentary basins along the coast. It is comprised of the Foz do Amazonas,

Pará-Maranhão, Barreirinhas, Ceará, and Potiguar Basins (Figure 4-1a). These basins began their development during the Early Cretaceous, as a series of several continental rift basins, and evolved through a complex evolution with the tectonic regime varying from predominantly normal (distension) to a predominantly strike-slip (transtension and transpression) regime. The geological evolution of this margin is similar to the West African margin, being characterized by a transform margin (Françolin & Szatmari, 1987; Matos, 2000; Milani & Thomaz Filho, 2000; Maia de Almeida et al., 2019).

The BEM has lately been the focus of considerable interest due to the well-documented large hydrocarbon discoveries within the conjugate transform basins of West Africa, including large oil fields in Ghana, the Ivory Coast, and Suriname (Huaicun, 2014; Exxon Mobil, 2020; GeoExpro, 2020). Still, the deepwater of the BEM is underexplored, only a few wells have been drilled, however available public domain data from ongoing seismic evaluation suggests that there is high potential for light oil discoveries in Upper Cretaceous turbidite sandstone reservoirs in stratigraphic traps. Previous works as Maia de Almeida et al. (2020) proved that reservoirs in a deepwater well comprise Cretaceous sandstones in a combined trap related to both an unconformity and a normal fault. Leopoldino Oliveira et al. (2020) identified a series of potential stratigraphic and structural traps, and associated petroleum plays, in rift and drift sequences of the Ceará Basin. That study was primarily based on 2D seismic data, which has its limitations in performing strong seismic geomorphology analyses.

Given this, in this study, three deepwater well boreholes and three-dimensional (3D) seismic reflection data have been examined with three main objectives: (i) identify deepwater architectural elements; (ii) use multiattribute analysis to characterize seismic facies which could be well related to sedimentary facies; (iii) identify the amplitude response of the lithologies and its fluid content on the boreholes and link the rock properties to seismic. These objectives will allow the integration of regional geology, 3D seismic reflection data, and exploration wells to better understand and interpret the large turbidites channels associated with a deepwater depositional system in the Ceará Basin.

Figure 4-1: Map of the Equatorial Atlantic Ocean highlighting the fracture zones and the marginal basins. b) The Ceará Basin sub-divided into four sub-basins: Piauí-Camocim, Acaraú, Icaraí and Mundaú. The study area is located in the Mundaú sub-basin. Structural data was compiled from Zalán and Warme (1985) and Morais Neto et al. (2003). The basins boundaries were provided by the Brazilian National Agency of oil, gas and biofuels (ANP) and boundaries of sub-basins were based on Morais Neto et al. (2003). c) Location of the four producer fields

(Xaréu, Atum, Curimã and Espada) of the Mundaú sub-basin. The location of the wells and seismic data are shown, as provided by the ANP. The topographic model in the figure was provided by NOAA (ETOPO1).

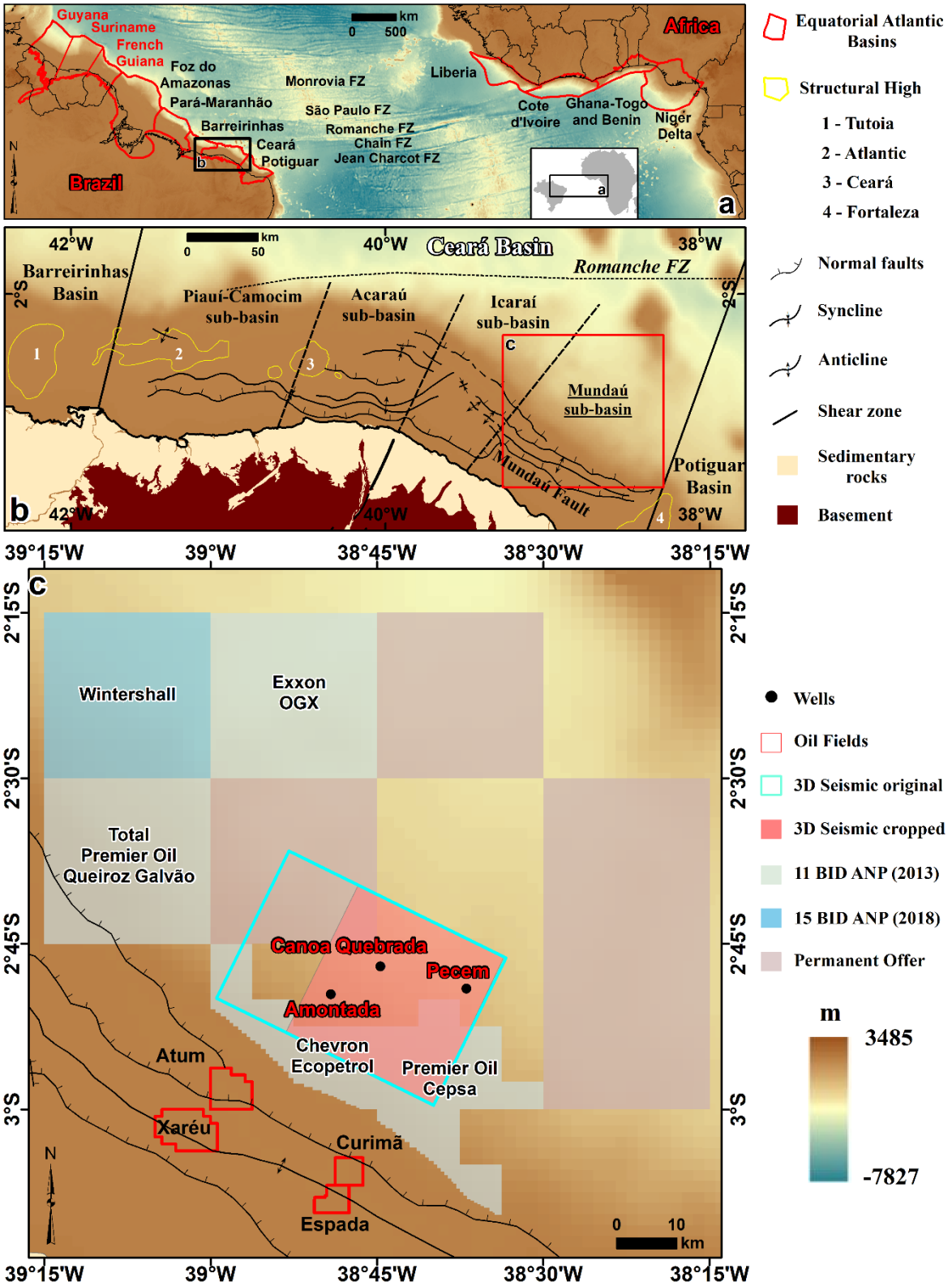

In addition to the multi-attribute seismic analysis, unsupervised machine-learning techniques including self-organizing maps (SOMs) and independent component analysis (ICA)

were applied. These techniques provided additional insights into the distribution and classification of the deepwater geological elements. Further, seismic geomorphology and facies analysis improved upon the interpretation of the internal and external architecture of the depositional elements, and so helped to identify and to predict the possible reservoirs related to the turbiditic sandstone. The well log modeling and rock-physics analysis helped to gain information regarding the relationship of the mineralogy, porosity, and fluid content with seismic amplitude. In addition to providing an improved understanding of the sedimentation patterns in the Albian to Turonian interval of the deepwater region, the rock physics analysis provided a 'ground truth' of data for interpreting the location of the main sediment transport pathways and sand-filled depocenters within the largely undrilled deepwater blocks, where previously seismic evaluation was the only option. This paper presents the first demonstration of subsurface large turbidite complex system based on the integration of the seismic attributes and machine learning techniques in the Ceará Basin.

4.2. GEOLOGICAL SETTING

The Brazilian Equatorial Margin evolved as a transform margin during the Lower Cretaceous by the fragmentation and continental breakup of northwest Gondwana. The BEM is composed by five sedimentary basins along the coast. There are, from west to east, the Foz do Amazonas, Pará-Maranhão, Barreirinhas, Ceará, and Potiguar Basins (Figure 4-1a). These basins began their development during the Early Cretaceous, as a series of several continental rift basins through a complex evolution with tectonic regime varying from predominantly normal (distension) to predominantly strike-slip (transtension and transpression) regime.

The main characteristics of the BEM's offshore basins are: a) their relatively late continental breakup when compared to the Eastern Brazilian Margin (EBM) (Françolin and Szatmari 1987, Szatmari et al., 1987; Matos, 2000), b) a continental rupture controlled by strike slip tectonics with predominant dextral kinematics (Matos, 2000; Basile et al., 2005), c) diachronous subsidence and uplift events on each margin segment controlled by divergent, transtensional or transpressional tectonics (Mohriak, 2003; Zálan, 2004), d) sub-basins that record contrasting histories in terms of their thermal, depositional, magmatic and deformation histories (Milani et al., 2000), and e) the absence of a transitional evaporitic sequence of Aptian age, as well as the absence of structures and sedimentation associated with salt tectonics (Mohriak, 2003; Zálan, 2004; Pellegrini and Severiano Ribeiro, 2018).

4.2.1. Ceará Basin

The Ceará Basin is bounded to the east by the Fortaleza High, to the west by the Tutóia High, to the south by the Precambrian basement, and to the north by the Romanche Fracture Zone (RFZ) (Figure 1b) (Costa et al., 1990). This basin presents transpressional and transtensional segments and, because of its distinct tectonic character along and across the BEM, it has been previously divided into four distinct sub-basins: the Mundaú, Icaraí, Acaraú, and Piauí-Camocim sub-basins (Morais Neto et al., 2003). The Piauí-Camocim is separated from the Acaraú sub-basin by the Ceará High. The Acaraú and Icaraí sub-basins have as common limit the Sobral-Pedro II lineament extension. In addition, the Icaraí is separated from Mundaú sub-basin by an important fault inflexion (Morais Neto et al., 2003).

Beltrami et al. (1994) suggested differences in the sedimentary record of the Mundaú, Icaraí-Acaraú and Piauí-Camocim sub-basins. The Piauí-Camocim sub-basin has the least complete sedimentary fill of the three sub-basins, with unconformities and depositional hiatuses of greater magnitude. The most complete stratigraphic record is that of the Mundaú sub-basin. For this reason, and because of the hydrocarbon oil fields, this sub-basin concentrates the largest amount of geological and geophysical data acquired to date. Condé et al. (2007) proposed a tectono-stratigraphic evolution for the Ceará Basin based mainly on data acquired in the Mundaú sub-basin.

4.2.2 Mundaú sub-basin

The Mundaú sub-basin is regionally structured by a major fault, the Mundaú Fault, which has normal offset in the NW-SE direction and is NE-dipping (Antunes et al., 2008) (Figure 1b). The tectono-sedimentary evolution of the Mundaú sub-basin consists of three major megasequences (Beltrami et al., 1994): syn-rift, transitional, and drift. The syn-rift phase is characterized by the development of NW-SE normal faults forming asymmetric half-grabens, and continental sedimentation marked by fluvial-deltaic sandstones and shales of the Mundaú Formation (Beltrami et al., 1994). The top of this unit is a regional stratigraphic reflector, called the Electric Mark 100 (Costa et al., 1990) or 1000 (Beltrami et al., 1994; Condé et al., 2007) and is interpreted to be the result of a period of regional flooding that affected the basin during the lower Aptian (Pessoa Neto, 2004).

The transitional sequence, the Paracuru Formation, is marked by the first marine incursions recorded in the sub-basin, within the fluvial, deltaic, and lacustrine sandstones. Limestones and subordinate evaporites (Trairi Member) were also deposited at this stage (~115 My) (Costa et al., 1990; Beltrami et al., 1994; Condé et al., 2007).

The drift or marine megasequence developed as a result of continental drift and a marked phase of thermal subsidence between the BEM and Equatorial Africa. The Ubarana Formation (from ~110 My to 65 My) comprises two members (Costa et al., 1990; Beltrami et al., 1994; Condé et al., 2007). The first one, the Uruburetama Member (~110 My to 75 My), corresponds to a marine transgression and consists of predominantly shales. The second member, Itapagé Member (from ~ 75 My to 65 My), corresponds to a regressive marine phase and consists of turbiditic shales and sandstones (Costa et al., 1990; Beltrami et al., 1994; Condé et al., 2007). The Guamaré Formation (from ~65 My to recent) consists of shelf carbonates, while the Tibau Formation (from ~65 My to recent) comprises proximal sandstones. The clastic continental sediments of the Barreiras Formation comprise the youngest unit of the basin (Condé et al., 2007).

Deepwater insights from Albian Base to Turonian

Figure 4-2a displays a stratigraphic chart summarized for this interval. Leopoldino Oliveira et al. (2020), based on five deepwater wells and 2D regional seismic interpretation, demonstrated that: a) the base of this sequence is composed of conglomerates representing deposits of low sea system tract. The top of this interval is related to a maximum flooding surface and anoxic event that has a very characteristic high-amplitude seismic character, and can be easily correlated throughout the Equatorial margin (Trosdtorf et al., 2007); b) the Pecém well present a low sand supply during the deposition at the base of this sequence, while the shale input was high, representing predominantly shelf to deepwater environments. However, the Canoa Quebrada and Amontada reveals a high sand supply in the whole sequence; c) the Cenomanian faults have a similar orientation to the rift faults, which seem to be linked at depth. This suggests that the Cenomanian faults formed as a result of a phase of reactivation of the older and deeper rift structures; d) the thickness of this interval reaches a greater depth to the northeast and northwest of the Mundaú sub-basin; e) the drift deposits were mainly influenced by sediment input from the continental shelf and slope instabilities.

The authors suggested the deepwater Ubarana Formation from Albian to Turonian age consists primarily of turbidites. It has a complex interplay between seabed geomorphology, sediment input from the shelf, and sediment transport. In this region, the main control on the distribution of turbiditic sands is the post-rift seabed geomorphology that was occasionally affected by sills. These features could develop highs that would form structures against which sands would onlap and pinch out, creating the potential for accumulation of reservoirs and

opportunity for stratigraphic traps to develop. These turbidites are extensive and are commonly associated with mass transport deposits, which is also seen in the east Brazilian margin (e.g. Fiduk et al., 2004; Mohriak, 2005; Gamboa et al., 2010). The interpreted turbiditic sandstones have reflectors with high acoustic impedance contrasts, low frequency, lens external geometry, and variable lateral extension, ranging from 5 to 8 km. These plays are very similar to the basin's African counterpart, with exception of the turbidites mixed by sills bodies that consists in an atypical play (Leopoldino Oliveira et al. 2020).

Figure 4-2: Correlation panel amongst 3D seismic reflectors and stratigraphic information from the Albian to Turonian age in the Ceará Basin (Condé et al., 2007). B) Well correlation panel showing interpreted gas indicator, gamma ray, sonic logs, density, porosity, and facies.

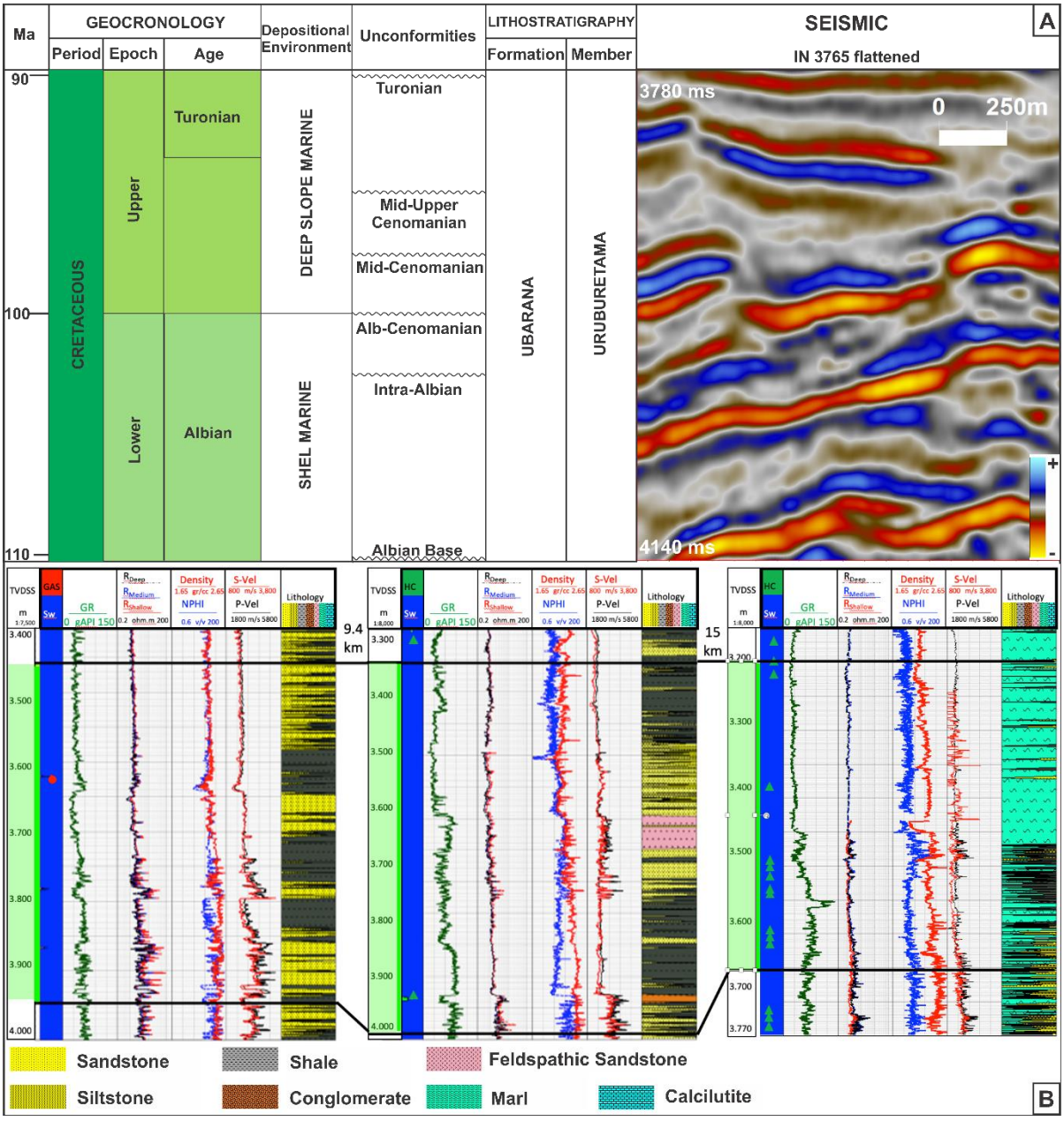

4.3. DATASET

This study is primarily based on a 3D seismic dataset in addition to three new exploration wells drilled for the oil industry between 2012 and 2013 (Figure 4-1c). This seismic survey was acquired in 2003 by CGG and covered ~1,107 km² of the deepwater Ceará Basin (Figure 4-1c). For the proposal of this research the seismic cube was cropped and covers an area of 765 km² with vertical geometry between -2772 and -5000 ms. It covers part of Premier Oil, Cepsa, Chevron, and Ecopetrol exploration blocks, as well as ANP's block of permanent offer (Figure 4-1c). The cropped seismic volume consists of 2233 inlines spaced 12.5 m with a 26.2° azimuth, and 2193 crosslines spaced 12.5 m. The central frequency is 25 Hz. The vertical resolution is a function of the P-wave velocity, given the highly variability of compressional velocity, varies from 14 m in the shallower region, to 70 m in the deepest interval. The seismic data are zero phase and normal polarity (SEG convention), where an increase in acoustic impedance is displayed as a positive amplitude (blue peaks) in the seismic cross section. The 3D post-stack seismic data was supplied with a standard processing flow and a quality control was conducted to determine issues associated with acquisition, noise and geological complexity for the whole cube. For example, a full prestack Kirchhoff time migration was applied to accurately image steep or overturned events. This step allows a better imaging geological setting characterized by complex structure increasing both vertical and lateral resolution.

The three exploration wells include a suite of wireline logs, drilling reports, and formation dynamic tester basic result. Our section of interest corresponds from Turonian to Albian age Formations, located between ~3330 m and ~3940 m (Figure 4-2b). We utilize stratigraphic markers and the associated ages from the three wells to aid in constraining the ages of major stratigraphic surfaces in the survey. We perform multimineral petrophysical evaluation to investigate, paramount reservoir properties (i.e. mineralogy, effective porosity and water saturation).

The borehole dataset consisted on shallow and deep resistivity curves, a total gamma-ray log (GR), corrected density, and neutron porosity. The compressional slowness and shear slowness were also recorded, having a larger interval, the compressional log, caliper log was also available to QC the borehole diameter, this was particularly critic due to the condition of the borehole, Amontada. Most of the geological information is provided by cuttings and sidewall core sample descriptions in well history reports, supplemented by borehole logs. Cutting samples were typically collected over 9 m intervals, while sidewall core sample spacing was more variable from Turonian to Late Albian age in two wells. The petrophysical and geomorphological analyses helped to calibrate the rock facies definition for training the deep

convolutional neural network (DCNN) while estimating S-wave velocity. Also, in the dataset a report of the modular dynamic formation tests is present to confirm the presence of hydrocarbon and the pressure intervals of the test. The check-shot in the three wells establishes an accurate time-depth relation with the seismic dataset. All of this data was supplied by the Brazilian National Agency of Oil, Gas and Biofuels (ANP).

4.4. METHOD

This research presents a general overview of the seismic geomorphology of the study area, aimed at delineating the turbidite channels, the primary depositional system for sands in this region. We used conventional seismic data interpretation techniques, 3D seismic attributes, and unsupervised machine learning techniques to investigate the seismic geomorphology and depositional environments from Albian to Turonian age interval (Figure 4-3). The geologic results are additionally correlated by applying a rock-physics model that leads to an improved understanding of lithology, water saturation, and porosity of the rocks, and their relation to seismic amplitudes.

In the first step, horizons were mapped and gridded to produce continuous surfaces with a grid cell size of 50 m. Then, the 3D seismic data set was cropped between these two horizons (Figure 4-4a and b). In this study, the Albian-Turonian interval consists, in part, of strong continuous reflectors incised by discontinuous reflectors with variable reflectivity (Figure 4-2a and 4-4d and e). A seismic geomorphology workflow was used to highlight structural and architectural elements by means of attribute analysis and well log interpretation (Figure 4-3), as well as the syn-sedimentary deposition of the sediments in this epoch.

Figure 4-3: Flow chart summarizing the methodology used in this work.

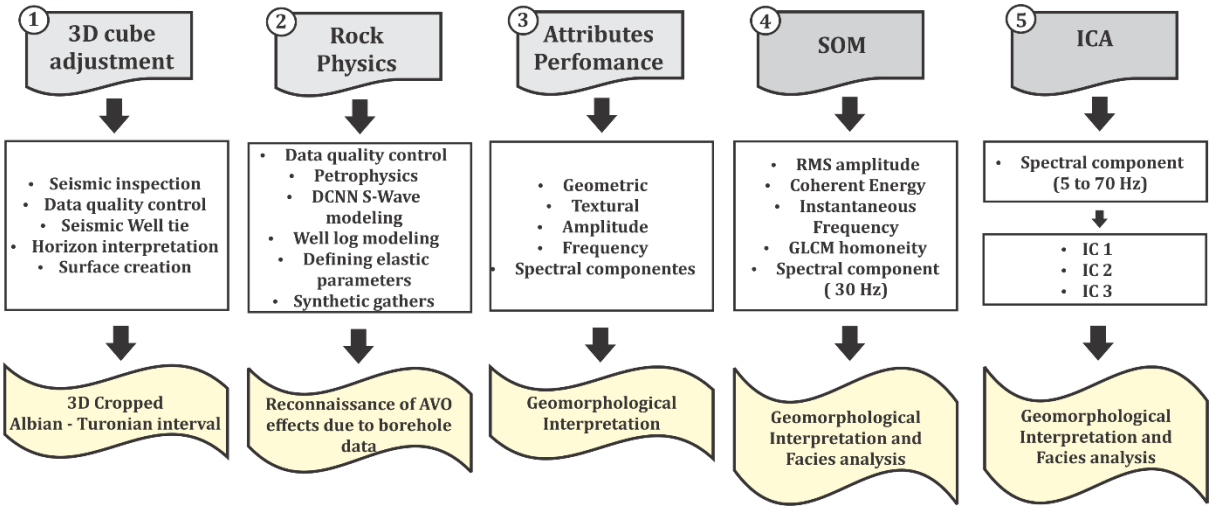

4.4.1. Seismic Attributes

After the seismic data was mapped, seismic attributes were generated based on the local dip and azimuth calculation of the 3D seismic data. For example, the coherence was calculated along volumetric dip and azimuth, which required more computational time than a coherence calculation without a dip search. Because of that, the dip-corrected coherence reveals features with geologic meaning, and not structure-induced anomalies. Attributes volumes, including root mean square (RMS) amplitude, sweetness, envelope, coherence, and spectral decomposition, were used to recognize the seismic geomorphology. Below is a summary of the attributes used in this study:

- The **RMS amplitude** is defined as the square root of the average of squares of the amplitude that is sensitive to map sand distributions (Brown, 2004). RMS amplitude map is widely used for the identification of channel sand bodies, direct hydrocarbon indicator (DHI), sand-rich shore bodies and high porosity (porous sands) (Taner et al., 1979).

- The **sweetness** attribute is calculated by dividing the reflection strength (or instantaneous amplitude envelope) by the square root of the instantaneous frequency (Radovich and Oliveros, 1998; Hart, 2008), and it is a useful attribute for detecting channels or other stratigraphic features. Usually, sweetness is used to map sand bodies because acoustic impedance contrasts between sands and shales tend to be high in clastic environments (Hart, 2008; Ahmad and Rowell, 2012).

- The **coherence** attribute is widely used in seismic interpretation and reservoir characterization to highlight faults and stratigraphic features since the 1990's (Bahorich and Farmer, 1995). Chopra and Marfurt (2007) define coherence as a measure of similarity between waveforms or traces. Coherence with high coefficients shows the similar traces, while low coherence coefficients highlight the discontinuities and anomalies over time or on horizon slices.

- **The envelope** is computed by taking the square root of the sum of the squares of the real and imaginary components (Taner et al., 1979). So, envelope (reflection strength) is sensitive to changes in acoustic impedance and thus to lithology, porosity, hydrocarbons, and thin-bed tuning (Chopra and Marfurt, 2007).

- **Spectral decomposition** has turn out to be a useful tool in delineating the paleo-channels of the seismic data during the past two decades. It is also quite helpful in predicting fault detection, lateral changes associated with changes in lithology, and the

depositional environments (Chopra and Marfurt, 2007). According to (Partyka et al., 1999), the lateral variation of frequency is associated with the changes in the sediment bed thickness along with lithology. So, as the spectral magnitude components are sensitive to impedance and thickness variations, they are thus good candidates for turbidite analysis (Lubo-Robles and Marfurt, 2019). Based on that, the seismic cube was decomposed on 14 components (5-70 Hz) using the continuous wavelet transform (CWT) method, which decomposes the seismic volume into phase and magnitude components at different time-frequency samples, often improving the temporal and vertical resolution and allowing us to interpret geologic features at different scales. These frequency components are similar to applying a band-pass filter to the volume and represent its information at a particular frequency (Chopra and Marfurt, 2015, 2016). The spectral magnitude components can be conveniently visualized using the three primary colors of red, green, and blue (RGB) in a single image (Figure 4-11).

Figure 4-4:Time-structural maps of the horizons at the study area: A) Albian base revealing the direction of sediments supply. B) Turonian top. C) Thickness map of the Albian base to Turonian interval. The location of three deepwater wells are shown. D) The 3D cube cropped showing the crossline 2251 and the 1BRSA 1114 CES well. Above it is displayed the original seismic cube and below is shown the flattened seismic cube. E) The crossline 2230 and the location of the phantom horizons interpreted.

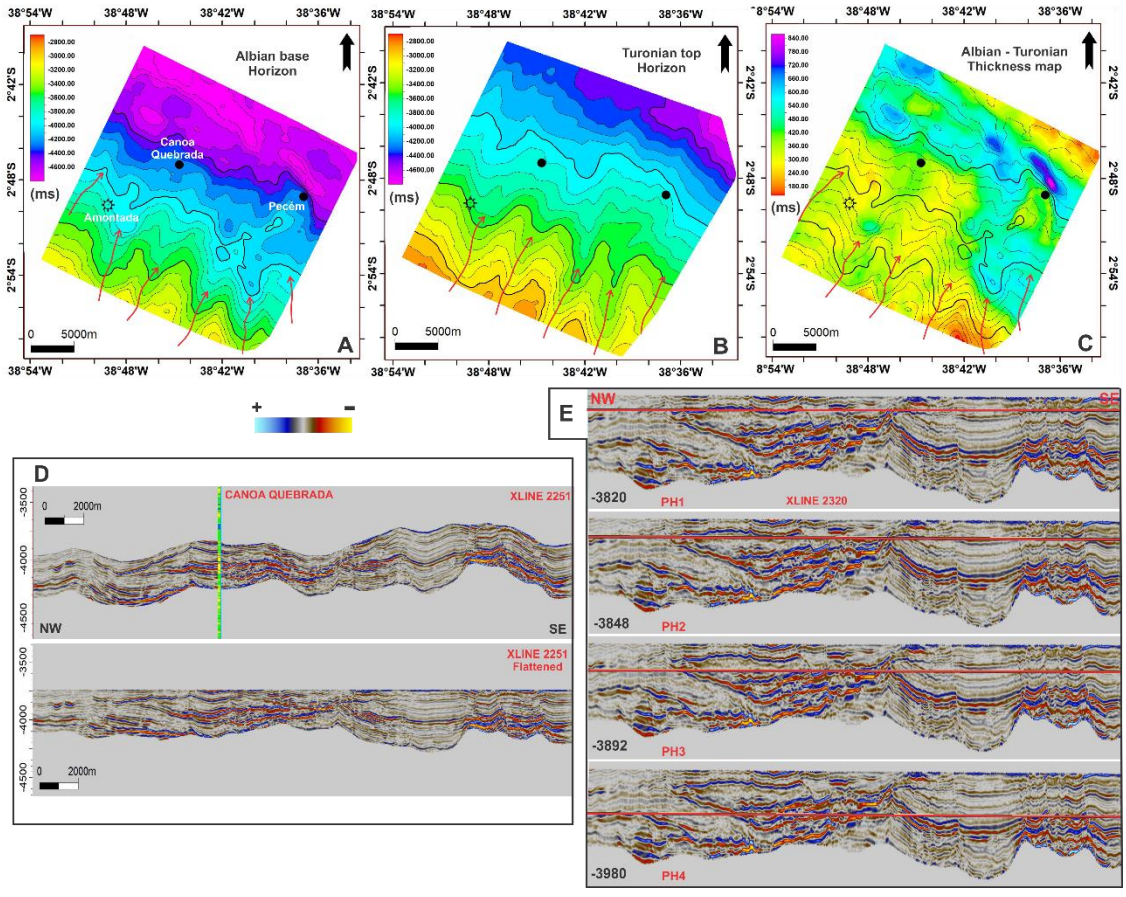

Different attributes highlight different features of interest. Combining them using multi-attribute analysis techniques provides a means to better understand the underlying geologic processes, and to better characterize geological features. Results of the attributes were then analyzed and compared at the same location to select the best attributes used on the unsupervised machine learning techniques. The RMS amplitude, sweetness, and envelope attributes were compared to well log facies distributions to check the validity of any relationship between this attribute and shale/sandstone content in the study area.

4.4.2 Rock Physics

In order to understand the seismic amplitude information and its link with the rock properties we required a theoretical rock physics model. The rock physics model bridges the petrophysical properties to the seismic information. In this analysis, we used borehole data from three wells drilled in the basin in a radius of 6 km.

We examined the borehole dataset to find a theoretical rock physics model that (i) corrects the velocity curves; (ii) to train the deep convolutional neural network (DCNN) into a confident S-wave and other curve estimations, (iii) to generate seismic synthetic gathers that allow us to classify the possible amplitude variation response in the Albian -Turonian interval. To overcome the first objective, we perform a petrophysical analysis to estimate the mineralogy, porosity and fluid content. Mineral estimation was necessary due to the presence of complex heterogeneities in the rock deposits of the Albian-Turonian interval (i.e. arkosic coarse sandstones, sandstones with calcite cement, marl intercalations in shales, feldspathic sandstones, silty feldspathic sandstones, marls, and calcilutites).

Once we better understood the petrophysical parameters, we modeled the curves to generate cleaner and sharper responses of the elastic curves. These petrophysical parameters and mineralogy were used as inputs to the DCNN model. Seven input parameters (water saturation, effective porosity, clay content, quartz content, calcite content, RHOB, Vp), were used, over thirty epochs and reached a calculated accuracy of 0.97. We calibrated and trained the S-wave modeling by using the existing S-wave information from the boreholes or other boreholes in the vicinity. The rock-physics model was selected qualitatively by investigating different rock physics templates for the various intervals. We compared the synthetic seismic gathers generated using elastic wave equations and traces with the trace observed in the seismic study. We then performed a perturbation study, to evaluate the possible responses in amplitude of different reservoir conditions. We modeled a 50/50 gas-brine scenario, 80/20 oil-brine

scenario and 30/30/40 gas-oil-brine scenario to look for these amplitude responses on the seismic and make a catalog of the possible AVO/AVA classes responses in the intercept and gradient domain (Figure 4-5).

Figure 4-5: AVO/AVA classes summary from generating seismic synthetic gathers and changing the reservoir conditions. Tight felspathic sandstones and conglomerates are the only lithology with a clear fluid vector definition. For all the other cases, the AVO/AVA response might be ambiguous, especially for the base of the Albian.

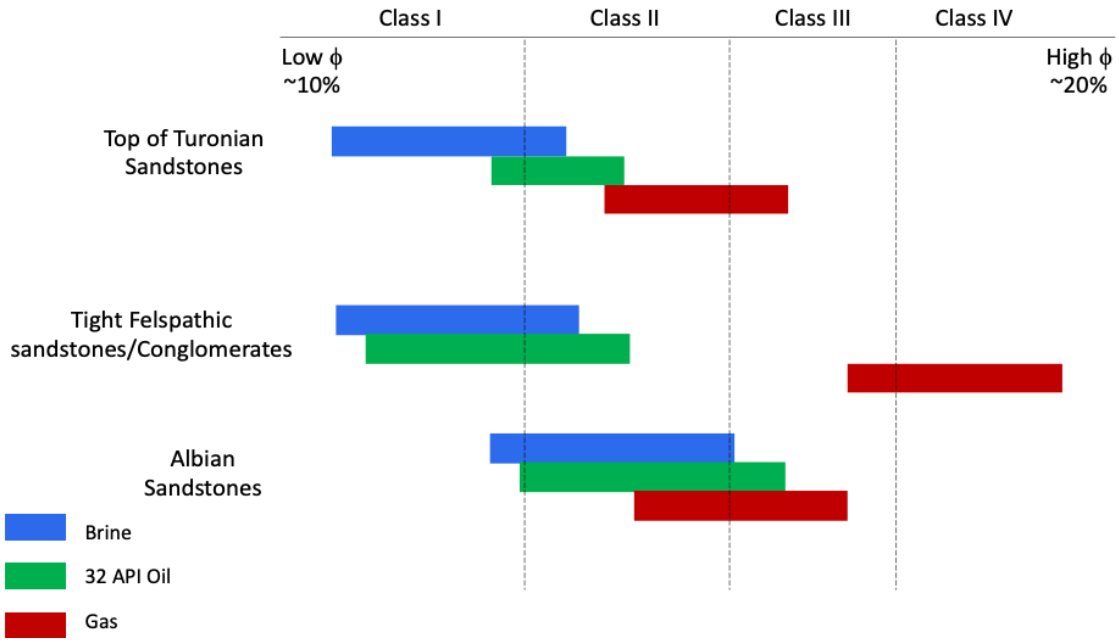

4.4.3 Machine Learning Techniques

To better evaluate the seismic facies, we employed self-organizing maps (SOM) and independent component analysis (ICA) algorithms to define the facies. The SOM is an unsupervised machine learning technique that was first introduced by Kohonen in 1982 and is frequently used in many areas to find patterns with similar characteristics within their respective datasets. Multiattribute analysis is laborious and time-consuming, and so to enhance this analysis, we chose to explore unsupervised machine learning methods to better characterize seismic facies in deepwater channels. The SOM algorithm was widely applied to define zones of interest in the oil and gas industry in the last decades (Linari et al. (2003), Coleou et al. (2003), Poupon et al. (2004), Verma et al., (2012), Roy et al. (2013), Roden et al. (2015), and Zhao et al. (2016)), and thus we chose to apply it herein.

For the SOM attribute inputs, we used: 1) RMS amplitude; 2) coherence energy; 3) instantaneous frequency; 4) GLCM homogeneity; and 5) spectral magnitude component 30Hz. These attributes were chosen based on Roden and Sacrey (2015) list of common seismic

attributes, their type, and interpretative use. The sweetness and envelope were not chosen to avoid redundancy since their response are similar to RMS amplitude attribute.

The ICA approach is directly related to projection pursuit (Huber, 1985), which is a statistical technique for finding “interesting” projections of multidimensional data. In turn, such projections are useful for optimal data visualization (Honório et al. 2014). This technique is considered as an extension of principal component analysis (PCA) (Hyvärinen et al., 2001), and it assumes that the signal has a non-Gaussian distribution. Therefore, considering that the seismic data can be viewed as signals with either super-Gaussian distributions (i.e., with positive kurtosis (Walden, 1985)) and non-Gaussian distributions, this assumption fits the fundamental assumption of ICA (Honório et al., 2014). We chose this technique to reduce the multiplicity of spectral data and enhance the most energetic trends inside the data that can be visualized using the three primary colors of red, green, and blue. In this study, we used this algorithm to extract the spectral response that can better delineate seismic features associated with different geologic features. 14 spectral magnitude components (5-70 Hz) attributes were used as input. This approach has been used to seismic analysis of carbonates (Li et al., 2014; Bueno et al., 2014), as well as fluviodeltaic system (Honório et al., 2014), and turbidite channels (Lubo-Robles and Marfurt, 2019).

The seismic cube has a considerable dip, for this reason to interpret the geomorphology and facies each attribute, spectral magnitude component, self-organizing map, and independent component were flattened against the Turonian horizon, which is equivalent to extracting phantom horizons parallel to Turonian top (Figure 4-4e). This approach helped us to do an ideal analysis of this interval. Four phantom horizons were created bracketing the top and bottom of our interest interval, resulting in an analysis interval of ~350 ms (Figure 4-4d and e). Distribution of sand-rich facies was characterized by combining the results of multi-attribute analyses, and supported by well validation.

4.5 RESULTS AND DISCUSSION

4.5.1 Geophysical characteristics of the Albian to Turonian interval

The seismic reflection profile shows the characteristic of channel sandstones as the convex bottom in the central area of the study area while on the eastern area the reflectors are parallel and continuous presenting more NW-SE fault-related deformation (Figure 4-4d). The difference in the velocities of sandstone and shale is minimal (Figure 4-2b) and becomes more significant in the feldspathic sands and conglomerates, as opposed to the shale and marls

(Figure 4-2a). The density shows larger contrast between the carbonate influenced lithologies than the sandstone and shales (Pecém vs Canoa Quebrada and Amontada). This combination of velocity trends and density variations suggest that there is an acoustic impedance contrast between the different lithologies, where the strongest amplitudes can be linked to calcite layers – feldspar sands or conglomerate deposits. This means that the seismic amplitude reflections can be observed on the seismic section, and used in the study area for channels detection. The Canoa Quebrada has a thick layer of almost 60 meters with a high gamma ray reading where the facies were registered as sandstones. The high gamma ray response is due to the potassium content in the arkosic sandstones which account for the high readings in the log, this effect is also evident on the P-wave and Density logs as an increase of values. (Figure 4-2b).

Results of the petrophysics, and facies analysis indicate the presence of a greater influx of sand-rich sediments close to the Amontada and Canoa Quebrada wells, while the Pecém well has a higher proportion of shale when compared to sandstone (Figure 4-2b). These three wells share a high input of calcite cement and a component of silica, borehole Amontada shows coarser sands, and Canoa Quebrada have a larger variability in the deposited sandstones varying from coarse sandstones, silty sandstones, feldspathic sandstones and conglomerates intercalated with shale deposit (Figure 4-2b). Borehole Pecém has a dominance of marl, shales, and sporadic conglomerate deposit, this creates a minimal velocity contrast between each lithology except the calcite layers that vary from 2 to 15 meters.

The petrophysical wireline interpretation suggests that the Amontada borehole is gas prone. This interpretation is confirmed by the drilling reports wherein a gas influx was observed when drilling thru a 30-meter-thick shaly sequence (Figure 4-2b). In contrast, the Canoa Quebrada borehole MDT reported two different intervals with oil shows in the zone of interest. The shallower oil interval was reported from a thin sandstone. The second oil show during the dynamic test happened on a low porosity conglomerate. The conglomerate thickness is around twenty meters, but, due to the low porosity and thinness, this interval was deemed uneconomic. Nevertheless, the presence of oil at this position of the stratigraphic section opens the possibility of more favorable facies and better rock reservoir conditions that could contain hydrocarbon.

The combination of low porosity, and the reported mineralogy yields into a high impedance interval, both for the reduced thickness sand and the conglomerate facies. The amplitude character of these is Class I for an 80/20 oil case or even Class IIn, for a 50% gas

saturation. The expected porosity range around this depth, based on the logs, would be 16 to 20%.

For the case of the channel feeder, we might expect a similar behavior, a small or null contrast between sandstones and shales, that would be a Class IIn or IIp, for all perturbations of the rock physics model that we perform. The input of the felspathic sandstones and conglomerates would show a Class I AVO/AVA. For these lithologies in the stratigraphic interval of interest represents the most observable amplitude anomalies with a clear hydrocarbon response (Figure 4-5).

On the other hand, the small to null contrast of the sandstones and shales are likely due to the compacted shales having a similar acoustic impedance with the cemented sandstones. The porosity decreases rapidly by the influx of sediments increasing overburden as can be seen in the effective porosity trends and, the mineralogy combination of the sandstones.

The Albian base horizon presents increased depths in the northwest of the study area with a uniform sediment distribution from upslope to deepwater (Figure 4-4a). In the east, close to the Pecém well, there is a structural high that changes with depth abruptly, down to a depocenter with a NW-SE trend. The slope has canyons and bypass zones that supply sediment in a NW-SE direction and in a NE-SW direction closer to Amontada (Figure 4-4a).

The Turonian top horizon reveals increased depths in the northeastern portion of the study area, with regular sediment distribution on the continental slope. The sediment supply zones are narrow (red arrows in Figure 4-4b) at this age and the sediment supply in the toe-of-slope has a more regular distribution when compared with the previous horizon described. The isopach map of the Albian to Turonian horizon demonstrates that there is a depositional thinning in the extreme northeastern zone, while in scattered areas, the thickness is observed to be greater (Figure 4-4c). In the eastern area of the slope, there is a subtle depocenter that is controlled by the upslope and a structural high near the Pecém well. Also, this structural high divide two depocenters in the northeastern portion of the area (Figure 4-4c).

4.5.2 Deepwater environments identification using seismic attributes analysis

Phantom horizon 1 (PH1 - youngest)

This horizon corresponds to the -3820 ms of the flattened cube. The variations of the amplitude values help us to detect and identify meaningful geological features on the RMS amplitude map. The calculated RMS displays scattered high amplitude anomalies all over the

study area, but they are primarily prevalent in the northwest and southeastern parts of the area. NW-SE trending faults are identified in the northeastern region of the area (light blue arrows Figure 4-6a). Three arbitrary seismic lines were extracted and are displayed in Figure 4-6a to better visualize the channels, point bars and levees (pink rectangle). The RMS map of this slice reveals a clear image of a wide channel-like feature (red arrow Figure 4-6a) as well as associated smaller channels, which are better visualized in the seismic vertical sections (Figure 4-6a). Coherence slices were generated and overlaid with envelope and sweetness attributes. The low coherence sinuous features are associated with the darker regions. The very dark regions on the horizon slices are interpreted as faults, while parallel and narrow, dark, sinuous zones surrounding bright, sinuous zones are interpreted as channels. An overlay of the sweetness with coherence shows the different geologic features seen on the previous attributes described above. Some features, similar to point bars, are observed in the central area (pink arrow - Figures 4-6b). Toward the north, the filled channel is better defined by the high sweetness values that follow a NW-SE direction to the edge of the seismic cube (Figures 4-6b). In the northeast, two depocenters are well-defined with high sweetness values on its edges, and the depocenters are separated by a series of NW-SE faults (dark and light blue arrows in Figures 4-6b). A few dendritic lobes are observed on the western part of the area, and are apparently feeding the smaller meandering channels that are characterized by high RMS, envelope, and sweetness values (purple and brown arrows in Figures 4-6). On the upslope, only a feeder channel is observed in the southwestern region (green arrow – Figures 4-6b). An overlay of the envelope and coherence in Figure 4-6c reveals the different geologic features seen on the previous attributes described above (i.e. channels, point bars, faults, depocenters). A dendritic lobe is observed on the western portion of the area and seems to feed small high sinuosity meandering channels that are characterized by high RMS and envelope values (brown arrows in Figures 4-6a and b).

Figure 4-6: Seismic attribute analysis of the phantom horizon 1: A) The RMS amplitude with the features interpreted. The location of three deepwater wells are shown as well as the location of the arbitrary seismic sections. Vertical seismic sections are shown in the top right. B) Sweetness map with features interpreted. C) Envelope with features interpreted.

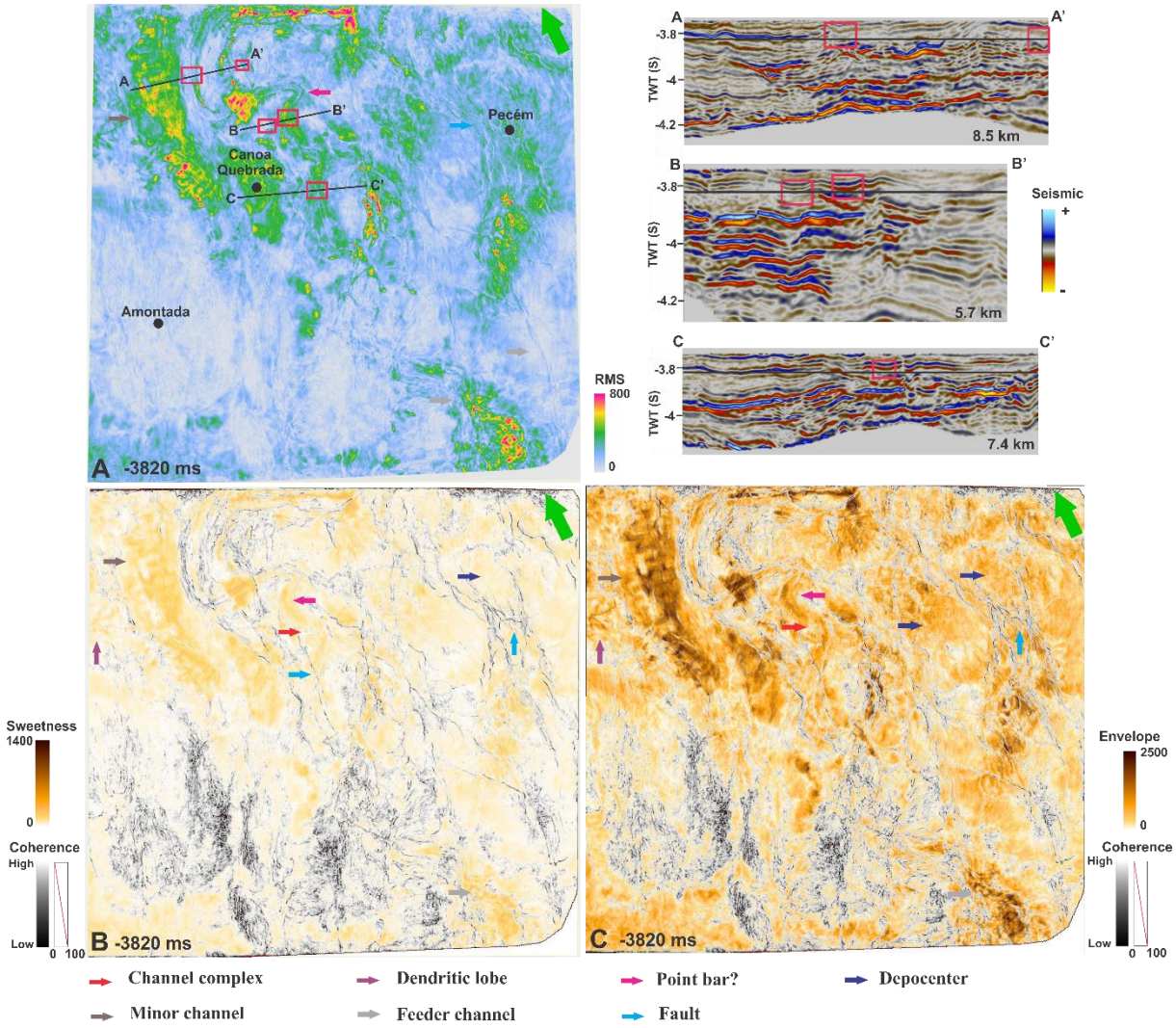

Phantom horizon 2 (PH2)

This horizon corresponds to the -3848 ms horizon of the flattened cube (Figure 4-4e). High RMS amplitudes are observed in the central region, and in some portions of the western and eastern regions of the area, primarily inside dendritic lobes and feeder channels (Figure 4-7a). Three arbitrary lines were extracted in Figure 4-7a to better visualize the channels, point bars and levees (pink rectangle) in the seismic data. A geological feature with high RMS amplitude and similar to a point bar is well defined in the central area (pink arrow in Figure 4-7a). The central meandering channel is wider and better delineated on this phantom horizon. The edges of the two depocenters are well defined in this time horizon when compared to the previous one, and the NW-SE faults are observed bounding these depocenters (Figure 4-7a). Also, the feeder channel in the southeast is wider and is linked more clearly to the main meandering channel (green arrow Figure 4-7a). A fan-like structure is characterized by a high RMS amplitude in the east (black arrow in Figure 4-7a). An overlay of the sweetness and coherence attributes reveal some features similar to point bars in the central area (pink arrow in

Figure 4-7b). To the north, the edge of the channel complex is better defined by high sweetness and coherence values (Figure 4-7b). At this time, the two depocenters have their edges well-imaged by high sweetness values, and the faults bounding them are more visible (dark and light blue arrows in Figure 4-7b). Two of dendritic lobe are revealed by high sweetness values on the western part of the area, and are apparently feeding smaller channels that are also characterized by high and low RMS and envelope values. On the upslope, a feeder channel observed in the last described horizon is barely seen in the southwest of the area (green arrow in Figure 4-7b). Overlay of the envelope and coherence maps provides a good image of the channel shape and the faults (Figure 4-7b). The sinuous features are interpreted as channel edges, while the straight features are interpreted as faults. This pattern is also observed in the seismic vertical sections. Two dendritic lobes with higher envelope values are imaged on the western portion of the area and seems to feed smaller channels that are characterized by high and low RMS and envelope values (Figure 4-7b). The same geological feature observed with the RMS amplitude are seen with these attributes, however the feature similar to a point bar is noted to have a longer length (pink arrow) (Figure 4-7b).

Figure 4-7: Seismic attribute analysis of the phantom horizon 2: A) The RMS amplitude with the features interpreted. The location of three deepwater wells are shown as well as the location of the arbitrary seismic sections. Vertical seismic sections are shown in the top right. B) Sweetness map with features interpreted. C) Envelope with features interpreted.

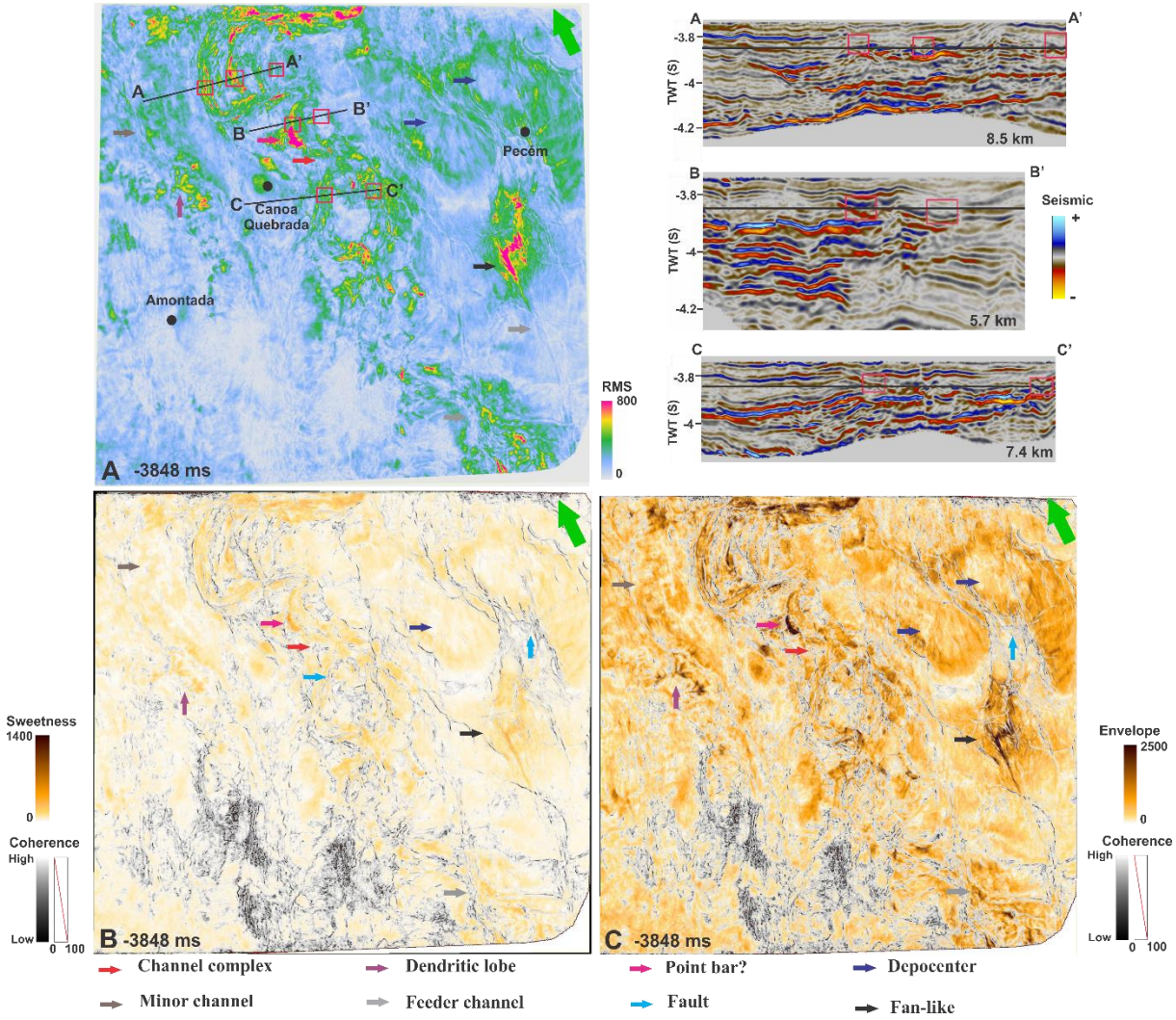

Phantom horizon 3 (PH3)

This horizon corresponds to the -3892 ms of the flattened cube (Figure 4-4e). The RMS amplitude displays high RMS anomalies mainly in the central area (main channel complex), and in the eastern part of the basin (Figure 4-8a). Images of small, channel-like features are observed in two areas: 1) the northwestern area (presenting a bifurcation and three distributaries), and 2) in the southeastern part of the basin, on the upslope, where the channels trend NW-SE, slightly parallel to the regional fault trend in the basin (Figure 4-8a). In the southwest of the area, near the Amontada well, a geological feature resembling a mass transport deposit has a few dendritic lobes that seem to feed into a smaller channel. In the northwestern area, the smaller channel bifurcates into three distributary flows (Figure 4-8a). Overlay of the sweetness with coherence shows the different geologic features seen on the previous attributes described above. Toward the north, the edge of the channel complex is no more well defined by the high sweetness and coherence values. Also, the channel complex does not change its direction as the previous horizons suggested (Figure 4-7). An overlay of the envelope and

coherence maps provides a good image of the channel complex, smaller channels, and the faults (Figure 4-8c). The same geological features observed with the RMS amplitude are seen with these attributes, however the feature similar to a point bar, presented in the previous horizon described, is no longer observed (Figure 4-8c). At this geologic time, the two depocenters have their central part well defined by a high RMS, envelope, and sweetness values and the faults separating them are more visible (dark blue arrows in Figure 4-8).

Figure 4-8: Seismic attribute analysis of the phantom horizon 3: A) The RMS amplitude with the features interpreted. The location of three deepwater wells are shown as well as the location of the arbitrary seismic sections. Vertical seismic sections are shown in the top right. B) Sweetness map with features interpreted. C) Envelope with features interpreted.

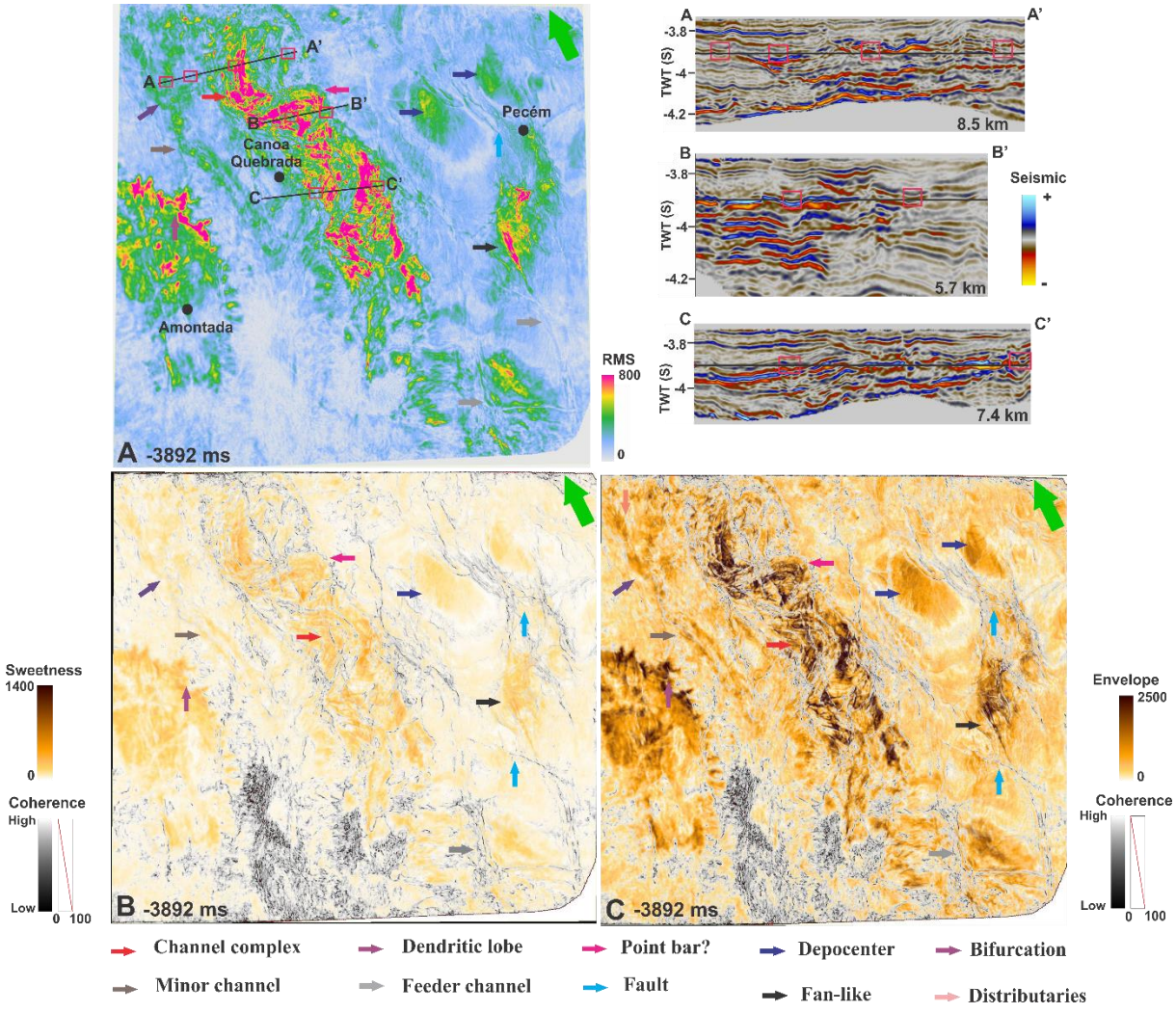

Phantom horizon 4 (PH4 – oldest)

Phantom Horizon 4 is the deepest horizon of the Albian – Turonian interval (Figure 4-4e). The RMS amplitude map displays scattered high RMS anomalies, mainly in the southeastern, and central part of the basin following a NW-SE trend (Figure 4-9a). Images of small, channel-like features are also observed. However, the main channel complex is not well

imaged as in the PH3 (red arrows in Figure 4-9a). In the middle part of the basin, channels are wider when compared to the previous described horizons and they follow a NW-SE trend. Two fan-like structures are characterized as a high RMS amplitude in the east of the area (black arrow in Figure 4-9a). A NW-SE fault is imaged cutting the channel feeder of one of these structures. The geological feature similar to a mass transport deposit is no longer seen on this horizon. Small channels with low RMS values are imaged in the northwest, and they are better defined in the A -A' seismic section (Figure 4-9a). The sweetness with coherence overlay shows the same geometries and orientations of the geologic features described in the younger intervals (Figure 4-9b). At this time, the center of the two depocenters have low RMS, envelope, and sweetness values (Figure 4-9). Overlay of the envelope and coherence maps provides a good visualization of the wider channel complex, smaller channels, and the faults (Figure 4-9). The same geological features observed with the RMS amplitude are seen with these attributes (i.e. channel complex, point bars, feeder channels, faults, depocenters, smaller channels).

We relate the seismic facies with lithologies from the Canoa Quebrada well report. Figure 4-10 demonstrates that the high RMS amplitude, sweetness and envelope values are associated with sand-prone seismic facies. It is possible to correlate the sand-prone seismic facies because the facies thickness is approximately 40 m; which is above the seismic resolution.

Figure 4-9: Seismic attribute analysis of the phantom horizon 4: A) The RMS amplitude with the features interpreted. The location of three deepwater wells are shown as well as the location of the arbitrary seismic sections. Vertical seismic sections are shown in the top right. B) Sweetness map with features interpreted. C) Envelope with features interpreted

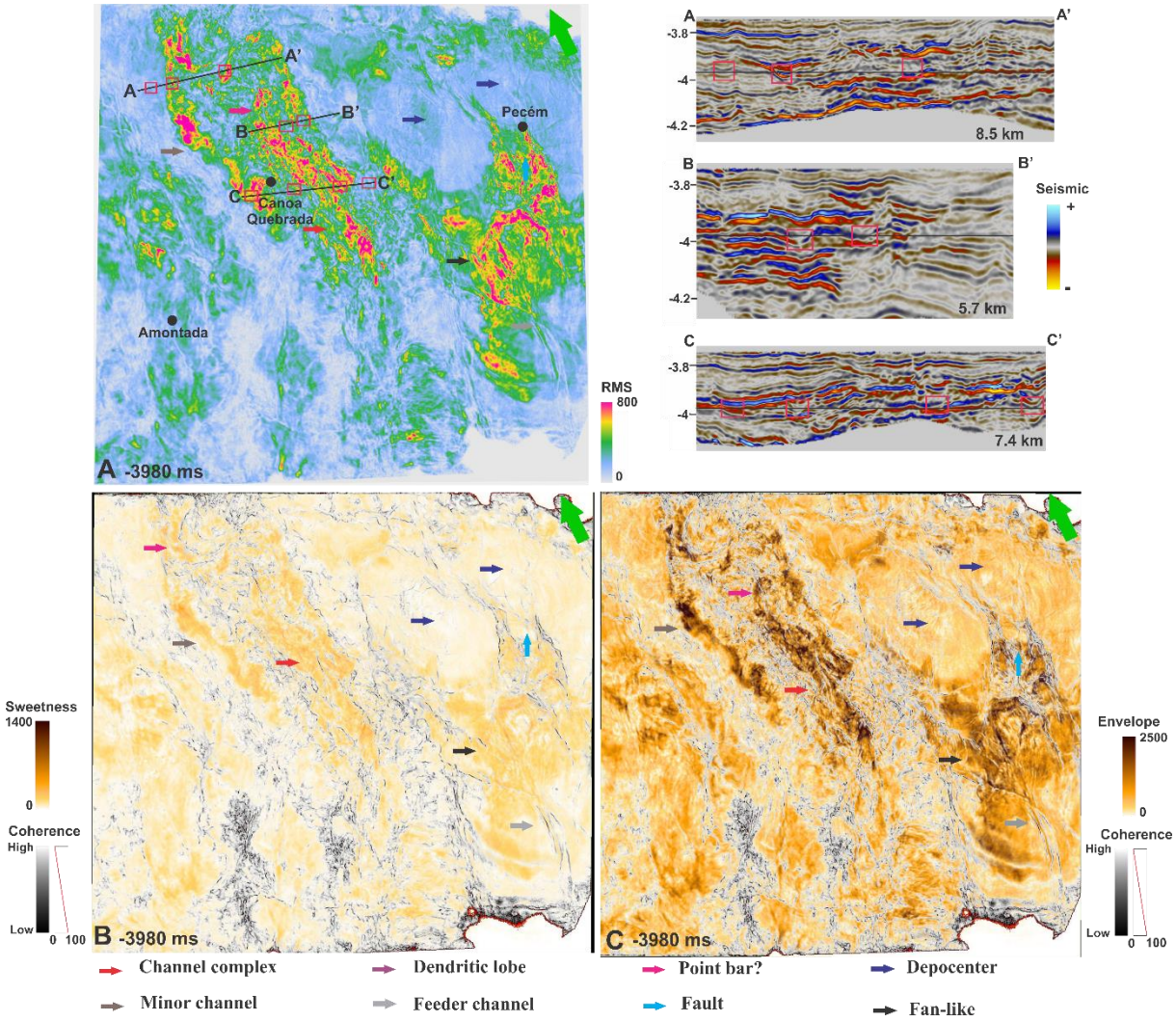

We relate the seismic facies with lithologies from the Canoa Quebrada well report. Figure 4-10 demonstrates that the high RMS amplitude, sweetness and envelope values are associated with sand-prone seismic facies. It is possible to correlate the sand-prone seismic facies because the facies thickness is approximately 40 m; which is above the seismic resolution.

Figure 4-10: Vertical seismic section showing the Inline 3765 and the 1 BRSA 1114 CES well: A) seismic amplitude section. B) RMS amplitude and its zoom in in the right. C) Sweetness its zoom in in the right. D) Envelope its zoom in in the right.

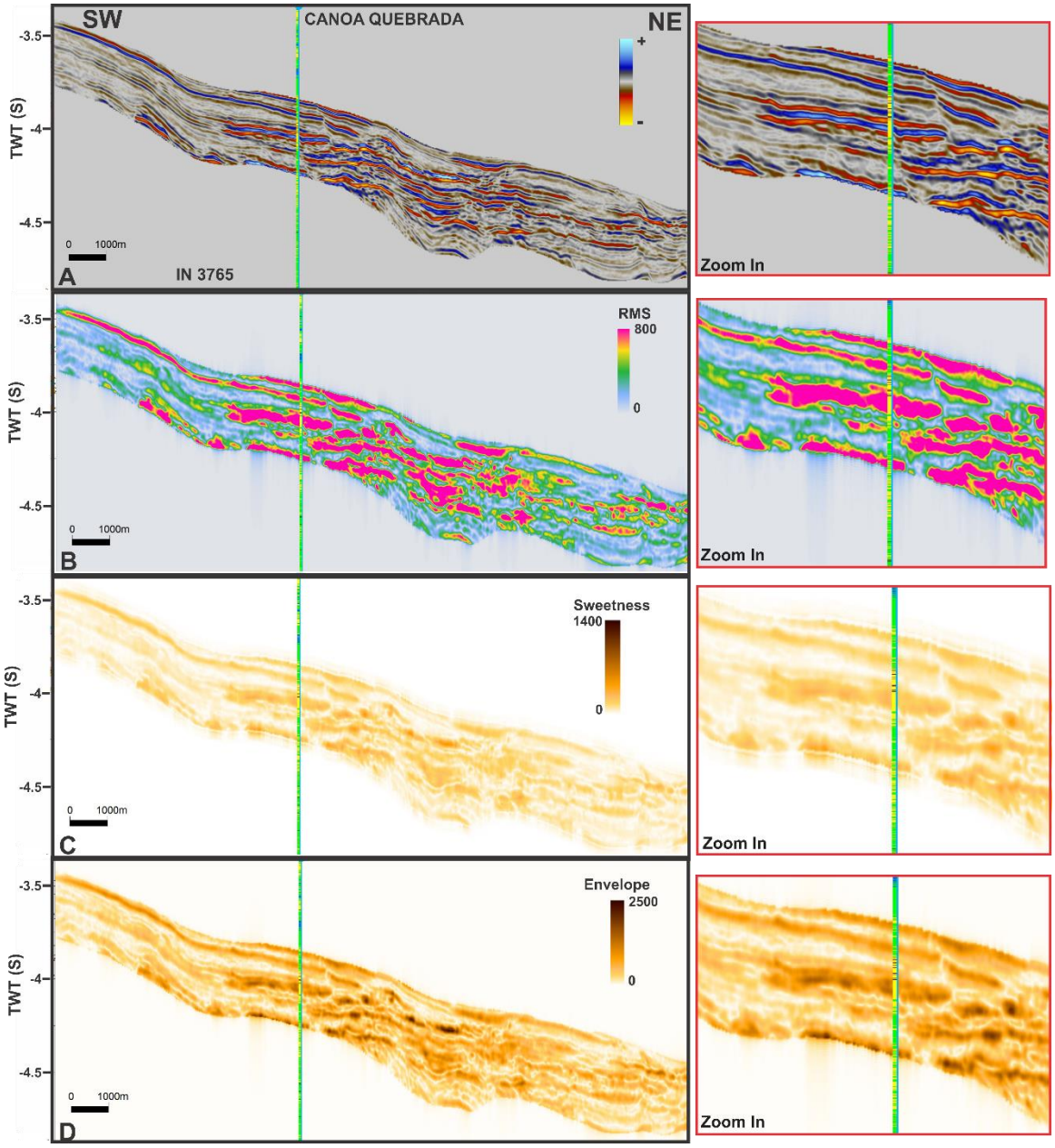

RGB blending interpretation

The RGB blending of three different spectral magnitude components (20, 30, and 50 Hz) provides better visualization of channel geometries compared to other single attributes as it combines together the channels delineated in different frequencies. For Phantom Horizon 1, this combination better delineates the meandering channel in the central part of the study area (Figure 4-11a). Also, note that the infill of the channel tends to tune at the low frequencies while their flanks are more coherent at approximately 30 Hz. Some thin beds tune at high frequencies of approximately 50 Hz. The meandering channels and smaller channels are better resolved in using this visualization technique. A few dendritic lobes are well imaged to the west, feeding smaller channels. In the northeastern region, the depocenter and its edges are well delineated at

20 and 30 Hz, respectively. One additional advantage of the spectral magnitude visualization is the improved definition of faults, coinciding with the improvement in imaging stratigraphic features.

Figure 4-51: Spectral magnitude components plotted against an RGB color using a combination of 20–30–50 Hz: A) Phantom horizon 1 (youngest); B) Phantom horizon 2; C) Phantom horizon 3; D) Phantom horizon 4 (oldest). The well locations are displayed as a white dot.

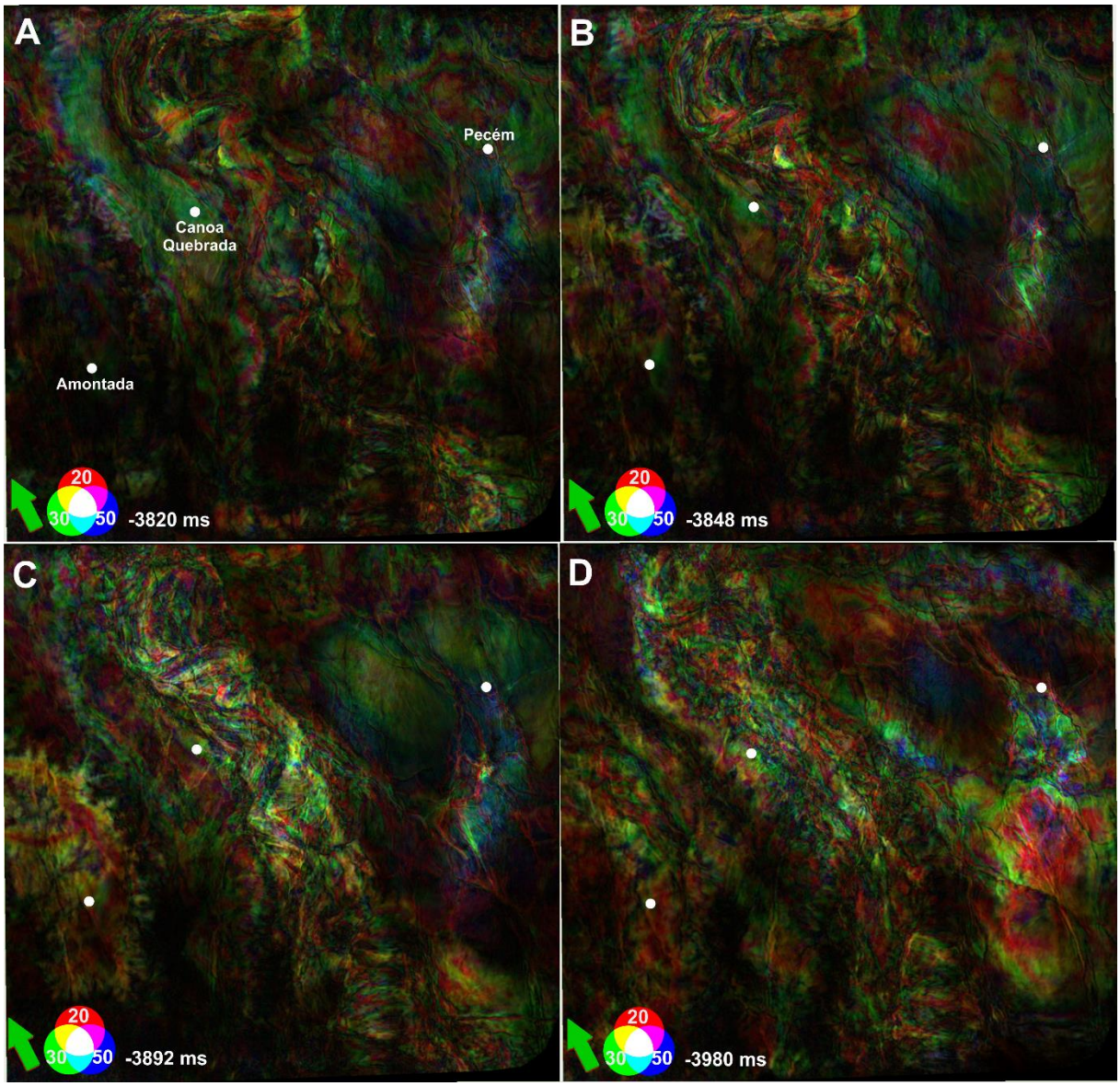

The PH2 period channel complex is wider compared with the PH1, with high sinuosity and follow a NW-SE trend. The central meandering channel is still well delineated, and the infill tends to tune at low frequencies, implying a thicker interval. The flanks are coherent at 30 Hz and the size of the channel at this level is smaller as compared to PH1. Moreover, the two depocenters are imaged on both horizons, but it is better highlighted at this horizon. In the southwest of the area, near the Amontada well, the geological feature similar to

a mass transport deposit has its central part tending to tune at the low frequency (20 Hz) while its edges are more coherent at approximately 30 Hz. This structure is linked with a few dendritic lobes that are feeding a straight smaller channel (Figure 4-11). A fan-like feature is delineated in the east of the area and its central part tends to tune at intermediate frequencies (30 Hz).

The PH3 period channel complex is wider compared with the PH2, with high sinuosity and follow a NW-SE trend. The central meandering channel is no longer well delineated because the various channels that are adjacent. However, some portions of the central meandering channel are still well delineated and the infill region tends to tune at low frequencies. The flanks are coherent at higher frequencies (30 and 50 Hz) (Figure 4-11c). The two depocenters are well imaged and their central portion tend to tune at intermediate frequencies (30 Hz). In the southwestern area, the geological feature similar to a mass transport deposit has a small channel tending to tune at the low frequency (20 Hz) while its edges are more coherent around 30 Hz. This structure is linked with a few dendritic lobes that are feeding a straight smaller channel (Figure 4-11c). The shape of this smaller channel was better imaged by low frequencies (20 Hz). The observation shows that at 30 Hz frequency, the channel flanks are better visualized (Figure 4-11c). The faults to the northeast are better highlighted at this horizon, and a fan-like feature is delineated in the east and its central part tends to tune at intermediate frequencies (30 Hz).

For PH4, the composite RGB image (Figure 4-11d) delineates thin beds inside the channels. Note that the infill of the small channels tends to tune at low frequencies while their flanks are more coherent at approximately 30 Hz. Also, some thin beds tune at high frequencies of approximately 50 Hz (Figure 4-11d). The wider channel complex follows a NW-SE trend and it is composed by small meandering channels. A fan-like deposit is well delineated in the east of the area and its central part tends to tune at low frequencies (20 Hz) while its edges are clearly better displayed at 30 Hz frequency. This horizon is more affected by faults than the horizons above described. Channels developed in this period are interpreted as meandering channels developed in a channel complex with energy.

The spectral magnitude components analysis provides greater resolution and detection of the layer-stacking heterogeneity, boundaries, and thickness variability than are possible with traditional broadband seismic attributes (Brown, 2008). For instance, the progression from red to green to blue indicates an increase in sedimentary thickness of the main channel-complex, and is observed from the deeper to shallower part of the depocenters in the

PH1 and PH2 (Figure 4-11a and d). The RGB blending provided insights in both stratigraphic and structural edges, as well as relative temporal thickness when comparing the frequencies in all the horizons (Figure 4-11). This is because as the amplitude contours move from thick towards thins as we proceed from low to high frequency. Also, the upper slope was better imaged when compared to the volumetric seismic attributes (Figure 4-11). This enhancement is because low-frequency components provide good images in poor data area due to the highest signal-to-noise ratio often exists at lower frequencies.

4.5.3 Unsupervised Machine Learning for Seismic Facies Classification

Geologic features seen on Self-organizing map

Figure 4-12 displays the seismic attributes chosen to SOM volumetric classification: 1) RMS amplitude; 2) coherence energy; 3) instantaneous frequency; 4) GLCM homogeneity (Figure 4-12); and 5) spectral magnitude component 30Hz as discussed in the Methodology. These attributes maps are also interpreted in terms of deepwater depositional elements.

Figure 4-62: Seismic attributes used to SOM clustering: A) RMS amplitude. B) Coherent Energy; C) Instantaneous Frequency; D) GLCM homogeneity.

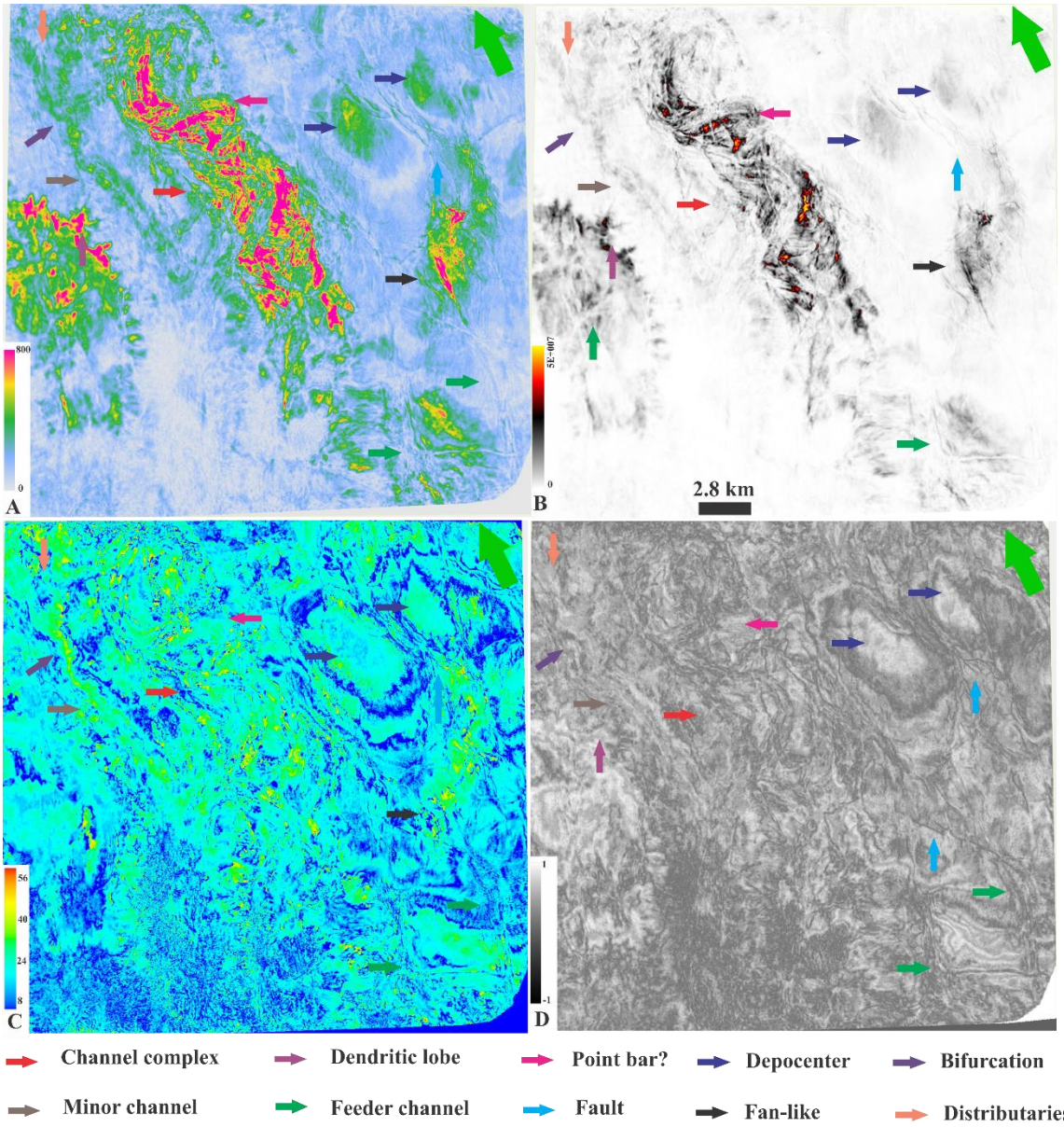

Figure 4-13 shows the four phantom horizons that illustrates the distribution of the seismic geomorphology that was also observed in the seismic attribute's analysis. However, in the upslope, the architectural elements are not well defined (e.g. feeder channels) and the geomorphology close to the Amontada well is not well characterized. A vertical slice is shown with our SOM facies classification (Figure 4-13e). From this classification, we can observe three distinctive colors (facies). The green colors represent the continuous high-amplitude facies, and the bright green represent the seismic reflector with a high impedance contrast. Comparing the results to the well facies, these colors are associated with a metric interbedded sandstones and shales (sandstone >> shale). The purple colors are more representative of the chaotic moderate amplitude facies. Figure 13e shows that the purple colors are associated with a subtle interbedded shales and sandstones (shales >> sandstones). The blue colors represent the weaker reflections that are more representative in the upslope (Figure 4-13a to e).

Figure 4-73: SOM results presented in the four phantom horizons that highlight the deepwater elements: Phantom horizon 1 (youngest); B) Phantom horizon 2; C) Phantom horizon 3; D) Phantom horizon 4 (oldest). The well locations are displayed as a white dot; E) Inline 3765 in seismic amplitude below and SOM result in the top. Evaluation of the seismic facies and sand-rich elements by using log facies information from the 1 BRSA 1114. CES

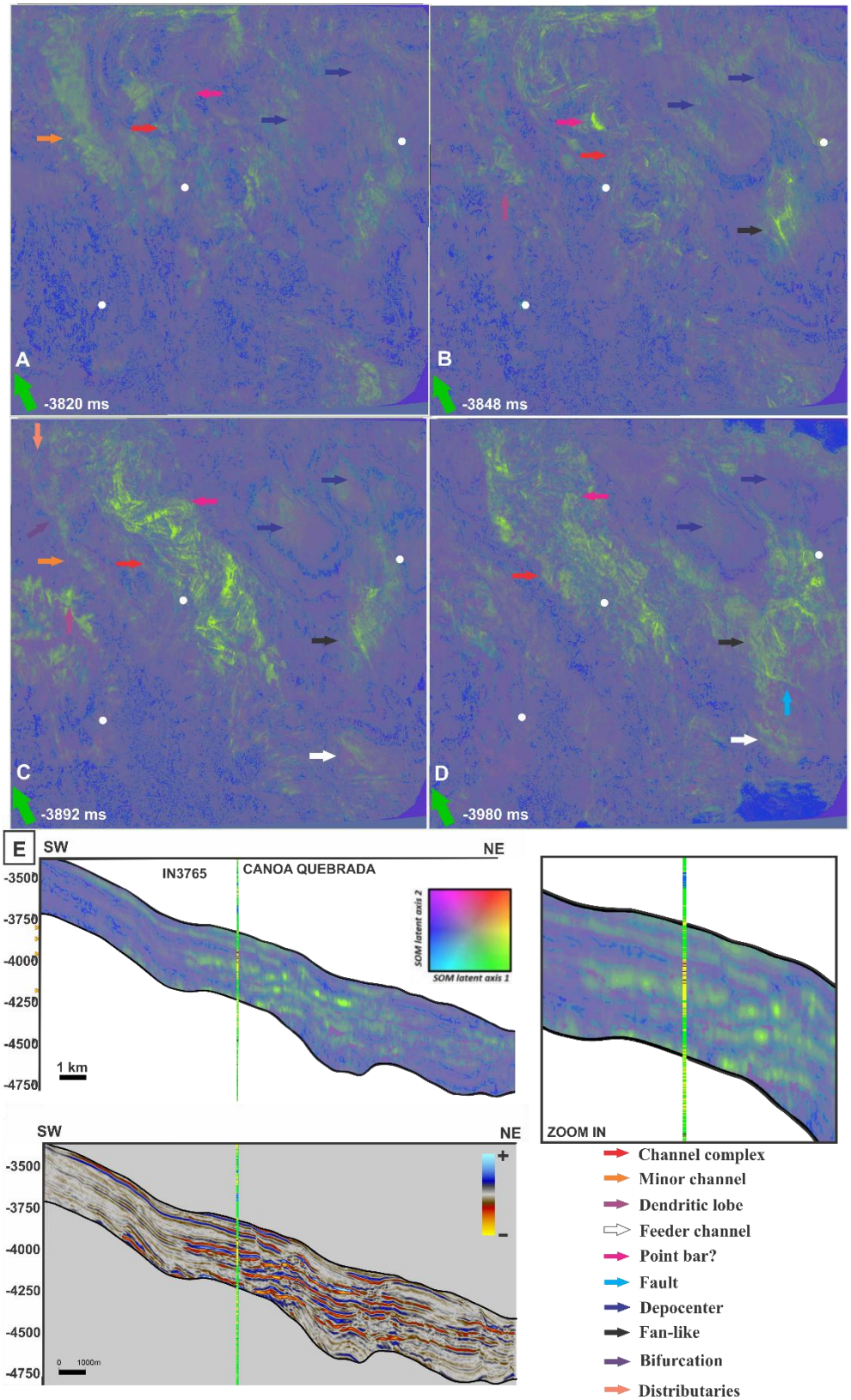

Observing the geomorphology of the phantom horizons, we notice that the green facies are distributed mainly in the channel complex, minor channels, dendritic lobes, and fan-like structure (Figure 4-13a to d). On the other hand, the purple facies are the most representative in the study area including almost the totality of the two depocenters (Figure 4-13e). These colors possibly indicate more shaley elements such marine shales commonly found in the basin floor, and mud-filled channels (small and large scale). The blue colors are distributed mainly in the upslope.

4.3.2. Geologic features seen on the independent components

Figure 4-14a displays the results of the Independent Component 1 (IC1) along Phantom Horizon 3 (-3891 ms). The IC1 results reveals the same deepwater elements previously seen with individual seismic attributes and with the SOM analysis. However, we note that IC1 presents less noisy, faults that are well delineated and clearer than the SOM results. Moreover, the channel-complex, smaller channel, faults, depocenters, point bars, and feeder channels are better delineated and internally resolvable in IC1 than the other ICs. In addition, the channel that bifurcates into three distributary channels toward the northwest is better delineated and internally resolved using IC1.

Figure 4-14b, displaying Independent Component 2 (IC2) more clearly images the large-scale geologic features such as the channel complex, depocenters, and smaller channels. However, the distributary channels are visible, but are difficult to definitively delineate using just IC2. Faults are also well exhibited when compared to the SOM results. As seen in IC1, IC2 exhibits a noise than the SOM. Figure 4-14c, for Independent Component 3 (IC3), still exhibits the largescale geologic features such as the channel complex, depocenters, and smaller channels. However, the smaller scale geologic features such as faults and feeder channels are less apparent with IC 3, than on IC1 and IC2. Although we can delineate the smaller channel, its bifurcation into three distributary channels is difficult to interpret on IC3.

Figure 4-84: Independent components in the phantom horizon 3: A) independent component 1. B) independent component 2. C) independent component 3. D) independent component 4.

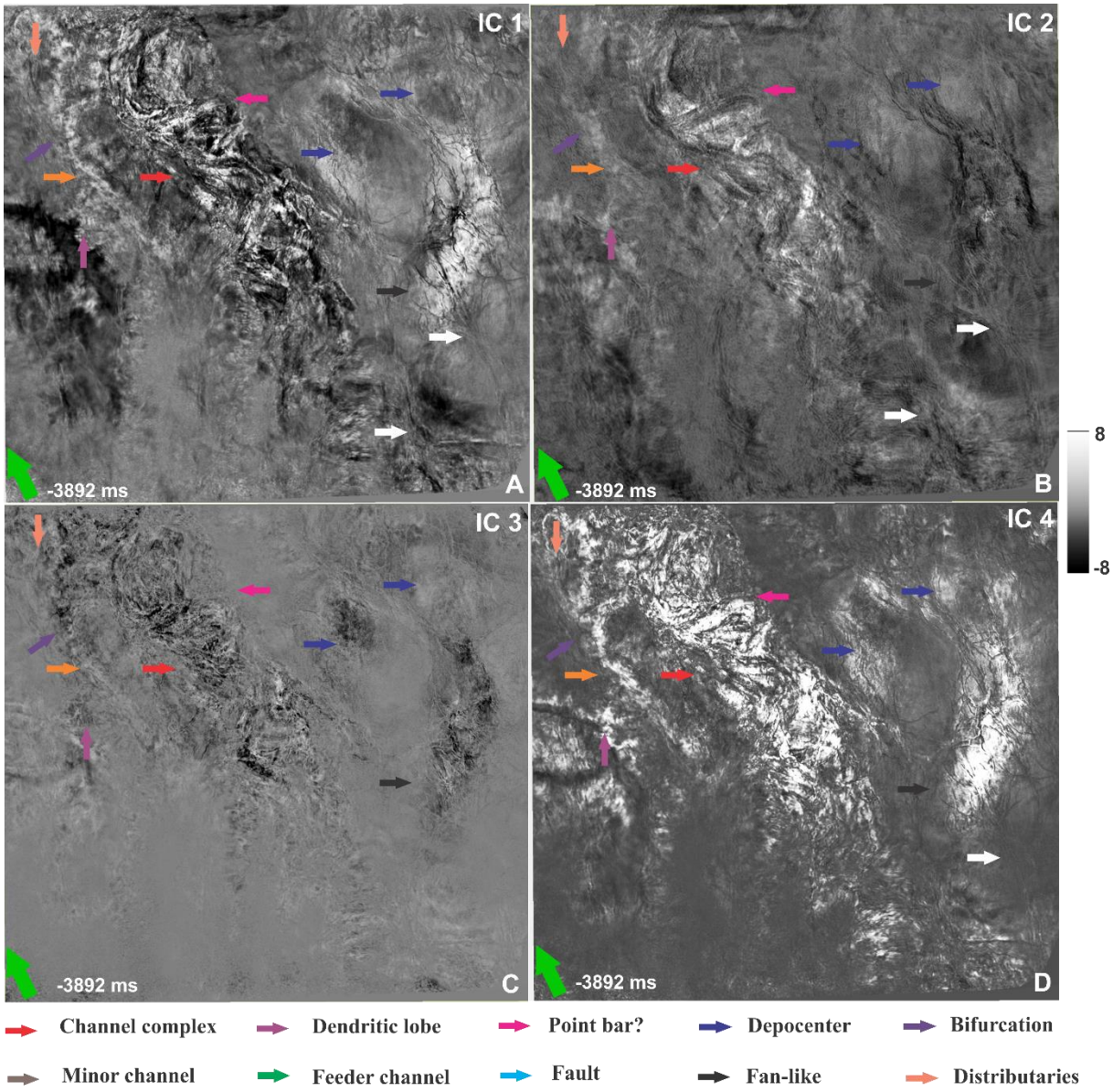

Independent Component 4 (IC4) better reveals the largescale geologic features such as the channel complex, depocenters, and smaller channel, as well as the small-scale geologic features as feeder channels and faults (Figure 4-14d). However, the channel complex is not internally well-resolved. The channel complex elements of IC4 have poor internal delineation when compared with IC1, IC2, and IC3. This observation is consistent with the objective of ICA, which seeks to best separate alternative patterns of independent sources (Lubo-Robles and Marfurt, 2019).

To accomplish the goal of making an unsupervised seismic facies analysis, we plot the independent components IC1, IC2, and IC3, which represent valuable geologic information, using an RGB color scheme (Figure 4-15). By construction, similar seismic facies will appear as similar colors. In Figure 15a, we note that the RGB blending using independent components at PH1 provides better resolution of geologic features when compared to SOM results. The

channel-complex, smaller channel, faults, depocenters, point bars, and feeder channels, as well as the small geological features (e.g. dendritic lobes and distributaries) are better delineated using the ICA method. It is also possible to notice that the ICA RGB blending provides better contrast between the distinct seismic facies.

As mapped in Figure 4-15b, the channel complex is characterized predominantly by green facies intercalated with some yellow and purple seismic facies, whereas the area close to the Pecém well has predominantly purple facies. The channel complex has a high variability of seismic facies; however, its shape is not well defined, and appears similar to braided channels. At PH3 (-3892 ms) (Figure 4-15c) the geological features close to the Amontada well is characterized by predominant green and purple seismic facies, whereas the dendritic lobe has yellow seismic facies. These dendritic lobes appear to feed the smaller channels, and this channel has the same seismic facies as its distributaries. The channel-complex has a greater variability of seismic facies and is well delineated (Figure 4-15c). At PH1, the channel-complex has predominantly green facies and purple facies as it trends towards northwest. The smaller channel in the northwest has predominantly yellow seismic facies when compared to the older horizons (Figure 4-15c). At PH4 (-3980 ms) (Figure 4-15d), the fan-like structure is highly variable with a mix of different seismic facies, the variability of which was better captured using ICA than SOM and attributes analysis.

Figure 4-15: ICA results presented in the four phantom horizons that highlight the deepwater elements: Phantom horizon 1 (youngest); B) Phantom horizon 2; C) Phantom horizon 3; D) Phantom horizon 4 (oldest). The well locations are displayed as a white dot; E) Inline 3765 in seismic amplitude below and ICA result in the top. Evaluation of the seismic facies and sand-rich elements by using log facies information from the 1 BRSA 1114 CES.

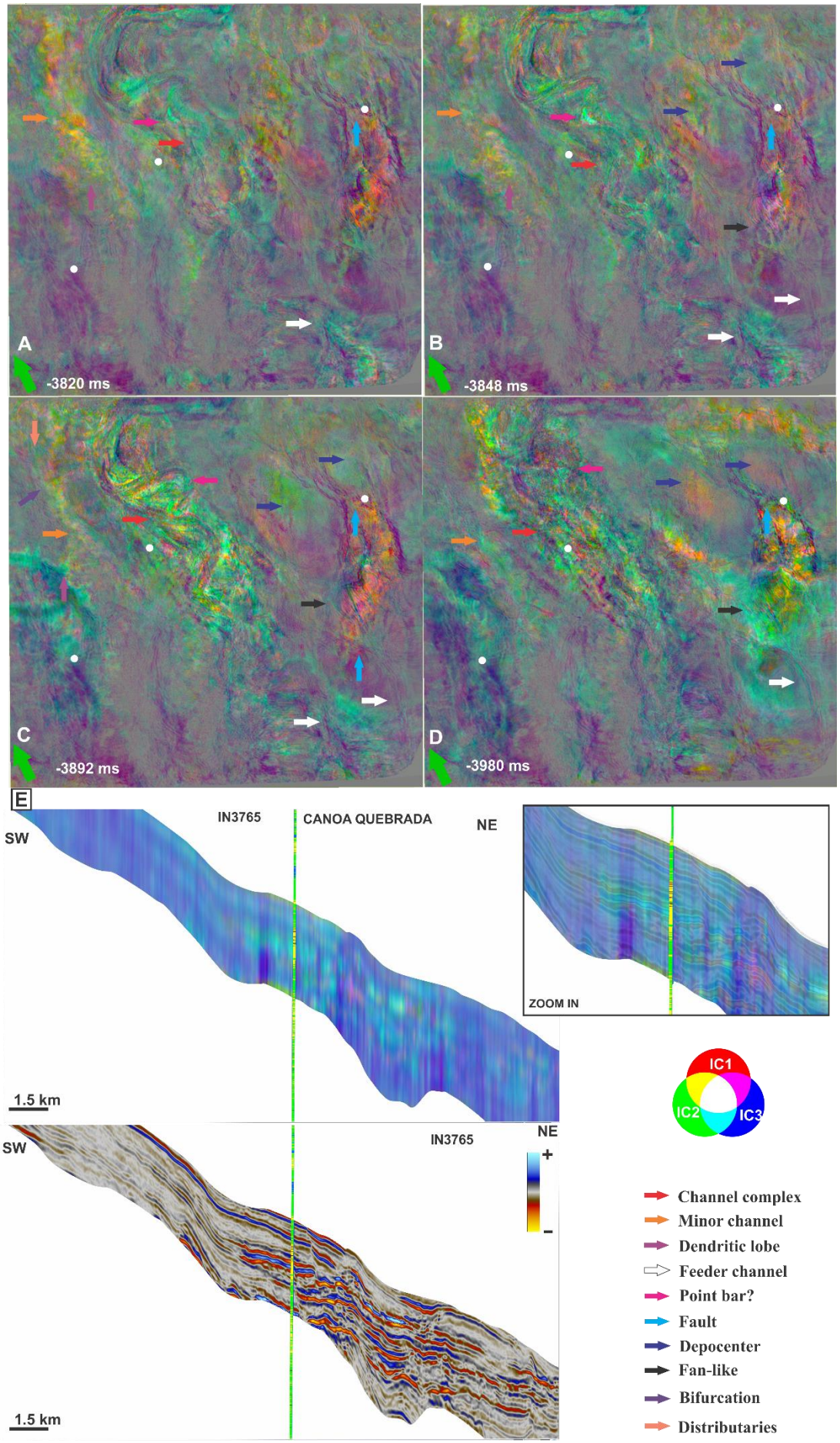
A
-3820 ms
B
-3848 ms
C
-3892 ms
D
-3980 ms
E
SW
IN3765
CANOA QUEBRADA
NE
ZOOM IN
1.5 km
SW
IN3765
NE
+
–
1.5 km
IC1
IC2
IC3
Channel complex
Minor channel
Dendritic lobe
Feeder channel
Point bar?
Fault
Depocenter
Fan-like
Bifurcation
Distributaries

To validate our interpretation of the seismic facies using principles of geomorphology and the ICA RGB blending to highlight the different architectural elements, we relate the seismic facies with lithologies analyzing the facies information from the Canoa Quebrada well report. Figure 4-15e demonstrated that the sandstone probably associated with sheet sands correlates with a mixture of bright yellow with green seismic facies associated with high amplitude and parallel reflectors. The blue and purple facies are associated with an interbedded shale and sandstone (shale >> sandstone).

4.5.4. Depositional Environment

The results from integration of various seismic attributes and unsupervised machine learning techniques reveal that significant differences in channel characteristics and morphology exist between Albian – Turonian interval. The PH4, the oldest, has a pattern similar to a braided channel with a high variability of seismic facies and not well-defined channels (Figure 4-15D). Braided channels do not have a main channel; besides they have a great capacity to transport sediments, and play a key role in erosion and deposition. It is important to highlight that this interval has a large number of erosive events that occurred between 10 Ma period (Condé et al., 2007) (Figure 4-2a).

A fan-like structure is well defined in the oldest study interval, near the Albian base horizon. At this time, the basin had high grained continental support, as its period is characterized as shelf marine (Figure 4-2a). The rift process was finalized by this point, and then the subsidence process allowed a horizontal distribution of the sediments. The faults at this time have a similar orientation to the rift faults. Leopoldino Oliveira et al. (2020) mapped the faults at this age and observed that these structures seem to be linked at depth, suggesting that these faults formed as a result of a phase of reactivation of the older and deeper rift structures. These faults are bounding the two depocenters that are displayed in the northeast of the study area. Additionally, is possible to notice that a NW-SE fault in the upslope is deforming the fan-like structure. This observation represents an insight about the upslope petroleum potential of the Ceará Basin since this feature is similar to the plays found in the Jubilee Field in Ghana. Lawrence Amy (2019) described the Jubilee plays as an Upper Cretaceous high-quality oil pay (Turonian in age) within a drift submarine fan sequence. The Jubilee field has stratigraphic pinch-outs plays linked to several large-scale normal basement linked faults.

The PH3 has a well-defined wide channel-complex, smaller channels, and distributaries. The sediment deposition in the channels was from the southeast to the northwest,

indicating that the main provenance was from the south, which is consistent with the regional geology of the area. It is observed that the sediment supply could also be from southwest close to the Amontada well. This observation can be verified by seismic attributes, SOM and ICA techniques (purple arrow in Figures 4-6 to 4-9, 4-13, and 4-15). The direction of the channels is in accordance with the relief of the paleogeographic map (Figure 4-4a, b, and c).

The youngest horizon (PH1) displays higher sinuosity channels that are straight compared to the oldest horizons. There is thought to be a strong relationship between slope angle and sinuosity, with sinuosity increasing as slope angle decreases passing from straight channels (feeder channels) to meandering channels (Schumm and Khan, 1972).

Comparing the attributes analysis, the interpretation of seismic spectral components (Figures 4-6 to 4-9, and 4-11) provides higher horizontal resolution, especially in the depositional boundary. In addition, the variations in the frequency decomposition of these deepwater elements provide some indication of the potential variation in depositional thickness.

The RMS amplitude, sweetness, and envelope displayed have values associated with thicker sandstones package. The high value of gamma-ray suggested that the package has arkosic sandstone, thus a clear indicative that the sediment source was close or the sediments were not reworked.

ICA shows better results than SOM in terms of delineating deepwater architectural elements of interest, reducing noise, and improving the contrast between different seismic facies. Although the Canoa Quebrada well is not drilled through one of the channel complexes, we believe that the validation of the seismic facies using this well can be extrapolated to the other zones of the seismic volume. Besides that, this well was considered for validation because the sandstone package is thicker than the seismic resolution (27 m).

4.6. CONCLUSION

This study of the Ceará Basin followed a seismic geomorphologic workflow to improve current understanding of its Albanian-Turonian interval, enhanced by the use of seismic attributes, rock physics modeling, and unsupervised machine learning. Primarily, this study found that:

- Meaningful geological features were successfully extracted from 3D seismic data using the RMS, coherence, envelope, sweetness, and spectral decomposition i.e. channel complex, point bars, feeder channels, faults, depocenters, dendritic lobes,

smaller channels and distributaries. The integration of all seismic attributes with well information helped to identify sand-rich deepwater elements;

- The rock-physics modeling gives meaningful insight to the seismic amplitude and its link with the rock parameters as fluid/porous system, also the rock-physics model helped in the S-wave estimation and curve modeling, keeping consistency with the elastic parameters and the rock properties.
- The ICA is a powerful technique to reduce dimensionality, extract valuable information from multiple seismic attribute volumes, and separate geologic features from noise. ICA provided better resolution than SOM analysis;
- Integration of seismic attributes and machine learning approach is more efficient for identifying depositional patterns than conventional seismic reflection data. Mainly, if the interpreter wants a quick overview of the exploration area using a huge 3D seismic cube. Also, these approaches can be applied to other underexplored basins in Equatorial Atlantic Margin for both exploration and production purposes;
- The deepwater upslope petroleum potential in stratigraphic traps were emphasized since a fan-like structure and an associated fault was mapped. This type of structures provided large volumes of hydrocarbon in the Equatorial Africa (Jubilee field) and it can be an important target for hydrocarbon exploration in the Brazilian Equatorial Margin.

References

Ahmad, M. N., and P. Rowell, 2012, Application of spectral decomposition and seismic attributes to understand the structure and distribution of sand reservoirs within Tertiary rift basins of the Gulf of Thailand: The Leading Edge, 31, 630–634

Antunes, A. F., E. F. Jardim de Sa, R. G. S. Araujo, and F. F. Lima Neto, 2008, Caracterização tectonoestrutural do Campo de Xareu (Sub-Bacia de Mundaú, Bacia do Ceara–NE do Brasil): Abordagem multiescala e pluriferramental: Revista Brasileira de Geociências, v. 38, no. 1, p. 88–105, doi:10.25249/0375-7536 .2008381S88105.

Bahorich, M. S., and S. L. Farmer, 1995, 3D seismic coherency for faults and stratigraphic features: The Leading Edge, 14, 1053-1058.

Basile C., J. Mascle, and R. Guiraud. 2005. Phanerozoic geological evolution of the Equatorial Atlantic domain. Journal of African Earth Sciences, 43:275-282. https://doi.org/10.1016/j.jafrearsci.2005.07.011

Beltrami, C. V., L. E. M. Alves, and F. J. Feijo, 1994, Bacia do Ceara: Boletim de Geociências da Petrobras, v. 8, no. 1, p. 117–125

Brown, A.R., 2004. sixth ed. Interpretation of Three-Dimension Seismic Data, vol. 42. American Association of Petroleum Geologists, Tulsa, Oklahoma, Memoir, pp. 295–308.

Bueno, J.F., B.C. Z. Honório, M.C. Kuroda, A.C. Vidal, and E.P. Leite. 2014, Structural and stratigraphic feature delineation and facies distribution using seismic attributes and well log analysis applied to a Brazilian carbonate field, Interpretation 2: SA83-SA92.

Chopra, S., and K. J. Marfurt, 2007. Seismic Attributes for Prospect Identification and Reservoir Characterization. Society of Exploration Geophysicists, Tulsa, OK (456 pp.)

Chopra, S., and K. J. Marfurt, 2015, Choice of mother wave- lets in CWT spectral decomposition: 85th Annual International Meeting, SEG, Expanded Abstracts, 2957–2961, doi: 10.1190/segam2015-5852193.1.

Chopra, S., and K. J. Marfurt, 2016, Spectral decomposition and spectral balancing of seismic data: The Leading Edge, 35, 176–179, doi: 10.1190/tle35020176.1.

Coleou, T., M. Poupon, and K. Azbel, 2003, Unsupervised seismic facies classification: A review and comparison of techniques and implementation: The Leading Edge, 22, 942–953, doi: 10.1190/1.1623635.

Conde, V. C., C. C. Lana, O. C. Pessoa Neto, E. H. Roesner, J. M. Morais Neto, and D. C. Dutra, 2007, Bacia do Ceara: Boletim de Geociências da Petrobras, v. 15, no. 2, p. 347–355.

Costa, I. G., C. V. Beltrami, and L. E. M. Alves, 1990, A evolução tectono-sedimentar e o “habitat” do óleo da Bacia do Ceara: Rio de Janeiro, Petrobras/Depex, Anais, Seminário de Interpretação Exploratória 1, p. 75 –85.

Exxon Mobil, 2020. Guyana project overview. Article Oct. 1, 2020. https://corporate.exxonmobil.com/Locations/Guyana/Guyana-project-overview#DiscoveriesintheStabroekBlock. (Accessed 12 November 2020).

Fiduk, J.C., E.R. Brush, L.E. Anderson, P.B. Gibbs, M.G. Rowan. 2004. Salt deformation, magmatism, and hydrocarbon prospectivity in the Espírito Santo Basin, offshore Brazil. In: Post, P.J., Olson, D.L., Lyons, K.T., Palmes, S.L., Harison, P.F., Rosen, N.C. (Eds.), Salt-sediment Interactions and Hydrocarbon Prospectivity: Concepts, Applications, and Case Studies for the 21st Century. GCSSEPM 24th Annual Research Conference, pp. 370-392.

Françolin, J.B.L., and P. Szatmari. 1987. Mecanismo de rifteamento da porção oriental da margem norte brasileira. Revista Brasileira de Geociências, 17:196-207

Gamboa, D., T.M. Alves, J. Cartwright, and P. Terrinha. 2010. MTD distribution on a 'passive' continental margin: The Espírito Santo Basin (SE Brazil) during the Palaeogene. Marine and Petroleum Geology, v. 27, (7), 1311-1324. DOI:10.1016/j.marpetgeo.2010.05.008

GeoExpro, 2020. Guyana–Suriname: The Hotspot That Keeps on Giving. Vol. 17, No 5, pp 36-37. https://www.geoexpro.com/articles/2020/11/guyana-suriname-the-hotspot-that-keeps-on-giving. (Accessed 12 November 2020).

Huaicun, J., 2014. Progress and revelation of exploration of large oil and gas fields around the globe. Sci. Technol. Rev. 32 (8), 76–83, 2014.

Hart, B. S., 2008, Channel detection in 3-D seismic data using sweetness: AAPG Bulletin, 92, 733–742, doi: 10 .1306/02050807127.

Honorio, B., A. Sanchetta, E. Pereira, and A. Vidal, 2014, Independent component spectral analysis: Interpretation, 2, no. 1, SA21–SA29, doi: 10.1190/INT-2013-0074.1.

Huber, P. J., 1985, Projection pursuit: Annals of statistics, 13, 435–475, doi: 10.1214/aos/1176349519

Hyvärinen, A., 1999a, Fast and robust fixed-point algorithms for independent component analysis: IEEE Transactions on Neural Networks, 10, 626–634, doi: 10.1109/72.761722.

Kohonen, T., 1982, Self-organized formation of topologically correct feature maps: Biological Cybernetics, 43,59–69, doi: 10.1007/BF00337288.

Lawrence A. Amy, 2019. A review of producing fields inferred to have upslope stratigraphically trapped turbidite reservoirs: Trapping styles (pure and combined), pinch-out formation, and depositional setting. AAPG Bulletin; 103 (12): 2861–2889. doi: https://doi.org/10.1306/02251917408

Leopoldino Oliveira, K.M., H. Bedle, R.M.G.C. Branco, A.C.B. Souza, F. Nepomuceno Filho, M.N. Normando, N. Maia de Almeida, and T.H. da Silva Barbosa. 2020. Seismic stratigraphic patterns and characterization of deepwater reservoirs of the Mundaú sub-basin, Brazilian Equatorial Margin. Mar. Pet. Geol. https://doi.org/10.1016/j.marpetgeo.2020.104310.

Li, F., and W. Lu, 2014, Coherence attribute at different spectral scales: Interpretation, 2, no. 1, SA99–SA106, doi: 10.1190/INT-2013-0089.1

Linari, V., K. Azbel, and M. Poupon, 2003, Seismic facies analysis based on 3D multiattribute volume classification, LaPalma field, Maracaibo, Venezuela: The Leading Edge, 22,32–36

Lubo-Robles, D., and K. Marfurt. 2019. Unsupervised seismic facies classification using ICA: Interpretation, 7, 3, Society of Exploration Geophysicists.

Maia de Almeida N.M., T. M. Alves, F. Nepomuceno Filho, G.S.S. Freire, A.C.B. Souza, M. N. Normando, K.M.L. Oliveira, and T.H.S. Barbosa. 2020. Tectono sedimentary evolution and petroleum systems of the Mundaú sub-basin: A new deepwater exploration frontier in equatorial Brazil. AAPG Bulletin, v. 104, no. 4 (April 2020), pp. 795–824. DOI:10.1306/07151917381

Matos R.M.D. 2000. Tectonic evolution of the equatorial south Atlantic. In: Mohriak W., Talwani M. (Eds.). Atlantic rifts and continental margins, p. 331-354. Washington, D.C., American Geophysical Union.

Milani E.J., J.A.S.L. Brandão, P.V. Zalán, and L.A.P. Gamboa. 2000. Petróleo na margem continental brasileira: geologia, exploração, resultados e perspectivas. Brazilian Journal of Geophysics, 18, 352-396. http:// dx.doi.org/10.1590/S0102-261X2000000300012

Milani, E.J., and A. Thomaz Filho. 2000. Sedimentary basins of South America. In: In: Cordani, U.G., Milani, E.J., Thomaz Filho, A., Campos, D.A. (Eds.), Tectonic Evolution of South America, vol. 31. International Geological Congress, Rio de Janeiro, pp. 389–449.

Mohriak W.U. 2003. Bacias sedimentares da margem continental brasileira. In: Bizzi L.A., Schobbenhaus C., Vidotti R.M., Golçalves J.H. (Eds.). Geologia, tectônica e recursos minerais do Brasil: textos, mapas & SIG, p. 87-165. Brasília, CPRM.

Mohriak, W.U. 2005. Interpretação geológica e geofísica da Bacia do Espírito Santo e da região de Abrolhos: Petrografia, datação radiométrica e visualização sísmica das rochas vulcânicas. Boletim de Geociencias da Petrobras 14 (1), 133 - 142

Morais Neto, J. M., O. C. Pessoa Neto, C. C. Lana, and P. V. Zalan. 2003. Bacias sedimentares brasileiras: Bacia do Ceara: Phoenix, v. 57, p. 1–6.

Partyka, G., J. Gridley, and J. Lopez. 1999. Interpretational applications of spectral decomposition in reservoir characterization: The Leading Edge, 18, 353–360, doi: 10.1190/1.1438295.

Pellegrini, B.S., and H. J. P. Severiano Ribeiro. 2018. Exploratory plays of Pará Maranhão and Barreirinhas basins in deep and ultra-deep waters, Brazilian Equatorial Margin. Brazilian Journal of Geology, 48 (3), 485-502. DOI: 10.1590/2317-4889201820180146

Pessoa Neto, O. C. 2004. Blocos basculados truncados por discordância angular: lições aprendidas em trapeamento combinado de hidrocarbonetos, Bacia do Ceará, Nordeste do Brasil. Boletim de Geociências Petrobras, Rio de Janeiro, v. 12, n. 1, p. 59-71.

Poupon, M., J. Gil, D. Vannaxay, and B. Cortilla. 2004. Tracking tertiary delta sands (UrdanetaWest, Lake Maracaibo, Venezuela): An integrated seismic facies classification workflow: The Leading Edge, 23,909–912.

Radovich, B. J., and R. B. Oliveros. 1998. 3-D sequence interpretation of seismic instantaneous attributes from the Gorgon field: The Leading Edge, 17, 1286–1293, doi: 10.1190/1.1438125.

Roden, R., T. Smith, and D. Sacrey. 2015. Geologic pattern recognition from seismic attributes: Principal component analysis and self-organizing maps: Interpretation, 3, no. 4, SAE59–SAE83, doi: 10.1190/INT-2015-0037.1.

Roy, A., B. Dowdell, and K. Marfurt. 2013. Characterizing a Mississippian tripolitic chert reservoir using 3D unsupervised and supervised multiattribute seismic facies analysis: An example from Osage County: Interpretation, 1, no. 2, SB109–SB124, doi: 10.1190/INT-2013-0023.1.

Schumm, S. A., and H. R. Khan. 1972. Experimental Study of Channel Patterns. GSA Bulletin; 83 (6): 1755–1770. doi: https://doi.org/10.1130/0016-7606(1972)83[1755:ESOCP]2.0.CO;2

Szatmari P., Françolin J.B., Zanotto O., Wolff S. 1987. Evolução tectônica da margem equatorial brasileira. Revista Brasileira de Geociências, 17:180-188.

Taner, M.T., F. Koehler, and E.E. Sheriff. 1979. Complex seismic trace analysis: GEOPHYSICS, 44, 1041-1063

Trosdtorf, I., Jr., P.V. Zalán, J.J.P. Figueiredo, and E.F. Soares. 2007. Bacia de Barreirinhas. B. Geoci. Petrobras, v. 15, n. 2, 331-339.

Verma, S., A. Roy, R. Perez, and K. J. Marfurt. 2012. Mapping high frackability and high TOC zones in the Barnett shale: Supervised probabilistic neural networks vs. unsupervised multi-attribute Kohonen SOM: 82nd Annual International Meeting, SEG, Expanded Abstracts, doi: 10.1190/segam2012-1494.1.

Walden, A. 1985. Non-Gaussian reflectivity, entropy, and deconvolution: Geophysics, 50, 2862–2888, doi: 10 .1190/1.1441905.

Zalán P.V. 2004. Evolução fanerozóica das bacias sedimentares brasileiras. In: Mantesso-Neto V., Bartorelli A., Carneiro C.D.R., Brito Neves B.B.B. (Eds.). Geologia do continente sul-americano: evolução da obra de Fernando Flávio Marques de Almeida, p. 595-1049 612. São Paulo, Editora Beca.

Zhao, T., J. Zhang, F. Li, and K. J. Marfurt. 2016,.Characterizing a turbidite system in Canterbury Basin, New Zealand, using seismic attribute and distance-preserving self-organizing maps: Interpretation, 4, no. 1, SB79–SB89, doi: 10.1190/INT-2015-0094.1

5. CONCLUSION

- The Aptian rift system in Mundaú sub-basin might supply further opportunities for structural trapping in the basin, and expectations of drift stratigraphic-structural traps through interconnecting faults. Four majors landward-dipping faults were mapped in all seismic data, which would have the potential to allow charging of deep- water drift reservoirs from rift source rocks.
- The seismic interpretation reveals evidence of Cretaceous to Paleogene magmatism in the region as indicated by the well imaged volcanoes and associated sills at depth. The proximity of deepwater turbidites plays with magmatic rocks could have established an atypical petroleum system.
- The variety of stratigraphic and structural features developed through the Cretaceous history of the basin offer high-trapping potential for a number of plays in the rift as well as in the drift sequences. The type of plays are: (1) the developed rift system with major faults which can act as long-distance migration pathways; (2) turbiditic bodies; (3) turbiditic bodies associated with magmatic intrusion. Identification of potential plays associated with turbiditic sandstones of the Ubarana Formation can be correlated to Jubilee play in Guinea Gulf and Zaedyus play in French Guiana.
- The sediments from Late Albian-Early Cenomanian-Turonian age are at depths ranging from 3048 to 4894 m in the deepwater and ultra-deepwater domains. Since the top depth of the oil window occurs from about 3400 to 3800 m in the deepwater Mundaú sub-basin, the analyses of geochemical data suggest that in this basin there must be generation of oil and/or gas at deepwater plays.
- Our data strongly suggest that the architecture of this basin is a volcanic passive margin. Volcanic passive margins are associated with the extrusion and intrusion of large volumes of magma, pre- dominantly mafic, and represent distinctive features of Larges Igneous Provinces, in which regional fissural volcanism predates localized syn-magmatic break-up of the lithosphere. The criteria used to justify our assertion are: (1) the presence of basement and rifts filled by volcanics (seaward dipping reflectors); (2) the absence of exhumed mantle between the continental crust and oceanic crust; (3) the large presence of igneous intrusions; (4) and the presence of a LIP in the equatorial margin, based on igneous intrusions between two basins near the Ceará Basin.

- Meaningful geological features were successfully extracted from 3D seismic data using the RMS, coherence, envelope, sweetness, and spectral decomposition i.e. channel complex, point bars, feeder channels, faults, depocenters, dendritic lobes, smaller channels and distributaries. The integration of all seismic attributes with well information helped to identify sand-rich deepwater elements;
- The rock-physics modeling gives meaningful insight to the seismic amplitude and its link with the rock parameters as fluid/porous system, also the rock-physics model helped in the S-wave estimation and curve modeling, keeping consistency with the elastic parameters and the rock properties.
- The ICA is a powerful technique to reduce dimensionality, extract valuable information from multiple seismic attribute volumes, and separate geologic features from noise. ICA provided better resolution than SOM analysis.
- Integration of seismic attributes and machine learning approach is more efficient for identifying depositional patterns than conventional seismic reflection data. Mainly if the interpreter wants a quick overview of the exploration area using a huge 3D seismic cube. Also, these approaches can be applied to other underexplored basins in Equatorial Atlantic Margin for both exploration and production purposes
- The deepwater upslope petroleum potential in stratigraphic traps were emphasized since a fan-like structure and an associated fault was mapped. This type of structures provided large volumes of hydrocarbon in the Equatorial Africa (Jubilee field) and it can be an important target for hydrocarbon exploration in the Brazilian Equatorial Margin.

REFERENCES

LEOPOLDINO OLIVEIRA, K.M., BEDLE, H., BRANCO, R.M.G.C., DE SOUZA, A.C.B., NEPOMUCENO FILHO, F., NOMANDO, M.N., MAIA DE DE ALMEIDA, N., DA SILVA BARBOSA, T.H. Seismic stratigraphic patterns and characterization of deepwater reservoirs of the Mundaú sub-basin, Brazilian Equatorial Margin. **Marine and Petroleum Geology**, *s.l*, V. 116, 1-2, June 2020. https://doi.org/10.1016/j.marpetgeo.2020.104310.

LIU, L., TANG, D., XU, H., LIU L. 2016. Reservoir Prediction of deepwater turbidite sandstones with seismic lithofacies control- A case study in the C block of lower Congo basin. **Marine and Petroleum Geology,** *s.l*, V. 71, 1-11, March 2016.

MAIA DE ALMEIDA N.M., ALVES, T.M., NEPOMUCENO FILHO, F., FREIRE, G.S.S., SOUZA, A.C.B., NORMANDO, M.N., OLIVEIRA, K. M.L., BARBOSA, T.H.S. Tectono sedimentary evolution and petroleum systems of the Mundaú sub-basin: A new deep-water exploration frontier in equatorial Brazil. **AAPG Bulletin**, *s.l*, v. 104, no. 4, 795-824, April 2020. DOI:10.1306/07151917381

MORAIS NETO, J.M.; PESSOA NETO, O.C.; LANA, C.C.; ZALÁN, P.V. Bacias Sedimentares Brasileiras: Bacia do Ceará. **Fundação Paleontológica Phoenix**, Aracaju, v. 57, 1-6 p, 2003.

OTC. 2018. Available in: http://2018.otcnet.org/special-events. Accessed in: September 2018.

PANG, X., CHEN, C.M., SHI, H.S., et al. Response between relative sea-level change and the pearl river deepwater fan system in the South China sea. **Earth Sci. Front**, *s.l*, v. 12, no. 3, 167-177, 2005.

PENG, D.J., PANG, X., CHEN, C.M., ET AL. From shallow-water shelf to deepwater slope-the study on deepwater fan systems in South China sea. **Acta sedimentological sinica,** *s.l*, v. 23, no 1, 1-11, 2005.

PETTINGILL, H.S., PAUL, W. Worldwide deepwater exploration and production: past, present, and future. **The Leading Edge**, *s.l*, v. 21, no 4, 371-376, April 2002.

SHANMUGAM, G., 2000. 50 years of the turbidite paradigm (1950s-1990s): deep- water processes and facies models-a critical perspective. **Marine and Petroleum Geology**, *s.l*,v. 17, no 2, 285-342, February 2000.

SILVA, S.R.P., MACIEL, R.R., SEVERINO, M.C.G. Cenozoic tectonics of Amazon Mouth Basin: **Geo-Marine Letter**, *s.l*, v. 18, 256-262, September 1998.

STOWA, D.A.V., MAYALL, M.. Deepwater sedimentary system: new models for the 21st century. **Marine and Petroleum Geology,** *s.l*,v. 17, no 2, 125-135, February 2000.

ZALÁN, P.V. & WARME, J.E. Tectonics and Sedimentation of the Piauí-Camocim Sub-basin, Ceará Basin, Offshore Northeastern Brazil. Rio de Janeiro: **Petrobras**, 1985. 71 p.

ZALÁN, P.V. 2015. Similarities and Differences between Magma-Poor and Volcanic Passive Margins – Applications to the Brazilian Marginal Basins. In: 14th International Congress of the Brazilian Geophysical Society, 2015, Rio de Janeiro, Brazil, 37-42 p. https://doi.org/10.1190/sbgf2015-007

APPENDIX 1 – LIST OF PAPERS AND ABSTRACTS RELATED TO THIS THESIS

Special section: Interesting features seen on seismic data

The importance of recognizing multiples in legacy data: A case study from the Brazilian equatorial margin

Karen M. Leopoldino Oliveira[1], Heather Bedle[2], Gabriel de A. Araujo[3], and Mariano Castelo Branco[1]

Summary

The Ceará Basin is a deepwater exploration frontier basin that comprises part of the Brazilian equatorial margin. This basin has been receiving renewed attention from the petroleum industry since the discovery of important deepwater oil fields in its African counterpart. However, detailed seismic stratigraphic, depositional, and structural frameworks for the Ceará Basin are still lacking in the literature. We have analyzed a series of 2D seismic data sets and stumbled into the pitfalls of migration artifacts (i.e., multiples) ultimately realizing that reprocessing was the best option to avoid the mistake of interpreting these artifacts as geologic features. Multiples can be difficult to identify in seismic data in which they mimic the true geology of the region, and they often present a pitfall for less experienced interpreters. Indeed, the identification and removal of multiples is crucial because they do not reflect the true geology in the subsurface and may otherwise lead to incorrect business decisions.

Geological feature: Stratigraphy of the Ceará Basin, offshore Brazil

Seismic appearance: Strong seismic horizons mimicking geological layering

Alternative interpretations: Multiples arising from poor seismic migration processing

Features with similar appearance: Strong seismic horizons reflecting basement and carbonates

Formation: Rift sequence of the Ceará Basin

Age: Cretaceous

Location: Ceará Basin, offshore Brazil

Seismic data: Obtained by the Brazilian National Petroleum Agency and reprocessed by the authors

Analysis tool: Reprocessing

Miscorrelating

An example of a seismic profile processed without a careful analysis of the velocity model is shown in Figures 1a and 2a, and it shows the occurrence of several multiples and noise (the red arrows) that mimic geologic events. These events are further exacerbated using seismic attributes such as the amplitude volume technique (AVT) (Bulhões and Amorim, 2005) (Figure 2a). Seismic interpreters can correlate and interpret these multiples as false horizons because they are well-marked and change their shape because it increases the order multiple (see the blue lines in Figure 1b).

Processing data

A conventional processing sequence was applied to marine seismic data. The main steps of the processing flow applied were (1) geometry definition, (2) deghosting, (3) deconvolution, (4) surface-related multiple elimination (SRME) multiple prediction, (5) spectral balance, (6) velocity analysis and normal moveout correction, (7) Kirchoff time migration, and (8) AVT attribute. To improve the recognition and removal of multiples, we calculated their depth location by modeling and subsequently extracted them (Figure 1a, the red arrows; Figure 1b, the blue and green lines).

We used the SRME (Verschuur et al., 1992) method that consists of attenuating multiples generated by the free surface. This method uses only the recorded data to predict all orders of free-surface multiples. Due to timing and amplitude errors that arise in practice, the predicted multiples are typically subtracted from the data using adaptive filtering.

The velocity model was improved using commercial seismic processing software that uses the constant velocity stack theory. In this method, the complete seis-

[1]Universidade Federal do Ceará (UFC), Programa de Pós-Graduação em Geologia, Campus do Pici, Bloco 912, Fortaleza, Ceará, CEP 60440-554, Brazil. E-mail: karenleopoldino@gmail.com (corresponding author); mariano@ufc.br.
[2]University of Oklahoma, School of Geosciences, 100 East Boyd Street, Suite 710, Norman, Oklahoma 73019, USA. E-mail: hbedle@ou.edu.
[3]Universidade Federal do Rio Grande do Norte, Departamento de Informática e Matemática Aplicada, Natal, CEP 59072-970, Brazil. E-mail: g.almeidaraujo@gmail.com.

Manuscript received by the Editor 2 October 2019; revised manuscript received 15 January 2020; published ahead of production 10 June 2020; published online 30 June 2020. This paper appears in *Interpretation*, Vol. 8, No. 4 (November 2020); p. SR17–SR21, 3 FIGS.
http://dx.doi.org/10.1190/INT-2019-0214.1.

Marine and Petroleum Geology 116 (2020) 104310

Contents lists available at ScienceDirect

Marine and Petroleum Geology

journal homepage: www.elsevier.com/locate/marpetgeo

Research paper

Seismic stratigraphic patterns and characterization of deepwater reservoirs of the Mundaú sub-basin, Brazilian Equatorial Margin

Karen M. Leopoldino Oliveira[a,b,c,*], Heather Bedle[c], R. Mariano G. Castelo Branco[a,b], Ana Clara B. de Souza[a], Francisco Nepomuceno Filho[d], Márcio N. Normando[a], Narelle M. de Almeida[e], Thiago H. da Silva Barbosa[f]

[a] Programa de Pós-Graduação em Geologia, Universidade Federal do Ceará (UFC), Campus do Pici, Bloco 912, Fortaleza, Ceará, CEP, 60440-554, Brazil
[b] Laboratório de Geofísica de Prospecção e Sensoriamento Remoto (LGPSR). Universidade Federal do Ceará (UFC), Campus do Pici, Bloco 1011, Fortaleza, Ceará, CEP, 60440-760, Brazil
[c] School of Geosciences, University of Oklahoma, 100 East Boyd St. Suite 710 Norman, OK 73019, US
[d] Departamento de Física, Universidade Federal do Ceará (UFC), Campus do Pici, Bloco 922, Fortaleza, Ceará, CEP, 60440-554, Brazil
[e] Departamento de Geologia, Universidade Federal do Ceará (UFC), Campus do Pici, Bloco 912, Fortaleza, Ceará, CEP, 60440-554, Brazil
[f] Departamento de Engenharia do Petróleo, Universidade Federal do Ceará (UFC), Campus do Pici, Bloco 709, Fortaleza, Ceará, CEP, 60440-554, Brazil

ARTICLE INFO

Keywords:
Brazilian Equatorial Margin
Ceará Basin
Petroleum exploration
Deepwater environments
Turbidites
Magmatism

ABSTRACT

In recent years, the Brazilian Equatorial Margin has drawn attention due to its similarity to areas with new hydrocarbon discoveries in the African conjugated margin, and in French Guiana. However, studies on the tectonic regimes associated with transform margins and their evolution, structures, and petroleum potential are still lacking due to the geological complexity of this region. To address this knowledge gap, research has been done to better understand the geological structures, as well as to identify potential hydrocarbon accumulations in the deepwater Ceará Basin. To achieve this, we performed an integrated interpretation of a large 2D seismic data, new exploratory borehole data, as well as older well data with revised biostratigraphy. This data analysis refines the basin architecture and the Cretaceous-Paleocene tectonic evolution, including implications for hydrocarbon prospectivity in the Ceará Basin deepwater. 2D seismic interpretation was performed using modern concepts of continental break-up. To accomplish this, the transition of continental-oceanic crust was taken into account for restoration of the sediments of the rift stage in the basin. The analysis also identifies potential hydrocarbon accumulations in turbiditic reservoirs and presents new insights about the dimensions of the underlying rift features situated in the continental slope. The results reveal a high potential for drift sequences in deepwater where the Late Albian-Early Cenomanian-Turonian sediments reach thicknesses of approximately 3048–4894 m. Moreover, this research shows evidence of Cretaceous to Paleocene magmatism, indicated by the well-imaged volcanoes and associated sills in the seismic data. This analysis indicates that the Mundaú sub-basin can be classified as a volcanic passive margin that was developed during the oblique dextral separation between South America and Africa. The variety of stratigraphic and structural features developed through the Cretaceous history of the Mundaú sub-basin offers a variety of potential hydrocarbon traps and plays in a number of rift and post-rift sequences.

1. Introduction

The Brazilian Equatorial Margin (BEM) in northeastern South America and the eastern part of the Equatorial South Atlantic Ocean is composed by five sedimentary basins along the coast. There are, from west to east, the Foz do Amazonas, Pará-Maranhão, Barreirinhas, Ceará, and Potiguar basins (Fig. 1a). These basins began their development during the Early Cretaceous, as a series of several continental rift basins through a complex evolution with tectonic regime varying from predominantly normal (distension) to predominantly strike-slip

* Corresponding author. Programa de Pós-Graduação em Geologia, Universidade Federal do Ceará (UFC), Campus do Pici, Bloco 912, Fortaleza, Ceará, CEP, 60440-554, Brazil.
E-mail addresses: karenleopoldino@ou.edu (K.M. Leopoldino Oliveira), hbedle@ou.edu (H. Bedle), mariano@ufc.br (R.M.G. Castelo Branco), anaclarageologia@alu.ufc.br (A.C.B. de Souza), nepomuceno@fisica.ufc.br (F. Nepomuceno Filho), mnormando@gmail.com (M.N. Normando), narelle@ufc.br (N.M. de Almeida), thiagohenrique@alu.ufc.br (T.H. da Silva Barbosa).

https://doi.org/10.1016/j.marpetgeo.2020.104310
Received 6 September 2019; Received in revised form 17 February 2020; Accepted 19 February 2020
Available online 22 February 2020

ACE 2020 ABSTRACT – AAPG ANNUAL CONVENTION &EXHIBITION

Session Title: Theme 7: Geophysical Techniques in Geological Characterization: Integrated Workflows. Your Session Role for this session: Poster Session

Seismic Attributes – a Promising Aid for Hydrocarbon Prediction in Deepwater of the Ceará Basin, Brazilian Equatorial Margin.

Karen M. Leopoldino Oliveira[1,2], Karelia Molina La Marca[2], Heather Bedle[2]

[1] Programa de Pós-Graduação em Geologia, Universidade Federal do Ceará (UFC), Campus do Pici, Bloco 912, Fortaleza, Ceará, CEP 60440-554, Brazil. Email: karenleopoldino@gmail.com

[2] School of Geosciences, University of Oklahoma, 100 East Boyd St. Suite 710 Norman, OK 73019. Email:karenleopoldino@ou.edu, karelialm@ou.edu, hbedle@ou.edu

The discoveries of the Jubilee field offshore Ghana in 2007, as well as the Pecém well in the Ceará Basin in 2012, and Pitu well in the Potiguar Basin in 2013 have attracted the attention of the oil industry to other global transform margins. However, studies on the tectonic regimes associated with transform margins and their evolution, structures, and petroleum potential are still lacking due to the geological complexity of these regions. To address this knowledge gap, research has been done to better understand the geological structures, as well as to identify potential hydrocarbon accumulations in the deepwater Ceará Basin. To achieve this, a large seismic data set was combined with new exploratory borehole data, as well as older well data that has been reexamined and the biostratigraphy updated. This data analysis refines the basin architecture and the Cretaceous-Paleogene tectonic evolution, including implications for hydrocarbon prospectivity in the Ceará Basin deepwater.

The analysis identifies potential hydrocarbon accumulations in turbiditic reservoirs and presents new insights about the dimensions of the underlying rift sections situated in the continental slope. The results also reveal a high potential for drift sequences in deepwater where the thickness of sediments reach from 3-6 km for the Late Albian-Early Cenomanian-Turonian sediments. Also, seismic attributes analysis and an unsupervised machine-learning technique called self-organizing maps were applied focusing on this Cenomanian-Turonian interval. These techniques provide additional insight to hydrocarbon potential in this area, and aided in understanding the distribution and classification of the deepwater geological elements. Further, seismic geomorphology and facies analysis were examined to improve interpretation of the internal and external architecture of the depositional elements, and so helped to identify and to predict the possible reservoirs related to the turbiditic sandstone.

Please Review Your Abstract. If The Abstract Is Final, Click "Submit Abstract" To Complete Your Submission.

Submit Abstract

Basinal variation of seismic attribute response in deepwater architectural element recognition

Karelia La Marca[1], **Javier Tellez**[1], Laura Lucia Ortiz Sanguino[1,2], Karen Maria Leopoldino Oliveira[1,3] and Heather Bedle[4], (1)University of Oklahoma Norman Campus, School of Geosciences, Norman, OK, United States, (2)Industrial University of Santander, School of geology, Santander, Colombia, (3)Universidade Federal do Ceará, Fortaleza, Brazil, (4)University of Oklahoma Norman Campus, School of Geoscienes, Norman, OK, United States

Abstract Text:

The advancement of seismic attributes and visualization techniques has allowed enhancing the study of seismic geomorphology from 3D reflection data. The study of deepwater deposits defines and characterizes architectural elements depending on their genesis, morphology, and position along the slope and basin floor. However, the geological configuration of every individual basin determines the dimensions, morphology, and lithological composition of its architectural elements. To understand how seismic attributes help to characterize geological settings, we employ multiple datasets with variable qualities, since few studies elaborate on compiling and discussing the differences between basins. We explore and compare the use of seismic attributes to highlight deepwater architectural elements in three different basins around the world: The Ceará Basin in Equatorial Brazil, The Taranaki Basin in New Zealand, and The North Carnarvon Basin in Australia, focusing on the deepwater sedimentary section in each case. Although the first two datasets are examples of siliciclastic environments and the North Carnarvon, a mixed carbonate-siliciclastic exponent, the architectural elements identified in all the datasets are similar as well as their attribute response. The results show that the most robust attributes to characterize deepwater elements such as incised channels, channel-levee systems, and lobes are geometric, amplitude derived, frequency, and textural attributes. These seismic attributes indicate morphological, lithological, bed stacking, and stratigraphic architecture that are key characteristics of architectural elements identification. Moreover, we found that the correndering of sweetness (lithology-proxy), coherence (morphology indicator) and curvature attributes, helps to define the internal configuration for most of the deepwater architectural elements. While each basin is unique, our results and comparisons serve as a guide that allows seismic interpreters to use the most meaningful attributes for deepwater seismic geomorphology characterization.

Session Selection:
EP034. Submarine and Seismic Geomorphology

APPENDIX 2 – LIST OF PAPERS AND ABSTRACTS OF THE BEM's RESEARCH GROUP

Journal of South American Earth Sciences 88 (2018) 700–714

Contents lists available at ScienceDirect

Journal of South American Earth Sciences

journal homepage: www.elsevier.com/locate/jsames

Architectural framework of the NW border of the onshore Potiguar Basin (NE Brazil): An aeromagnetic and gravity based approach

Karen M. Leopoldino Oliveira[a,b,*], David L. de Castro[c], R. Mariano G. Castelo Branco[a,b], Diógenes C. de Oliveira[c], Eduardo N.C. Alvite[b], Caio C.A. Jucá[b], Jonathan L. Castelo Branco[b]

[a] Programa de Pós-Graduação em Geologia, Universidade Federal do Ceará (UFC), Campus do Pici, Bloco 912, Fortaleza, Ceará, CEP 60440-554, Brazil
[b] Laboratório de Geofísica de Prospecção e Sensoriamento Remoto (LGPSR -UFC), Brazil
[c] Programa de Pós-Graduação em Geodinâmica e Geofísica, Universidade Federal do Rio Grande do Norte, Natal, 59078-970, RN, Brazil

ARTICLE INFO

Keywords:
Potential field methods
Euler deconvolution
Basement heterogeneity
Brasiliano lineaments
Equatorial Margin

ABSTRACT

On the basis of qualitative and quantitative geophysical interpretations, studies on tectonostratigraphic evolution were carried out in NW onshore Potiguar basin. Airborne magnetic and terrestrial gravity data were acquired in order to investigate tectonostratigraphic relationships in a poorly studied area of this oil-bearing Early Cretaceous basin. The present integrated study determined the main geophysical lineaments, basin internal geometry and depth of intra-basement magnetic and gravity sources, characterizing geological domains in terms of lithostructural elements. The depth of geophysical sources was estimated using 2D and 3D Euler deconvolution. 2D forward gravity modeling was also performed along three transects. The results unravel crustal partitioning, characterized by NE-SW lineaments with local E-W to NW-SE inflexions. The geophysical patterns are directly related to basement grain, which is Brasiliano in age. In fact, the Jaguaribe shear zone, that is not clearly marked on the surface, appears much more pronounced in the various geophysical maps and gravity models. The Ponta Grossa and Fazenda Belém shear zones show similar geophysical signatures to the Jaguaribe shear zone and appear to limit a low-related gravity features. Another important magnetic lineament was revealed by 2D Euler deconvolution and was named Retiro shear zone. 2D gravity modeling shows the basin geometry in depth, which presents shallow depocenters that may be associated with hydrocarbon reservoirs to the east, such as the Fazenda Belém oil field. An evolutionary tectonic model of this reservoir is proposed comparing our results and previous geological studies. This study indicates that a few faults, which occur in the NW edge of Potiguar Basin and form depocenter boundaries, oblique to the main transform continental margin in NE Brazil, have the orientation, kinematics and geometry as the main rift faults. Thus, our final model suggests that the grabenlike depocenter could be the westernmost expression of the NE Brazilian Rift System that generated a series of rift basins along the Borborema Province in the Early Cretaceous. The still unknown deposition of rift-related sequences to the west of Fazenda Belém oil field is probably associated with raised area that remained active when the eastern sector of the Potiguar basin presented overall subsidence. It is likely this basement structural configuration is topographic highs and lows, keeping geodynamics relationships with strike-slip fault regimes installed in the Atlantic Equatorial Margin during Aptian.

1. Introduction

The Equatorial and South Atlantic opening was preceded by an extensive continental rifting in the NE-most South American platform (e.g., Chang et al., 1988; Heine et al., 2013). The Early Cretaceous extensional event led to a series of rift basins, named Northeast Brazilian Rift System (NEBRIS) by Matos (1992), inserted in the Precambrian Borborema Province and São Francisco Craton (Fig. 1). In Barremian, the extensional kinematics changed, moving the rifting east- and northwards to the current continental margin and leaving behind a roughly N-S, 1000-km long sequence of aborted rifts and small grabenlike basins. The onshore Potiguar Basin is the northernmost member

* Corresponding author. Programa de Pós-Graduação em Geologia, Universidade Federal do Ceará (UFC), Campus do Pici, Bloco 912, Fortaleza, Ceará, CEP 60440-554, Brazil.
E-mail addresses: karenleopoldino@alu.ufc.br (K.M. Leopoldino Oliveira), david@geologia.ufrn.br (D.L. de Castro), mariano@ufc.br (R.M.G. Castelo Branco), dcoliveira2005@yahoo.com.br (D.C. de Oliveira), eduardocapelo01@gmail.com (E.N.C. Alvite), c.alvesjuca@gmail.com (C.C.A. Jucá), jonathancastelobranco@gmail.com (J.L. Castelo Branco).

https://doi.org/10.1016/j.jsames.2018.10.002
Received 30 July 2018; Received in revised form 28 September 2018; Accepted 3 October 2018
Available online 03 October 2018
0895-9811/

Tectono-sedimentary evolution and petroleum systems of the Mundaú subbasin: A new deep-water exploration frontier in equatorial Brazil

Narelle Maia de Almeida, Tiago M. Alves, Francisco Nepomuceno Filho, George Satander Sá Freire, Ana Clara Braga de Souza, Márcio Nunes Normando, Karen M. Leopoldino Oliveira, and Thiago Henrique da Silva Barbosa

ABSTRACT

The Brazilian equatorial margin (BEM) evolved in response to transform motion between Brazil and Africa. In 2012, Petrobras drilled the Pecém well in the Mundaú subbasin (Ceará Basin) of the BEM to record the first deep-water oil discovery in the region. This work investigates the deep-water evolution of the Mundaú subbasin focusing on its structural and sedimentary evolution, and characterizes the petroleum systems in this new exploration frontier. For such purposes, poststack seismic reflection, borehole, and geochemical data were used. Three tectono-stratigraphic sequences representing synrift (Mundaú Formation), transitional (Paracuru Formation), and drift strata (Ubarana Formation) were divided into seven seismic units. Different tectonic domains were interpreted: proximal, distal, and Romanche Fracture Zone. Typical structures of transform margins, such as marginal ridges and marginal plateaus, were not identified in the Mundaú subbasin. Instead, the subbasin was predominantly deformed by transtensional movements. The Mundaú and Paracuru Formations are mature within the oil window, whereas the Ubarana Formation is immature. Main reservoir intervals consist of approximately 1-m (~3.28-ft)-thick intercalations of sandstone between shales, siltstones, and marls. The seal rocks comprise shales in the Ubarana Formation, whereas the hydrocarbon trap is related to an unconformity and a normal fault. This work concludes

Manuscript received November 3, 2017; provisional acceptance January 25, 2018; revised manuscript received April 14, 2018; revised manuscript provisional acceptance July 30, 2018; 2nd revised manuscript received March 14, 2019; 2nd revised manuscript provisional acceptance June 6, 2019; 3rd revised manuscript received June 7, 2019; final acceptance July 15, 2019.
DOI:10.1306/07151917381

AUTHORS

NARELLE MAIA DE ALMEIDA – *Programa de Pós-Graduação em Geologia, Universidade Federal do Ceará (UFC), Fortaleza, Ceará, Brazil; Instituto Federal do Rio Grande do Norte, Natal, Rio Grande do Norte, Brazil; narellemaia@gmail.com*

Narelle Maia de Almeida completed a B.Sc. in geology from UFC (2011), a master's degree in geodynamics and geophysics from the Federal University of Rio Grande do Norte (2014), and a Ph.D. in geology from UFC (2018). She is a professor at the Federal Institute of Rio Grande do Norte, Natal, and studies shallow and deep water on continental margins, sedimentary basins, marine and petroleum geology, and geophysics.

TIAGO M. ALVES – *3D Seismic Lab, School of Earth and Ocean Sciences, Cardiff University, Cardiff, United Kingdom; alvest@cardiff.ac.uk*

Tiago Alves completed a B.Sc. (1997) in engineering geology in Lisbon and a Ph.D. (2002) from the University of Manchester. He heads the 3D Seismic Lab, Cardiff University, since 2012. A sea-going marine researcher with close ties to the International Ocean Drilling Program, he undertakes research on deep-water continental margins, fluid migration in sedimentary basins, reservoir engineering, and geoenergy as an all-encompassing theme.

FRANCISCO NEPOMUCENO FILHO – *Departamento de Física, UFC, Fortaleza, Ceará, Brazil; nepomuceno@fisica.ufc.br*

Francisco Nepomuceno Filho holds a master's degree from University of Texas and a Ph.D. from the Universidade Estadual de Campinas. He worked at Petrobras as an executive manager for petroleum exploration and production in Brazil and as head of Petrobras's London office dedicated to presalt technology. He is coordinator of the Center of Excellence in Petroleum Geophysics and chief executive officer of the Technological Park of the UFC.

GEORGE SATANDER SÁ FREIRE – *Programa de Pós-Graduação em Geologia, UFC, Fortaleza, Ceará, Brazil; freire@ufc.br*

Marine and Petroleum Geology 122 (2020) 104599

Contents lists available at ScienceDirect

Marine and Petroleum Geology

journal homepage: www.elsevier.com/locate/marpetgeo

Research paper

A three-dimensional (3D) structural model for an oil-producing basin of the Brazilian equatorial margin

Narelle Maia de Almeida [a,*], Tiago M. Alves [b], F. Nepomuceno Filho [c], George Satander Sá Freire [a,d], Ana Clara B. Souza [d], Karen M. Leopoldino Oliveira [d], Márcio Nunes Normando [d], Thiago Henrique S. Barbosa [e]

[a] Departamento de Geologia, Universidade Federal do Ceará (UFC), Campus do Pici, Bloco 912, Fortaleza, Ceará, CEP 60440-554, Brazil
[b] Cardiff University. 3D Seismic Lab, School of Earth and Ocean Sciences, Cardiff University, Cardiff, United Kingdom
[c] Departamento de Física, Universidade Federal do Ceará (UFC), Campus do Pici, Bloco 922, Fortaleza, Ceará, CEP 60440-554, Brazil
[d] Programa de Pós-Graduação em Geologia, Universidade Federal do Ceará (UFC), Campus do Pici, Bloco 912, Fortaleza, Ceará, CEP 60440-554, Brazil
[e] Departamento de Engenharia do Petróleo, Universidade Federal do Ceará (UFC), Campus do Pici, Bloco 709, Fortaleza, Ceará, CEP 60440-554, Brazil

ARTICLE INFO

Keywords:
Atlantic ocean
Equatorial Brazil
Ceará basin
3D seismic
Oil fields
3D modelling

ABSTRACT

Hydrocarbon discoveries in Equatorial Brazil, Equatorial Africa and French Guiana-Suriname-Guyana have recently confirmed their importance as new exploration frontiers. The Mundaú sub-basin, located on the Brazilian Equatorial Margin, comprises four producing fields in shallow waters: Xaréu, Atum, Espada e Curimã. In order to understand the structural and seismic-stratigraphic frameworks of an oil-producing region in Equatorial Brazil, this work addresses the 3D geometry and spatial distribution of main faults in the Curimã and Espada fields. The occurrence of hydrocarbons in the Mundaú sub-basin is compared with fields in other parts of the Brazilian Equatorial Margin and Equatorial Africa. Data from 12 wells and a 3D post-stack time-migrated multichannel seismic volume are used to define nine (9) seismic-stratigraphic units: the syn-rift Mundaú Formation (Units 1, 2, 3 and 4); the transitional Paracuru Formation (Unit 5); and the drift Ubarana (Uruburetama and Itapagé Members, Units 6 and 7), Tibau and Guamaré Formations (Units 8 and 9). The study area is dominated by NW-SE planar normal faults, basinward-dipping, that form multiple half-grabens, and tilted blocks with small anticlines and synclines genetically related to a transtensional system. Three types of plays are recognised in the Mundaú sub-basins: structural, combined (structural-stratigraphic) and stratigraphic (turbiditic). In the eastern part of the study area, where the basement is shallow, no oil was found. Conversely, oil was discovered in an anticlinal trap formed over a hanging-wall block analogous to fields on the Côte D'Ivoire-Ghana transform margin. This work shows that combined traps on footwall blocks are successful plays near the shelf break of the Mundaú sub-basin, in similarity with the Espoir and Baobab fields in Ivory Coast. Furthermore, turbiditic reservoirs in drift units are analogous to the Stabroek block in Guyana and prospects in the Gulf of Guinea. The structural and petroleum-play analyses in this work are therefore crucial to understand the multiple geological processes leading to the trapping of hydrocarbons in the larger Equatorial Atlantic Ocean.

1. Introduction

The Ceará Basin is located on the Brazilian Equatorial Margin (BEM) between the Potiguar Basin to the southeast and the Barreirinhas Basin to the northwest (Fig. 1). The BEM developed as a typical continental margin of the transform type (Matos, 2000). The bulk of its development was dominated either by oblique extension (transtension) or by pure and simple shear movements, all responding to a dominant dextral sense of movement in transfer (syn-rift) and transform (post-rift) faults. In this portion of the late Gondwana supercontinent, continental rupture and breakup took place in an East-West direction, creating shorelines with two predominant directions: NW-SE in transtensional portions, and E-W

* Corresponding author.
E-mail addresses: narelle@ufc.br (N. Maia de Almeida), alvest@cardiff.ac.uk (T.M. Alves), nepomuceno@fisica.ufc.br (F. Nepomuceno Filho), freire@ufc.br (G.S.S. Freire), anaclarageologia@alu.ufc.br (A.C.B. Souza), karenleopoldino@gmail.com (K.M. Leopoldino Oliveira), mnormando@gmail.com (M.N. Normando), thiagohenrique@alu.ufc.br (T.H.S. Barbosa).

https://doi.org/10.1016/j.marpetgeo.2020.104599
Received 3 January 2020; Received in revised form 31 May 2020; Accepted 15 July 2020
Available online 22 July 2020

Journal of South American Earth Sciences

GEOCHEMICAL CONSTRAINTS ON THE ORIGIN AND DISTRIBUTION OF CRETACEOUS SOURCE-ROCKS IN THE CEARÁ BASIN, BRAZILIAN EQUATORIAL MARGIN

--Manuscript Draft--

Manuscript Number:	
Article Type:	Research Paper
Keywords:	Organic geochemistry; Petroleum system; Cretaceous; Hydrocarbon generation; Spatial distribution map.
Corresponding Author:	Ana Clara Braga de Souza, M.D. Universidade Federal do Ceará Campinas, SP BRAZIL
First Author:	Ana Clara Braga de Souza, M.Sc
Order of Authors:	Ana Clara Braga de Souza, M.Sc
	Daniel Rodrigues do Nascimento Jr., PhD
	Alessandro Batezelli, PhD
	Karen Maria Leopoldino Oliveira, M.Sc
	Narelle M. de Almeida2 Maia de Almeida, PhD
	Francisco Nepomuceno Filho, PhD
	Márcio Nunes Normando, M.Sc
	Thiago Henrique da Silva Barbosa, B.Sc
Abstract:	The Ceará Basin is an offshore basin located in Northeast Brazil. It is part of a series of Brazilian Equatorial Margin basins, generated during the breakup of West Gondwana and the opening of the Equatorial South Atlantic Ocean. In this present study, geochemical data such as total organic carbon (TOC), calculated vitrinite reflection (Ro cal), and pyrolysis indexes (eg., hydrogen index-HI, oxygen index-OI, maximum temperature-Tmax, and relative hydrocarbon potential-RHP) were investigated in two areas: middle and outer shelf. This research included the study of Mundaú, Paracuru, and Ubarana Formations, covering rift, breakup-sequence, and drift phases, respectively. Altogether, 1571 core samples of organic-rich rocks from 15 boreholes were selected. This work aims to determine the origin of these organic-rich rocks and to evaluate their source rock potential. Additionally, it will allow us to identify, predict, and map the most productive organic facies and the best feature related to the characterization of the generation and expulsion of the petroleum systems. The geochemistry results indicate that the source rocks from the rift supersequence have Type III kerogen and were thus considered gas-prone. Rock-Eval pyrolysis reveals a fair to excellent source-rock potential, and its spatial distribution is related to fault boundaries. The source rocks from the breakup-sequence are the main generating and presents a broad mixture of organic matter types. Characterized by abundant organic matter, indicating a high hydrocarbon potential and classified as oil and gas-prone. Source-rock spatial distribution from the breakup-sequence initially goes towards the depocenter of the basin and then back towards the land. The advance to land is observed from the highest values of TOC. This latest change is accompanied by a higher hydrogen index (HI) and more significant hydrocarbon potential (RHP) values. This interval is interpreted in this study as the main geochemical mark of the Ceará basin and define the most promising range for hydrocarbon generation. The source rocks from the drift phase contain less promisor source rocks. They were appointed as an organic-rich stratum, mainly in distal areas. This phase has an immature to early oil-window thermal conditions with kerogen Type II and II-III and IV. On the middle shelf, the hydrocarbon expulsion threshold corresponds to a depth of about 1635m, which is shallower than in located closer to the outer shelf border (2106m). In the deep waters, the hydrocarbon expulsion threshold corresponds to 3632m. This result allows us to classify Ceará Basin as a high-heat-flow basin, corroborating its recent classification as

49º Congresso Brasileiro de Geologia
20 a 24 de agosto de 2018 – Rio de Janeiro

NEW INSIGHTS ON TECTONIC FRAMEWORK OF POTIGUAR BASIN, BASED ON POTENTIAL FIELD DATA

Oliveira, K.M.L.[1], Castelo Branco, R.M.G.[1], de Castro, D.L.[2], Oliveira, D.C.[2], Nepomuceno Filho, F.[1], Souza, A.C.B.[1], Almeida, N.M.[1,3] , Normando, M.N.[1], Barbosa, T.H.S.[1]

[1]Federal University of Ceará; [2]Federal University of Rio Grande do Norte; [3]Instituto Federal do Rio Grande do Norte

ABSTRACT: This research presents the internal geometry of the northwestern edge of Potiguar Basin (Fazenda Belém oil field - NE Ceará State), and its structural framework based on magnetic and gravity anomalous patterns and density distribution in depth derived from 2D gravity modeling. To achieve this goal we used older magnetic airborne survey and new terrestrial gravity data. Interpretation of magnetic and gravity anomalies was based on data processing and depth analysis techniques, which provided a geological map of the crustal domains concealed in this part of the basin. Thus, the number, location and internal geometry of gravity and magnetic sources were used to generate the initial geophysical model constrained by 2D Euler solutions of magnetic and gravity data. The study area shows structural lineaments characterized by lineaments in the NE-SW direction with E-W and NW-SE inflexions. The spatial arrangement of geophysical domains is related to distribution of deep crustal lineaments, which are associated with continuity of the main Brasiliano shear zones. The Jaguaribe shear zone is not well marked on the surface, but appears well pronounced on subsurface as shown in geophysical maps and models. The Ponta Grossa and and Fazenda Belém lineaments, in turn, present similar characteristics and seem to limit possible grabenforms structures westernmost edge of Potiguar basin. Another lineament with expression and depth similar to others presents well marked by 2D Euler deconvolution in northwest of Ponta Grosa lineament and was named Fazenda Retiro Grande lineament. 2D gravity modeling in three profiles point out the geometry of western edge of the Potiguar basin, which could be grabenforms felled areas, with implications on the westward continuity of the Fazenda Belem petroleum system. The shallower alignments located in the SE sector are interpreted as faults or intrabasin discontinuities, which may represent reactivations of the main shear zones. Finally, an evolutionary tectonic model of Fazenda Belém oil field is proposed comparing our results and previous geological studies. This study indicates that a few faults that occur in the NW edge of Potiguar Basin and form graben boundaries, oblique to the main transform margin, havethe same orientation, kinematics and geometry as the main rift faults. Thus, our final model suggests that the grabenlike depocenter could be the westernmost expression of the NE Brazilian Rift System that generated a series of rift basins along the Borborema Province in the Early Cretaceous. However, it is still necessary to identify rift sequence deposited within this depocenter to confirm that Fazenda Belém grabenlike structure is coeval to the Neocomian Potiguar Rift ~100 km far to the east. This work provides new insights that can contribute to a better understanding of the process of continental rifts and transform margin evolution.

KEYWORDS: GRAVITY 2D MODELING; GEOPHYSICAL MAPPING; EQUATORIAL MARGIN.

49º Congresso Brasileiro de Geologia
20 a 24 de agosto de 2018 – Rio de Janeiro

SEQUENCE STRATIGRAPHY FROM THE DRIFT PHASE OF MUNDAÚ SUB-BASIN USING WELL LOGS DATA

Souza, A.C.B.[1]; Oliveira, K.M.L.[1]; Almeida, N.M.[1,2]; Normando, M.N.[1]; Nascimento Junior, D.R.[1]; Nepomuceno Filho, F.[1]; Barbosa, T.H.S[1].

[1]Universidade Federal do Ceará; [2]Instituto Federal do Rio Grande do Norte.

ABSTRACT: The Ceará Basin is an offshore basin located in Northeast Brazil and is part of a series of basins of the equatorial margin of Brazil. This basin is subdivided according to tectono-sedimentary aspects in four sub-basins. In this work, we study the Mundaú sub-basin, which concentrates oil and gas exploration activities and has a thick and complete sedimentary record. The distribution of depositional environments in a sedimentary basin reflects the spatial and temporal variations in physical processes at the shoreline and the relationship between the sediment supply rate and the accommodation development space. A complete stratigraphic cycle was studied from the recognition of the stratigraphic sequence, which typically includes two or more systems tracts. This work aims to define and characterize these stratigraphic discontinuities in well logs and from this provide a stratigraphic model for the Ceará Basin. The standard log data (i.e. gamma ray-GR, sonic-DT and density-RHOB) were used to interpret the stratigraphic units. All the data was provided by ANP. The methods consist of identify key surfaces bounding, subdivide the sediment packages and correlate their continuities.The recognition of systems tracts and their relation to the depositional processes were based on the identification and interpretation of key surfaces, such as; maximum flooding surface (MFS), maximum progradation surface (MPS), marine condensed interval (MCI), downlap surface (DS) and sequence boundary (SB). Some key surfaces of regional expression were recognized in the two major units. Unit 1 marks beginning of the drift sedimentation. This unit includes the Uruburetama and Itapajé members, both belonging to the Ubarana Formation. Uruburetama member comprises mainly retrograde patterns and its base is comprised of shales and an abrupt upward increasing in the GR. These two members are distinguished by a SB described as steeply rising upwards in the GR and DT logs. Itapajé member has retrograde and prograde intervals recognized by coarsening upward patterns, which constitute DS.Bow and blocky trend also occur as thick stratigraphic unit. In general, the prograde sequences are less thick at the top of the unit. Thus, this unit ends up with fining upward and followed by a coarsening upward pattern.The latter sequence of Unit 1 marks a subsequent process of progradation. This sequence is delimited at its base by a MPS and marks the SB that begins the aggrading phase. Unit 2 comprises the Tibau and Guamaré Formations and is initially marked by irregular trends which are interpreted as aggrade intervals. Usually these aggrade intervals are followed by fining upward patterns that point out transgressive patterns interpreted as MFS. In general, Unit 2 is less thick than the other sequences found in Unit 1. In conclusion, these stratigraphic information are parameters for interpreting and measuring depositional processes in Ceará Basin.

KEYWORDS: KEY SURFACES, SYSTEMS TRACTS, CEARÁ BASIN.

ACOUSTIC INVERSION FEASIBILITY FOR RESERVOIR CHARACTERIZATION IN CEARÁ BASIN

Normando, M.N.[1]; Souza, A.C.B.[1]; Oliveira, K.M.L.[1]; Almeida, N.M. [1,2]; Nascimento Júnior, D.R.[1]; Nepomuceno Filho, F. [1]; Barbosa, T.H.S.[1]

[1]Universidade Federal do Ceará; [2]Instituto Federal do Rio Grande do Norte

ABSTRACT: The economic environment of recent years, characterized by low price of petroleum barrel, brought again the importance of production in mature fields that are responsible for about 70% of worldwide hydrocarbon production. These reservoirs still have some significant volume of remaining oil in place that needs to be drained optimally, with new wells drilled in the best locations. Reservoir characterization studies are essential to try identifying these regions with hydrocarbon as they allow a good understanding of the field. Acoustic inversion can help to identify and quantify areas in the reservoir favorable for oil accumulation through well data analysis (porosity and impedance, mainly) and seismic data analysis (amplitudes of 2D seismic lines or 3D seismic cubes). Thus, the main objective of this work is to evaluate the feasibility of seismic inversion studies in reservoirs from Ceará Basin. For this purpose, we used well and seismic data set from Ceará Basin, covering the four main fields in production (Xaréu, Curimã, Atum and Espada) and a new exploration frontier in deep water. The whole data set was provided by ANP (National Petroleum Agency). The methodology used here is based on where the reservoir has a good correlation between the properties porosity and impedance, at the end of the seismic characterization process, it is possible to obtain maps or cubes of porosity that can be integrated in the geological and geostatistical modeling, building a model more realistic and reliable. Seismic amplitudes represent the impedance contrasts between the different layers. However, for reservoir characterization, it is necessary to have the properties of the layers and not properties on the interfaces. Seismic inversion process converts the interface property (amplitude) into a layer property (impedance). In general, the wells from Ceará Basin have a good correlation between porosity (NPHI) and acoustic impedance (AI), around 80-90% (some wells with 98-99% of correlation). Furthermore, it is possible to observe clearly the facies behavior: non-reservoir facies have low porosities and high impedance; reservoir facies have high porosities and low impedances. These initial results suggest that a reservoir characterization study using acoustic seismic inversion could generate properties (porosity maps or cubes, for instance) to build a more consistent reservoir model for Ceará Basin area.

KEYWORDS: RESERVOIR MODELING, PETROPHYSICAL PROPERTIES, INTEGRATED STUDIES.

49º Congresso Brasileiro de Geologia
20 a 24 de agosto de 2018 – Rio de Janeiro

3D STRUCTURAL MODEL FOR AN OIL-PRODUCING REGION, CEARÁ BASIN, BRAZILIAN EQUATORIAL MARGIN

Almeida, N.M.[1,2]; Alves, T.M.[3]; Nepomuceno Filho, F.[1]; Freire, G.S.S.[1]; Souza, A.C.B.[1]; Oliveira, K.M.L.[1]; Normando, M.N.[1]; Barbosa, T.H.S.[1]

[1]Universidade Federal do Ceará; [2]Instituto Federal do Rio Grande do Norte; [3]Cardiff University

RESUMO: Faults can act either as conduits or barriers for hydrocarbon migration, because they have anisotropic flow properties that relate to their complex three-dimensional structures. The Mundaú sub-basin, Ceará basin, is an oil and gas producer with four fields in its shallow waters (Xaréu, Atum, Espada e Curimã). Exploration started in 1970's and has continued to the present day. Tectono-sedimentary units consist of the Mundaú Formation (syn-rift); the Paracuru Formation (transitional) and the Ubarana, Tibau and Guamaré Formations (post-rift). Three types of plays are known in the basin: turbiditic, combined (structural-stratigraphic) and structural. The structural plays may be classified as rotational, transpressive, transtensive or footwall-related. In parallel, we know that Curimã and Atum oil fields comprise examples of combined traps, relating to the erosional truncation of tilted blocks limited by normal faults. Despite that, the geometry and distribution of these faults are unknown. This work aims at recognizing the 3D geometry and spatial distribution of faults in an area that includes the Curimã and Espada fields, answering key questions: What are the typical faults geometries in the Curimã and Espada fields? How are the faults distributed in the subsurface? In what way(s) these faults influence hydrocarbon accumulations? For such purpose, we used 3D seismic and well data. The seismic volume consists of 172 inlines spaced 75 m, and 663 crosslines, spaced 25 m. The inline length is ~16,6 km and the crosslines are ~12,8 km, comprising a total area of ~212 km². The depth reaches 5.000 ms twt and each seismic trace has 1.251 samples, with 4 ms interval sample. The well data comprise standard log suites (i.e. gamma ray, sonic, density and resistivity), check-shots, lithological data and formation tops. All the dataset used in this work was supplied by ANP Brazil. In the study area, there are extensional basinward-dipping faults that formed multiple half-grabens. The basement is NNW-dipping. In the ENE region of the area where the basement is higher, i.e. close to the 1_CES_115 well, the Paracuru Formation was eroded and this well was dry. The 4_CES_0128 well reached a dome structure near the Paracuru top, in between two important normal faults. In contrast with 1_CES_115, this well found oil in Ubarana and Pararuru Formations. Others wells, such as 4_CES_0024 and 3_CES_0037D, were drilled reaching the top of structural/combined traps on the footwall of different faults to find oil. Therefore, we mapped the faults and different structural petroleum plays and understood the importance of a multi-faceted structural component to the entrapment of hydrocarbons in the Ceará Basin.

PALAVRAS-CHAVE: 3D SEISMIC, FAULTS, OIL.

49º Congresso Brasileiro de Geologia
20 a 24 de agosto de 2018 – Rio de Janeiro

PETROLEUM SYSTEMS OF DEEP-WATER MUNDAÚ SUB-BASIN, CEARÁ BASIN, NEW EXPLORATION FRONTIER

Almeida, N.M.[1,2]; Alves, T.M.[3]; Nepomuceno Filho, F.[1]; Freire, G.S.S.[1]; Souza, A.C.B.[1]; Oliveira, K.M.L.[1]; Normando, M.N.[1]; Barbosa, T.H.S.[1]

[1]Universidade Federal do Ceará; [2]Instituto Federal do Rio Grande do Norte; [3]Cardiff University

RESUMO: Transform margins were not a significant target for oil industry until the discovery of the Jubilee field offshore Ghana in 2007. Likewise, discoveries have been realized in Equatorial Brazilian margin as the Pecém well in Ceará basin in 2012 and Pitu well in Potiguar basin in 2013. Thus, these findings have attracted the attention of the oil industry to the Brazilian Equatorial margin. The main objective of this work is characterize the petroleum system of the deep-water Mundaú sub-basin, including the understanding of the source rocks, reservoirs, seal rocks and entrapment. We used 2D post-stack seismic and data of Pecém well (1_BRSA_1080) comprising standard log suites (i.e. gamma ray, sonic, density and resistivity), checkshots, lithologic data and formation tops. We also used geochemical data including Total Organic Carbon (TOC) and Rock-Eval pyrolysis. All the dataset was granted by ANP. The tectono-sedimentary evolution of deep-water Mundaú sub-basin consists of three major megasequences: syn-rift (Mundaú Formation), transitional (Paracuru Formation) and post-rift (Ubarana Formation). TOC% values for source rocks in the Mundaú Fm. are between 0.46% and 1.97%, indicating poor to good generation potential. The values of Paracuru Fm. are between 1.16% and 3.56%, indicating good to excellent generation potential while the source rocks in the Ubarana Fm. are 3.63% and 4.19% indicating an excellent generation potential. The results indicated Type II kerogen dominantly. The Tmax ranges from 424 to 449°C which places Mundaú and Paracuru Formations within the oil window. The samples of these formations are thermally (early) mature. However, the samples of Ubarana Fm. are considered thermally immature. A plot of S1 versus TOC classified the samples of Mundaú and Paracuru Formations as autochthonous hydrocarbons, indicating that the oil produced has not migrated from far source rocks. This means that hydrocarbons were accumulated very close to where they were produced. The reservoirs consist of thin intercalations of sandstones between shales, siltstones and marls. Oil was found in fluid samples and using gas detectors in several intervals mainly near the top of Paracuru Formation. The seal rocks are composed of transgressive shales of Ubarana Formation while the hydrocarbon trap is mixed (structural-stratigraphic), related to an unconformity and a normal fault. Until now, with the available data, we can conclude that Paracuru Fm. is the main source and reservoir unit of deep-water Mundaú sub-basin. However, we can not rule out the possibilities of: 1. Source rocks and reservoirs at Mundaú Fm. related to the onset of rifting in Equatorial Brazil and 2. Reservoirs at Ubarana Fm. related to the migration by faults from syn-rift and transitional source rocks to post-rift reservoirs.

PALAVRAS-CHAVE: SOURCE ROCKS, OIL RESERVOIR, MIXED TRAP.

APPENDIX 3 –LIST OF FIGURES

Figure 1-1: (a) Regional topographic and bathymetric map of the Equatorial Atlantic showing conjugate margins in Brazil and Africa as well as the larger oceanic fractures zones in the area; (b) The Ceará basin is divided in four sub-basins: Piauí-Camocim, Acaraú, Icaraí and Mundaú; (c) Relative location of the four producer fields (Xaréu, Atum, Curimã and Espada) of the Mundaú sub-basin. The location of the wells and 3D seismic data are shown. The topographic model is from the National Oceanic and Atmospheric Administration (NOAA). The structural data was compiled from Zalán & Warme (1985), Silva et al., (1999), and Morais Neto et al., (2003). The basin boundaries are from ANP and the sub-basins boundaries were adapted from Morais Neto et al., (2003).....14

Figure 1-2: The location of the wells, seismic data (2D), and the blocks of ANP Bidding Rounds are displayed. Also, four producer fields (Xaréu, Atum, Curimã, and Espada) in the Mundaú sub-basin are outlined.....16

Figure 2-1: a) Seismic reflection section with the presence of the first multiple of the seabed and red layer multiple (red arrows) mixing with the signal and noise – a location map view is shown with the seismic profile, the Pecém well and the exploration blocks in Ceará Basin, Brazilian Equatorial Margin; (b) two multiples related to the seabed and another derived from a slightly deeper horizon. Blue lines refer to seabed reflector and the green line refers to the red line layer. 20

Figure 2-2: (a) Seismic line obtained by Brazilian National Petroleum Agency (ANP) with the presence of multiples (red arrows); (b) reprocessed seismic line and true horizons can be mapped without bias. Note that multiples and noise were extracted and the seismic signal is much better defined. Both lines are displayed with the amplitude volume technique (AVT) attribute as described by Bulhões and Amorim, (2005). 22

Figure 2-3: The three panels of velocity analysis of this seismic line. (a) the supergather panel is shown on the left as a function of time and offset; (b) the semblance panel; (c) the stacked section with each vertical red line representing a location where the velocity analysis was performed and green line the current location in analysis; (d) the result of this process is shown in a 2D velocity model.....23

Figure 3-1: (a) Regional topographic and bathymetric map of the Equatorial Atlantic showing

conjugate margins in Brazil and Africa as well as the larger oceanic fractures zones in the area; (b) The Ceará basin is divided in four sub-basins: Piauí-Camocim, Acaraú, Icaraí and Mundaú. The Romanche Fracture Zone and positive gravity anomalies were mapped using data from the World Gravity Map (WGM2012). The topographic model is from the National Oceanic and Atmospheric Administration (NOAA). The structural data was compiled from Zalán & Warme (1985), Silva et al., (1999), and Morais Neto et al., (2003). The basin boundaries are from ANP and the sub-basins boundaries were adapted from Morais Neto et al., (2003). 28

Figure 3-2: The location of the wells, seismic data (2D), and the blocks of ANP Bidding Rounds are displayed. Also, four producer fields (Xaréu, Atum, Curimã, and Espada) in the Mundaú sub-basin are outlined. The black polygon frame indicates the area presented in Figures 8, 9, 10 and 11.....31

Figure 3-3: Ceará Basin litho-, chrono-, and tectonostratigraphic columns with the representation of the units recognized in the study area (modified from Conde et al., 2007). BS: Breakup sequence; UBA: Ubarana Fm.; GUA: Guamaré Fm.; TIB: Tibau Fm.....32

Figure 3-4: (a) Correlation panel among the five deepwater wells showing interpreted seismic units, gamma ray, sonic logs, and calculated Vshale; (b) Four deepwater wells displaying the Paracuru Fm. interval of gamma ray and facies. The rocks of the Trairi Member are interbedded calcilutites and shales with high values of gamma ray. The 1 BRSA 1114 CES well data reveals that the Paracuru Formation in deepwater is composed of interbedded sandstones and shales in a subtle thickening pattern to the top; c) The five deepwater wells revealing the Unit 4 and 5 lithotypes. GR: Gamma Ray; Vsh: V shale; RS: Rift Sequence; BS: Breakup Sequence; DS: Drift Sequences.....35

Figure 3-5: Seismic section showing the continental shelf, slope and deepwater segments in the study area. (a) On the continental shelf, the border fault controls the extensional faults, which form half-grabens and the basin depocenter; (b) The slope segment is characterized by SDRs and the four major landward-dipping faults mapped in this basin. A thick rift depocenter as well as anticline structures are interpreted. Synthetic and antithetic faults are interpreted in drift sequence; (c) The deepwater segment is characterized by a thick drift sedimentary package, several high-amplitude reflectors, and high-angle and Cenomanian faults. The 1BRSA 1080 CES is shown in the up left. The Moho is interpreted on slope segment as a high-reflectivity zone around 9000 ms twt. Profile location (green line) is displayed on the right. Vertical scale

in two-way traveltime (ms twt). The units mapped in this study are presented in yellow text.37

Figure 3-6:SW-NE dip seismic sections with stratigraphy uninterpreted and interpreted. The uninterpreted sections show the major antithetic faults and Mid-Eocene reflector. a) Interpreted section shows several anticline structures on the continental slope where it is related to the rift stage. Oligocene faults are shown in this section. Reflector SDRs were interpreted in the basement. The 1 BRSA 1080 well and its hydrocarbon evidence are labeled (black dots); b) Oligocene faults and SRD reflectors were also interpreted in this section; c) Interpreted section shows the interpreted horizons and Cenomanian reactivation faults. Note that seismic in C AVT attribute was not applied. The location is depicted in all the stratigraphic uninterpreted sections. Vertical scale in two-way traveltime (ms twt). The units mapped in this study are presented in yellow text. 40

Figure 3-7: NW-SE strike seismic sections with stratigraphy uninterpreted and interpreted and the location of the BRSA 1080 well is shown together with the location of hydrocarbon evidence (black dots); a) Interpreted section showing the presence of magmatic bodies as sills and vent. Mass transport and a paleocanyon is interpreted in the drift sequences. Red polygon indicates the area displayed in Figure 13a; b) Several sills and a magmatic body are shown in this section; c) Paleocanyons, canyons, and a basement high were interpreted in this section. The location is depicted in all the stratigraphic uninterpreted sections. Vertical scale in two-way traveltime (ms twt). The units mapped in this study are presented in yellow text. 42

Figure 3-8: Structural maps from ten major horizons interpreted with seismic, and two structural maps migrated in time and depth. The location of five deepwater wells and the four major faults are shown. Parts (a) through (j) display time structure maps, parts (k) and (l) display depth structures. CS: continental shelf; OC: oceanic crust. 44

Figure 3-9: Isochron maps from eight units from the studied seismic lines, and one isochron map migrated in depth. These maps show sediment thickness distribution. The location of five deepwater wells and the four major faults are also shown in the figure for reference. Parts (a) through (i) display time structure maps, part (j) displays the depth structure. CS: continentalshelf; OC: oceanic crust. 45

Figure 3-10: (A) SW-NE schematic geological section showing the architecture of the segments and stratigraphic interpretation. Note the thick package of rift sequences in the continental slope

segment, and the thick package of drift in the deepwater segment. The projected location of the BRSA 1080 well, the oil discovery, is marked. (B) The isochron map of the syn-rift sequences. (C) The thickness map of the Transitional sequence (breakup sequence). (C) The thickness map of the drift sequences. COB: Continental-oceanic boundary; CS: continental shelf; OC: oceanic crust; TWT: two-way traveltime.....48

Figure 3-11: Interpreted depositional environments in the drift units and location of the five deepwater wells used in this study. The drift deposition in slope segment reveals an active dynamic of erosion with canyons and gullies developed during its evolution. CS: continental shelf. 51

Figure 3-12:(a) Plot of total organic carbon (TOC) versus depth showing the source rock generation potential; (b) Tmax versus Depth displaying the maturity of organic matters; (c) Hydrogen Index versus Tmax showing the maturity and the kerogen type; (d) Modified Van Krevelen diagram presenting the primary composition. 53

Figure 3-13:Figure 13: Seismic lines with stratigraphy uninterpreted and interpreted detailed section showing magmatic bodies. a) NW-SE strike section interpreted showing sills, vents and magmatic bodies; b) SW-NE dip section showing several high-amplitude reflectors associated with sills and a massive magmatic body. Red polygon indicates the area in Figure 14b; c) SW-NE dip section showing sills, vents, a mini-volcano, and a large magmatic body. Red polygon indicates the area in Figure 14c. All the magmatic features with the exception of the vents are presented in this area until the late Eocene.....55

Figure 3-14:SW-NE dip seismic lines with stratigraphy uninterpreted and interpreted detailed section showing turbiditic bodies in deepwater. a) Interpreted section showing several bright spots and turbidites of the Late Albian to Turonian possibly saturated with hydrocarbons. These turbidites were interpreted with updip pinch-out and some of them are associated with magmatic bodies. Also, mass-transport are clearly associated with these turbidites. Turbidites from the Late Eocene were also interpreted with updip pinch-out and associated with magmatic bodies (red forms); b) Interpreted section showing several high-amplitude reflectors with patterns probably associated with turbidites of the Late Albian to Turonian; c) Interpreted section showing turbidites of the Late Albian to Turonian. Faults connecting rift, transitional, and drift sequences were interpreted near these turbiditic bodies. This indicates a possible play where the migration occurs directly from rift and transitional source rocks to drift turbiditic

reservoir. The seismic section B and C are also shown in a larger view in Figure 13 60

Figure 3-15: SW-NE oriented seismic lines with stratigraphy uninterpreted and interpreted detailed section showing turbiditic bodies in deepwater. a) Interpreted section showing turbidites of the Late Albian to Turonian age. Faults connecting rift, transitional, and drift sequences were interpreted near these turbiditic bodies. This indicates a possible play where the migration occurs directly from the rift and transitional source rocks to drift turbiditic reservoir; b) Interpreted section showing turbidites of the Late Albian to Turonian where updip pinch-out was interpreted. These reflector patterns show interbedding of turbidite and shales; c) Interpreted section displaying turbidites of the Late Albian to Turonian with updip pinch-out. Faults connecting rift, transitional, and drift sequences were interpreted near these turbiditic bodies. This indicating a possible play where the migration occurs directly from the rift and transitional source rocks to drift turbiditic reservoir. The 1 BRSA 1114 well and its hydrocarbon evidence are labeled (black dots).....62

Figure 4-1: (A) Map of the Equatorial Atlantic Ocean highlighting the fracture zones and the marginal basins. B) The Ceará Basin sub-divided into four sub-basins: Piauí-Camocim, Acaraú, Icaraí and Mundaú. The study area is located in the Mundaú sub-basin. Structural data was compiled from Zalán and Warme (1985) and Morais Neto et al. (2003). The basins boundaries were provided by the Brazilian National Agency of oil, gas and biofuels (ANP) and boundaries of sub-basins were based on Morais Neto et al. (2003). C) Location of the four producer fields (Xaréu, Atum, Curimã and Espada) of the Mundaú sub-basin. The location of the wells and seismic data are shown, as provided by the ANP. The topographic model in the figure was provided by NOAA (ETOPO1). 75

Figure 4-2: Correlation panel amongst 3D seismic reflectors and stratigraphic information from the Albian to Turonian age in the Ceará Basin (Condé et al., 2007). B) Well correlation panel showing interpreted gas indicator, gamma ray, sonic logs, density, porosity, and facies. 80

Figure 4-3: Flow chart summarizing the methodology used in this work. 82

Figure 4-4:Time-structural maps of the horizons at the study area: A) Albian base revealing the direction of sediments supply. B) Turonian top. C) Thickness map of the Albian base to Turonian interval. The location of three deepwater wells are shown. D) The 3D cube cropped showing the crossline 2251 and the 1BRSA 1114 CES well. Above it is displayed the original

seismic cube and below is shown the flattened seismic cube. E) The crossline 2230 and the location of the phantom horizons interpreted. 84

Figure 4-5: Seismic attribute analysis of the phantom horizon 1: A) The RMS amplitude with the features interpreted. The location of three deepwater wells are shown as well as the location of the arbitrary seismic sections. Vertical seismic sections are shown in the top right. B) Sweetness map with features interpreted. C) Envelope with features interpreted. 90

Figure 4-6: Seismic attribute analysis of the phantom horizon 2: A) The RMS amplitude with the features interpreted. The location of three deepwater wells are shown as well as the location of the arbitrary seismic sections. Vertical seismic sections are shown in the top right. B) Sweetness map with features interpreted. C) Envelope with features interpreted. 92

Figure 4-7: Seismic attribute analysis of the phantom horizon 3: A) The RMS amplitude with the features interpreted. The location of three deepwater wells are shown as well as the location of the arbitrary seismic sections. Vertical seismic sections are shown in the top right. B) Sweetness map with features interpreted. C) Envelope with features interpreted. 94

Figure 4-8: Seismic attribute analysis of the phantom horizon 4: A) The RMS amplitude with the features interpreted. The location of three deepwater wells are shown as well as the location of the arbitrary seismic sections. Vertical seismic sections are shown in the top right. B) Sweetness map with features interpreted. C) Envelope with features interpreted 95

Figure 4-9: Vertical seismic section showing the Inline 3765 and the 1 BRSA 1114 CES well: A) seismic amplitude section. B) RMS amplitude and its zoom in in the right. C) Sweetness its zoom in in the right. D) Envelope its zoom in in the right. 96

Figure 4-10: Spectral magnitude components plotted against an RGB color using a combination of of 20–30–50 Hz: A) Phantom horizon 1 (youngest); B) Phantom horizon 2; C) Phantom horizon 3; D) Phantom horizon 4 (oldest). The well locations are displayed as a white dot. .. 98

Figure 4-11: Seismic attributes used to SOM clustering: A) RMS amplitude. B) Coherent Energy; C) Instantaneous Frequency; D) GLCM homogeneity. 100

Figure 4-12: SOM results presented in the four phantom horizons that highlight the deepwater elements: Phantom horizon 1 (youngest); B) Phantom horizon 2; C) Phantom horizon 3; D) Phantom horizon 4 (oldest). The well locations are displayed as a white dot; E) Inline 3765 in

seismic amplitude below and SOM result in the top. Evaluation of the seismic facies and sand-rich elements by using log facies information from the 1 BRSA 1114. CES 102

Figure 4-13: Independent components in the phantom horizon 3: A) independent component 1. B) independent component 2. C) independent component 3. D) independent component 4. 103

Figure 4-14: ICA results presented in the four phantom horizons that highlight the deepwater elements: Phantom horizon 1 (youngest); B) Phantom horizon 2; C) Phantom horizon 3; D) Phantom horizon 4 (oldest). The well locations are displayed as a white dot; E) Inline 3765 in seismic amplitude below and ICA result in the top. Evaluation of the seismic facies and sand-rich elements by using log facies information from the 1 BRSA 1114 CES. 105